THE STATE OF WATER AND CELL MORPHOLOGY IN DEEPLY FROZEN *POPULUS*

by
Allen Gene Hirsh

Dissertation submitted to the Faculty of the Graduate School
of the University of Maryland in partial fulfillment
of the requirements for the degree of
Doctor of Philosophy
1985

APPROVAL SHEET

Title of Thesis: The State of Water and Cell Morphology
In Deep Frozen Populus

Name of Candidate: Allen Gene Hirsh

Thesis and Abstract Approved: th. Solomos

Theophanes Solomos
Professor
Department of Horticulture

Date Approved: 6/7/85

ABSTRACT

Title of Dissertation: The State of Water and Cell Morphology in Deeply Frozen Populus

Allen Gene Hirsh, Doctor of Philosophy, 1985

Dissertation directed by: Dr. Theophanes Solomos, Associate Professor
Department of Horticulture

By using differential scanning calorimetry, electron microscopy, light microscopy, and freezing survival experiments, it is shown that superhardy Populus balsamifera v. Virginiana (Sarg.) is capable of withstanding liquid nitrogen (LN_2) temperatures because of the formation during cooling, at a temperature of about -30°C and cooling rates less than 30°C/hr, of aqueous glasses in the intracellular solutions.

In more detail, the major findings concerning the state of intracellular water are: (1) the bulk of the intracellular contents go through an equilibrium glass transition at about -28°C during slow (<5°C/hr) cooling; (2) smaller additional amounts of intracellular material go through equilibrium glass transitions at about -47°C and -70°C; (3) as a result of the resistance to homogeneous nucleation of these glass forming intracellular solutions when they are in equilibrium with extracellular ice at $\leq$-20°C, cooling/warming at any combination of rates from 3°C/hr to 1200°C/min between -20°C and -196°C is non-injurious to fully hardened wood; (4) death associated with quench cooling in LN_2 from -15°C is correlated with the devitrification, (cold crystallization) near -90°C upon warming of the very low temperature glass forming component, followed by further devitrification of the higher temperature components, especially between -30°C and -20°C; and (5) the vacuolar compartment appears least resistant to devitrification and capable of thereby causing death even when the cytoplasm resists devitrification.

In addition, it was found that when fully superhardy wood is cooled slowly (3°C/hr) after being imbibed with water (doubling total water content) massive intracellular freezing occurs. Despite the fact that total tissue water of tender Populus (summer wood) is 2x that of the artifically water loaded hardy wood on a gram H_2O/gram dry weight basis, tender wood cooled at 3°C/hr to -50°C does not display intracellular freezing. It is killed by -2°C. It is shown that in both tender and hardy wood <10% of water is extracellular. Thus a significant excess of extracellular water appears to cause intracellular freezing and this may be a major reason for the large water loss seen in the fall 'hardening off' of most temperature zone woody plants.

It is also shown that during slow cooling, the plasma membranes of both hardy and tender Populus cells stick to and collapse the cell wall, but that these membranes stay smooth in the case of superhardy cells and wrinkle markedly in the case of tender cells. Membrane-associated particles appeared to clump in the membranes of slowly cooled tender cells but not in the slowly cooled hardy cells.

Key words: cell morphology, freezing, freezing stress, cold hardiness, Populus, glass, DSC, membrane stress, freeze-fracture, freeze-etch, electron microscopy.

ACKNOWLEDGEMENT

I would not have been able to realize my childhood dream of investigating the mysteries of cold hardiness without an immense amount of friendship and consideration. To Dr. Harold Meryman and Dr. Robert J. Williams, who hired an eccentric nurseryman off the street, and to Dr. Theo Solomos, who sheltered a homeless waif against the terrors of State U., my debt of gratitude is too large to repay. I owe also a special debt of gratitude to Dr. Russell Steere and his brilliant assistant Eric Erbe. Their skilled electron microscopy made an extraordinarily difficult investigation possible. I also want to thank the other members of my committee, Drs. Greer, Goode, Stimart, and Racusen for their time, especially in view of the onerous tome they were first asked to read.

Without the special help and patience of Monica Hufnagel, Longine Wonders, Carol Norsworthy, Mary Douglas, and Dr. Tsuneo Takahashi, all of our lab, I would have foundered in this project at the onset. The awesome task of processing hundreds of photographs would have been impossible without the help of Joe Watson, also of the Red Cross.

A special note of thanks to my friends, Joe Gray and Bob Angell of Potomac Garden Center, good friends who helped me afford graduate school, and let me collect poplar on Bob's property.

A very special note of thanks to Dr. Arthur Karlin, in whose laboratory at Columbia I first learned how difficult and demanding it is to be good.

Thanks to Greg Leon, who made it much easier to brush 16 years of rust off my Fortran, and Jarrett Burton, who introduced me to the world of freeze etch electron microscopy.

Finally, love and thanks to my parents, brother and friends, who encouraged me to begin again.

Table of Contents

List of Figures, Graphs and Plates

Page #

VI Discussion

A. Introduction

A vast amount of work has been done on the causes of freezing injury in higher plants that are not completely resistant to the stresses induced by slow cooling (<.5 C per minute). Numerous workers have pointed to solution concentration (cell desiccation) during loss of cell water to extracellular ice as a major stress (32,40,52,75,93). Other workers have investigated the breakdown of membrane organization during freezing (22-25,28,40,55,56,89). Still other workers have identified supercooling of intracellular solutions, culminating in massive intracellular freezing at some critical temperature, as a major cause of death in some cellular groups of higher woody plants (26,43). This supercooling is made possible by the resistance to passage of ice crystals through the hydrophobic layer of plasma membranes and the well known ability of some liquids (especially water) to supercool several tens of degrees centigrade below their equilibrium freezing point before spontaneously freezing (2,4,61). The latter is called homogeneous nucleation. It occurs well below the freezing point because for a crystal nucleus of radius r the free energy of formation is, to a first approximation, given by:

$$\Delta G_{formation} = - [\Delta G_{bulk}] \times [4\pi r^3] + 4\pi r^2 \times \gamma$$

where: $-\Delta G_{bulk}$ = the free energy of formation of a unit volume of ice from the melt at a temperature below the equilibrium point.

γ = the free energy of formation of a unit area of interface between crystal nucleus and melt.

Since the terms are of opposite sign and different exponential depend-

ency on r, the free energy goes through a maximum and small nuclei tend to be unstable. The detailed kinetics and statistical mechanics are complex and poorly understood (47,61). In the macroscopic environment liquids usually contain microscopic colloidal contaminants that act as catalytic nucleators at temperatures near the freezing point. Living cells are generally free of such nucleators internally (41,55).

Relatively little work, albeit much speculation, has centered on completely resistant (superhardy) woody tissues. These are tissues that do not supercool intracellularly. They may be cooled, when in the winter dormant state, at rates <0.5 C/min to the temperature of liquid nitrogen (-196°C) and then warmed at the same or a slower rate until they thaw and sustain no measurable injury. This ability to withstand slow cooling to and slow thawing from such low temperatures is the definition of superhardiness. These superhardy woody tissues have an additional resistance to cold stress which allows one to speak of different degrees of superhardiness. They can be very rapidly cooled from a high subzero temperature to that of liquid nitrogen and then warmed very slowly without injury. The degree of superhardiness is then defined as the maximum subzero temperature (Tq) at which the fast cool (quench) can commence with no difference in mortality between quenched samples and unquenched controls upon slow warming. Thus one can speak of partially superhardy (lower T_q) vs. fully superhardy tissue. T_q can range as low as -60°C and as high as -20°C in populus in different stages of hardening. Those samples of Populus balsamifera having a T_q of less than -20°C are termed partially superhardy, those with a T_q of -20°C are termed fully superhardy. Presumably this maximum achievable termperature varies from species to species.

Workers who have looked at these tissues (8-10,13,15,37,40-42,48-

50,62-68,70-73) have failed to establish unequivocally even the state of water in these tissues at extreme subzero temperatures, let alone the packing of membranes, or chemical organization of the cytoplasm.

The goal, then, of this thesis work has been to characterize the state of water in deeply frozen tissue of such a superhardy species (Populus balsamifera var. virginiana Sarg.) as a function of cooling rate, water content of the tissues, and state of cold resistance (this plant ranges from total resistance to -196°C in the period from late November to early March to complete cellular destruction at -2°C from early May to mid October).

To accomplish this goal, primarily four techniques have been used: light microscopy, freeze-fracture freeze-etch electron microscopy, thermal analysis, and mortality studies after quench freezing.

Light microscopy allows one to visualize the response of previously stressed and unstressed cells to freezing, vapor phase drying, and dehydrating solutions. This leads to information about what sort of stresses the plant actually faces in vivo, as well as the various strains one might expect from a given stress.

Electron microscopy allows one to observe directly the presence or absence of ice crystals in the tissues and thus can provide evidence of the state of water during freezing stress. It also yields additional information about cell morphology during stress.

Thermal analysis (differential scanning calorimetry, DSC) allows one to quantitatively measure first order (freezes and melts) and/or second order (glass transitions) phase changes occurring in the tissues as a function of cooling and heating protocols. It addresses the fundamental question of whether intracellular water in deeply frozen Populus

is a glass (a solid with 'frozen-in' liquid order), is complexed in crystalline hydrates with water bound by strong dipole - dipole interactions to salts and organic molecules, or is ice.

B. A Short History

In 1970, Weiser (93) wrote a classic monograph on cold resistance in woody plants. In that monograph, he referred to a final stage of hardening which he claimed was induced by temperatures in the range of -30°C to -50°C. This idea he derived from the work of Tumanov and Krasavtsev (37,91). This 'hardening', Weiser claimed, would allow plants to attain levels of cold resistance not normally attained in nature. At about the same time as these Russian workers were investigating the extremes of cold hardiness in woody plants, Sakai and his coworkers at the Low Temperature Institute in Japan were pursuing similar studies (64,70). Sakai came to somewhat different conclusions than Weiser. Sakai found that increased hardening in extremely hardy tissue was not observed at storage temperatures <-20°C. Furthermore, he found that when far northern trees are fully hardy, they could stand slow freezing to any subzero temperature. He also presented evidence that the fully hardened wood of such trees could withstand freezing at rates up to thousands of degrees centigrade per minute if they were first cooled at several degrees centigrade per hour to -20°C or lower. Unfortunately, the evidence he presented was not definitive. He rewarmed the quenched (quick cooled) samples much more rapidly (several tens of degrees per minute or more) than they would thaw in nature (<5°C/hr). He also measured viability in these samples by their ability to plasmolyze (shrink in hypertonic solution) and deplasmolyze without lysing. He conducted the viability measurements immediately after thawing. Since Levitt has shown that hardy cells that are lethally stressed by freezing may yet retain the ability to plasmolyze and deplasmolyze for several days after thawing (41), it is not clear that Sakai was actually

looking at living cells after his freezing experiments. Sakai postulated that the tissue he was working with froze intracellularly when quench cooled from so high a temperature as -20°C and that the quick warming was necessary to prevent the recrystallization of small ice crystals to large ice crystals that often occurs in quickly frozen solutions when they are warmed at a slow rate (47).

Ignoring most of Sakai's work, Weiser surmised that there might be a 'quasi-crystalline' ordering of remaining intracellular water at temperatures of -30°C to -50°C which would make the cells immune to injury from further cooling. He also urged workers to study the problem of the state of intracellular water at low temperatures calorimetrically and spectroscopically, especially by use of (nuclear magnetic resonance spectroscopy, NMR).

The study of water in deeply frozen, very hardy tissue was begun in the mid 1970's using NMR (13,15,26,27) and continues at the present time (43,88). This technique proved very useful for measuring the amount of liquid water present in samples down to the temperature range of -50°C to -70°C. However, the very properties of NMR which allow it to measure liquid water quantitatively made water in the solid state invisible to the techniques then in use. This is true whether the water is in the crystalline array or a solid glass because in both cases the spin-lattice relaxatin becomes very long and the spin-spin relaxation very short. Thus the techniques could not be used to distinguish different solid forms of water.

Simultaneous with the use of NMR a large amount of differential temperature analysis (DTA) was being done (7,14). This work provided strong evidence that in many very hardy (but not superhardy) plants, intracellular water of living xylem cells supercools to temperatures

between -20°C and -40°C, and the point at which it freezes is highly correlated with the killing point of the tissue. This method is not quantitative though, and superhardy tissues are display no events on DTA records at temperatures much below the initial freezing point of extracellular water. What little actual calorimetry was done (26,31,32,55) was confined to the accurate measurement of the amount of water frozen at high subzero temperatures in moderately hardy crop plants or accurate measurements of the amount of supercooled xylem water freezing in very hardy plants.

The only other major work on superhardy plants during the period of the last twenty years has been on the characterization of biochemical changes in superhardy trees during hardening (8-10,38,42,62,67,78-83,97). These workers have discovered that there are noteworthy changes in every major type of cellular constituent except the DNA. Soluble protein increases and its composition changes. In general, soluble sugar levels increase, and the lipid composition of the membrane changes. The only biochemically based model is by Levitt (41), whose SH hypothesis of protein-protein denaturation by abnormal S-S bond formation during extreme osmotic stress has not enjoyed experimental confirmation (41).

The suggestion that intracellular glass formation might be an important strategy in these plants appears to have been made only by Williams (94) in this laboratory. He extracted a compound from Cornus stolonifera that has an equilibrium glass transition of -47°C. That is to say, a compound characterized by an aqueous freezing point depression of 47° when the glass transition temperature of the solution is also -47°C. He speculated that this would in fact eliminate osmotic stress

at very low temperatures in the plants, which do in fact resist temperatures below -47°C when cooled slowly.

Concurrent with these investigations of very hardy plants, studies of the physical chemistry of solutions have led to large amount of calorimetric data on glass formation in aqueous systems. This includes studies of inorganic salt solutions (1-5,11,34,36,51), organic polymer solutions (21,44,47,59,77) and theoretical attempts to extend the results of these studies to living tissue (57,58,60). Especially germane to the work reported here are the studies of Franks and co-workers (21). They approached the problem of analyzing aqueous polyvinylpyrrolidone solutions thermodynamically much as I have approached the analysis in the Populus wood: utilizing differential scanning calorimetry coupled with electron microscopy of the solutions.

Another important development of the last several years has been that of freeze-fracture freeze-etch electron microscopy. Numerous workers have applied this technique to the analysis of frozen aqueous solutions (18,39,46,53), and quickly frozen biological tissue, including Populus (19,20,30,54,76,84-86,90). However, studies of slowly frozen tender plant tissue (98), or quickly frozen hardy tissue (69) done specifically to investigate frost damage have utilized the more traditional fix-and-section method of producing specimens for electron microscopy.

This thesis is the first simultaneous application of light microscopy, freeze fracture electron microscopy, calorimetry, and quenching studies to the determination of the state of water in superhardy tissue.

C. Overview of the Study

The characterization of the state of water in the frozen Populus tissue entails determination of: (1) the amount and distribution of water in liquid and solid form as a function of temperature, and (2) the form(s) the water takes as a solid: (a) ice crystal, (b) hydrate (bound water), or (c) glass.

The fact that frost tender Populus in active growth is killed completely by temperatures as high as $-2^{o}C$ means that there is no correlation between either intracellular freezing or intracellular glass formation and freezing resistance in the tender wood. In contrast, superhardy Populus is resistant to temperatures below $-140^{o}C$ at which point all known forms of liquid water have solidified (1,3,5,11,51). Thus the form(s) and distribution(s) of solid H_2O in the frozen wood may be a crucial element in the frost resistance of superhardy Populus.

One can postulate at least five general models by which the Populus could resist extreme subzero temperatures. These in turn lead to six basic questions which, when answered may suggest which of the five models is closest to the actual in vivo situation.

The five models are as follows:

(1) The superhardy cells could lose most of their water and volume during slow freezing to temperatures $\leq -20^{o}C$. Thus they would be tolerant to both extreme freezing dehydration and osmomechanical stress. Freezing dehydration is the loss of intracellular water to extracellular ice during cooling. Osmomechanical stress is the set of forces that build up in cellular structures as a consequence of cellular volume loss due to the equilibration of internal cell solutions to increasing external solution osmolality (such as from increasing ice formation

during cooling). This model implies that large amounts of special water-binding or glass-forming substances are not synthesized during hardening off in the autumn.

(2) The superhardy cells could produce a large amount of hydrate forming (water-binding) material intracellularly during hardening off such that subsequent slow freezing to <-20°C removes all free liquid water from the cells, leaving only hydrate water of greater thermodynamic stability than ice. Since the hydrate forming material has a large mass in this model, it could significantly reduce total loss of cell volume during freezing. Thus this model postulates that the cells' constituents are highly resistant to dehydration (loss of fluid water), and that the cells avoid osmomechanical stress.

(3) The superhardy cells could produce a large amount of aqueous glass forming material intracellularly during hardening off. As a result there would be only a modest loss of volume between 0°C and -20°C. Near -20°C the intracellular solution would become a largely inert glassy solid. This model postulates that the cells avoid both dehydration and osmomechanical stresses by increasing intracellular viscosity during freezing until the glass transition of the bulk of the cell sap is reached at or just below -20°C.

(4) The superhardy cells could allow intracellular ice to form during slow freezing from 0°C to -20°C either by heterogeneous nucleation or by growth of extracellular ice through cell membranes into the cells' interiors. This model postulates that the slow growth of ice into the cells can be controlled so as to cause no irreversible damage. Osmomechanical stress would be avoided.

(5) Superhardy cells could remain liquid intracellularly to temperatures far lower than -20°C but by -20°C the intracellular solution

could have concentrated to such a point that all homogeneous (or heterogeneous) nucleation would be depressed during further cooling. Since all nucleation would be depressed, no devitrification would occur on warming and the cells could be termed perfect supercoolers. Depending on the amount of natural cryoprotectant necessary to effect complete elimination of homogeneous nucleation, the cells might be osmomechanical stress avoiders or tolerators. Since the cells would be supercooled, they would to some extent avoid dehydration stress. The intracellular solutions would go through equilibrium glass transitions at very low temperatures, according to this model.

Several types of organisms appear to use either a combination of models 1 and 2 or model 5 to withstand deep dehydration and/or freezing stress. Brine shrimp, for example, can dehydrate to 1-2% total water content (hydrate water) and remain viable. According to studies by Clegg (16) and Crowe (17), this is due to replacement during dehydration of all non-hydrate water by sugars such as trehalose. These sugars appear to be water-replacing compounds and the shrimp retain only a small amount of hydrate water. This is a combination of aspects of models 1 and 2.

Hardy (but not superhardy) northern trees of the genus Abies appear to undergo partial loss of bud tissue water, allowing suppression of homogeneous nucleation to -70°C (12). This is similar to model 5 but less complete, in that homogeneous nucleation is not completely suppressed.

To distinguish which of the models most closely approximates the actual freezing events in the superhardy Populus, one must answer the following six questions: (1) How is water partitioned between intra-

cellular and extracellular space during freezing and what is the cell volume as a function of dehydration? (2) Is the low water content of the hardened wood necessary for the survival of the tissue. (3) Are ice crystals present in the intracellular fluids of slowly frozen Populus. (4) During a two step cooling procedure consisting of slow cooling to a high subzero temperature followed by fast cooling from that temperature to the temperature of liquid nitrogen, how high a temperature does the second step (fast cooling) have to commence at for there to be ice present in the intracellular fluids, formed either after the cooling or during subsequent warming? (5) How does the formation of ice intracellularly in a two step cooling procedure as described in question (4) correlate with mortality upon thawing the tissue after such cooling? (6) If the intracellular solutions of superhardy Populus resist ice formation during non-lethal freezing, is the intracellular water present mostly as hydrate or as inert aqueous glass; and if the latter, at what temperature(s) are the equilibrium glass transitions?

Biological Materials and Methods

Hardy twigs were harvested and used either fresh, stored at +4°C on moist perlite, or stored at -20°C with ice in a mechanical freezer until ready for use. Experiments were always accompanied by a control. Experiments usually involved two groups of twigs in large-capped polyethylene centrifuge tubes (6 per tube) placed into a Neslab alcohol cold bath (ULT-50 or ULT-80, Neslab Company, Needham, Mass.) and cooled to the appropriate temperature (T*) at 3°C/hr (henceforth always referred to as slow cooling). The experimental group was then plunged into liquid nitrogen with the caps removed from the tubes so that the liquid was in direct contact with the twigs, or, if it was plunged into dry ice, the twigs were directly buried in dry ice. In LN_2, boiling ceased in <10 sec so that the estimated cooling rate was $\geq$1,200°C/min. This rate was further corroborated by inserting thermocouples into the cortex of the twigs and measuring the cooling rate with a Bailey Bat 10 digital thermometer (Bailey Instruments, Saddlebrook, N.J.), 5 sec response time. It was found to be 1200°C/min from -20°C to-144°C. The twigs so quenched were then either (1) immediately reinserted into the Neslab bath at T* for fast rewarming to the bath temperature (10°C/min as measured by thermocouples in the twigs), (2) stored either in dry ice or LN_2 depending on the experiment, then reinserted into the bath after the bath was warmed to a higher temperature at 3°C/hr or (3) stored as in (2), then reinserted after the bath was cooled at 3°C/hr to lower temperature. These slow changes were required because the control samples remained in the bath throughout. Thus most comparisons were between samples frozen at <5°C/hr and samples frozen at 1200°C/min.

For fully superhardy Populus (for definitions of partial and full

superhardiness see page 2 of Introduction), slow freezing to -70°C and subsequent slow warming results in almost zero mortality and it appeared unnecessary to have a third unfrozen control. After reinsertion into the bath, both sets of twigs were slowly warmed until thawed (or occasionally warmed as fast as the bath would go at 1/2 to 1°C/min) and then placed in wet perlite in beakers covered with parafilm and stored for no less than 2 days at +4°C before being moved to a well lit shelf at room temperature. Mortality and growth were monitored for three to five weeks by observation under the dissection microscope and by plasmolysis-deplasmolysis in 1.25 osmolal $CaCl_2$ solutions in a light microscope. The latter was often recorded on videotape. Simultaneously, the maturation of buds and/or callosing (growth of undifferentiated tissue) was monitored during this period. The callose could be easily distinquished at 50x in the dissection microscope by the gradual appearance over a period of several days of piles of large disorganized cell masses protruding from the cut end or sides of the twigs.

Since the statistical comparisons were pairwise, an exact probability test based on the Polya Urn model was devised. The latter refers to the probability of picking n live twigs and m dead twigs out of an urn containing A>n live twigs and B>m dead twigs if the picking is done without replacement. Thus the null hypothesis was that both experimental and control observations came from the same group with a total mortality that of experimental plus control. A computer program was written calculating the probability of choosing the observed experimental group from such a larger group plus the probability of choosing all less likely groups. The test is thus two tailed.

The equation for the probability of choosing a particular set of n,m is:

$$\frac{(n + m)!\ A!\ B!\ ((A + B) - (n + m))!}{n!\ m!\ (B - m)!\ (A - n)!\ (A + B)!}$$

The Fortran program for the computation for this expression plus all less likely events is shown in Appendix II.

Appendix I describes the experiments in detail. It gives the dates of collection, storage temperatures and exact thermal treatments for all quenching experiments. It displays the results of the statistical tests which were performed on the callosing/budbreak data and the mortality data.

Materials and Methods for DSC

(A) Theory: Differential scanning calorimetry is a technique, developed originally by the Perkin Elmer Corporation of Norwalk, Connecticut, for measuring the power necessary to keep an experimental sample isothermal with respect to a reference sample when both samples are being heated or cooled at a constant rate. Figure (1) is a schematic of the physical structure of the heart of the measuring apparatus. The heavily outlined figure is the sample pan holder (labeled (A)), a platinum cup. The rectangular regions (labeled (B)) containing the symbols R_S and T_S on the left, and T_R on the right represent the sample pans. These are aluminum sample holders, one type of which can be sealed against up to 3 atmospheres of pressure by simply crimping an aluminum top over it. Thus accurate measurements can be made on volatile materials. The region labelled R_o is the region of contact between the sample pan and the sample pan holder. Usually, this is largely a thin air space (the area of actual metal to metal contact is small because the bottoms of the sample pans are not perfectly flat). Immediately below this region, in the area labelled T_p, are temperature sensors (small amplitude saw-tooth labeled (C)), which are highly accurate platinum resistance thermometers, and the resistance heaters (large saw-tooth labeled (D)). Both of these are located just beneath the floor of the platinum sample pan holder. The large rectangle enclosing the two cups represents the large aluminum block heat sink. This is held at liquid nitrogen temperature during studies conducted at temperatures below 0^oC. The R's represent various thermal resistances (unit = degrees/unit power). Thus R is the resistance of the heat conduction path from the platinum cup to the heat sink, R_e the source

Figure 1

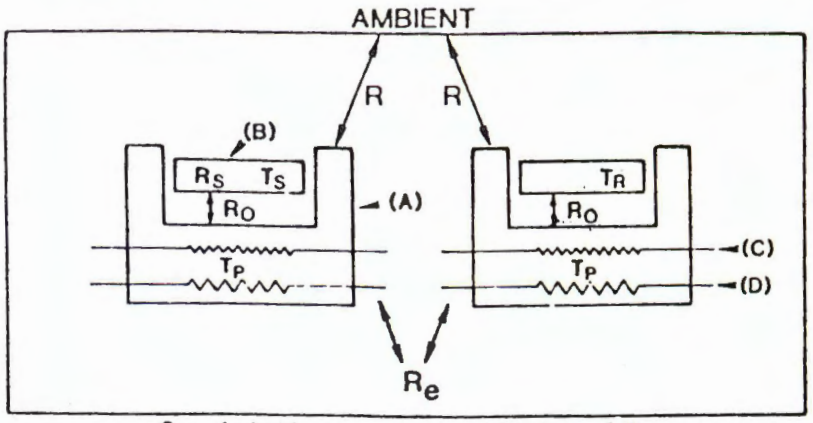

Sample holders, sensors, and heaters of the Differential Scanning Calorimeter

Figure 1 Schematic of Differential Scanning Calorimeter.

A - Platinum sample holding cup

B - Aluminum sample pan

C - Pt resistance thermometer (sensor)

D - Ohmic heating element

R - Thermal resistance of holding cup to surround

R_s - Internal thermal resistance of sample

R_o - Thermal resistance of sample pan-holding cup contact

T_p - Temperature of sensor

T_r - Temperature of reference sample

T_s - Temperature of experimental sample

Figure reproduced with permission of Perkin Elmer Corporation, Norwalk, Connecticut.

resistance of the electronic circuits, R_o the resistance from the sample pan to the temperature sensor, R_s the internal resistance of the sample.

The system maintains isothermality between sample and reference by reading the average voltage of the two sensors 60 times per second and comparing each reading to a reference voltage determined by a clock in the microprocessor unit of the DSC. The clock is ramping the reference voltage between the starting and final voltages of the scan so as to provide a highly linear ramp of temperature at the rate set by the experimenter. Since the platinum resistance thermometer has accurately known resistance values at any temperature at which the machine operates, the high gain amplifier is programmed to use the difference between the average voltage of the thermometers and the reference voltage to increase or decrease the voltage to the heaters so as to bring the $\triangle V$, the average voltage the minus the reference voltage as close to zero as possible. In between these adjustments of the average voltage of both samples to the reference voltage of the temperature ramp, and also at 60 times per second, the difference in voltage between the sensors is fed into an amplifier and current is supplied to both heater circuits so as to minimize the difference in voltage between the sensors. The amount of current needed may be more in the sample than the reference, or vice versa. In either case, since the resistance of the heater is known to great accuracy, by Ohm's law the differential power between sample and reference necessary to maintain isothermality can be determined directly from the differential current.

This isothermal measurement technique is a great improvement over classical differential temperature analysis. The latter system works by the placing of a sample and a reference in contact with a thermally controlled heat sink and measuring the differential voltage between two

thermocouples, one in contact with the sample, one with the reference. Since the temperature difference between the sample and reference is a complex function of absolute temperature, geometry, and any phase changes the sample is undergoing, quantitative information is often impossible to obtain from the older systems.

The question of the sensitivity of the DSC measurements to sample thermal resistance is crucial. To analyze this we first note that the temperature of each sample obeys the heat equation. To the extent that the two sets of heat sources (the resistance heaters in each cup and the experimental and control samples themselves) can be considered sources and/or sinks with each set in an approximately spherically symmetric heat conducting environment, the following equation holds:

$$W_t(r) = -\frac{1}{R_d} \times \frac{\partial T(r)}{\partial r}$$

where $W_t(r)$ = power flow at radius r

R_d = resistance to heat flow per unit distance

r = radial distance from source/sinks

$T(r)$ = absolute temperature at radius r

For small devations from isothermality between the two sets of sources the differential temperature and power flow from the two sets of sources to the sensors can be shown to obey the following equation:

$$\Delta T = W_s (R_s + R_o + R) + W (R_o + R)$$

ΔT = differential temperature between the two sensors

R_s = thermal resistance of experimental sample

$R_o + R$ = thermal resistance of the rest of the system (symmetric with respect to both sets of samples)

W = differential power flow from the two heaters

W_s = differential power to or from the control sample and experimental sample

Since this system is locked into a negative feedback loop, the following is also true:

$$W = -K\Delta T$$

Where K is the feedback amplifier gain. In other words, the differential power output of the sample heater vs reference heater is proportional by way of the feedback loop to the temperature difference sensed by the sensors. Algebraic rearrangement yields:

$$W = -W_s \frac{\left[1 + \frac{R_s}{R_o + R}\right]}{\left[1 + \frac{1}{(R + R_o)\,K}\right]}$$

This is <u>not</u> the equation Perkin Elmer publishes in its technical explanation (Thermal Analysis Newsletter No. 9, 1970, Perkin Elmer Corp., Norwalk, Connecticut). They assume R_s, the internal resistance of the sample is much less than R_o (they set it equal to zero), which in turn is much less than R. Under those circumstances, which <u>are</u> true for most samples, $W = \sim -W_s$ for a large K, i.e. a high gain amplifier, and a large R, which is how the system is engineered. Even if R_o is large, the machine will yield accurate results as long as $R_s << (R_o + R)$. Frozen wood, unfortunately, has a large R_s. Thus, one can see that the heater will tend to put out too much power. This can be seen clearly when the ice to water melt (ice is a poor thermal conductor) is used as a temperature and enthalpy standard. Even at scan rates as low as 10°C/min the machine will sometimes produce nearly 3 times as much power as it should to melt the water. It is not a repeatable phenomenon from sample to sample though, because the thermal contact between the sample pan and

the ice is variable. If the contact is good, the accuracy for the melting of ice is usually $\pm$ 1%. Of course, this introduces a note of uncertainty into the calculations done on the wood samples. For the slow scans ($\leq 5^{\circ}C$/min) the results with ice are acceptable, but often appear to overestimate enthalpies by 10-15%. At warming or cooling rates higher than that the calculation of enthalpies or glass transitions must be viewed as possible overestimates. Since the control substances were all run as water solutions, and most of them yielded reasonable results, I believe that most of the biological enthalpy calculations are good rough estimates. Nevertheless, when energy readings appeared too high after data analysis of these samples, conductance problems were assumed.

The differential current readings, which are proportional to the differential power, are fed through an electronic signal processing unit that averages approximately 30 readings at a time, to a microcomputer. They are then displayed on a power vs. temperature graph in real time on a video screen. After the scan has ended these data can be stored permanently on a magnetic disk and manipulated by means of Perkin Elmer software (TADS Standard Software Kit, P.N. 0419-0355, Perkin Elmer Corp., Norwalk, Connecticut), written in Basic. The TADS software allows one to rotate the curve through an angle θ, expand the power and temperature scales, integrate peaks to obtain enthalpies, calculate the ΔC_p of glass transitions and compare two curves simultaneously. Since the slope of a curve on a power vs. temperature scale is physically meaningful, representing $\frac{\partial Cp}{\partial T}$, the rotation of the curve to eliminate machine generated slope (systematic bias) must be done with caution. If a slope comparison is to be made between two curves that have been so

manipulated, it is best to normalize them, if the masses of the two samples were different, and then align those portions of the curves wherein the samples could have been expected to have the same specific heat capacity. These cautions do not generally apply to the integration of peaks or the determination of the ΔC_p of a glass transition.

(B) Preparation of Samples: If the samples were control substances such as aqueous $CaCl_2$, or aqueous PVP, then aliquots were placed in sealable aluminum sample pans (P.N. 0219-0062 Perkin Elmer Corp.) and sealed with a crimper press (P.N. 0219-0048, Perkin Elmer Corp.). The sealed sample pan was then weighed on a Cahn Electrobalance (Model G, Cahn Instrument Co., Paramount, Calif.). Since the water in these samples is volatile, the sample pan was generally left in place on the scale for ten minutes to test its seal. After weighing, the sample pans were transferred to the platinum sample pan holders of the DSC-4 and control of the temperature was accomplished using the DSC microprocessor and microcomputer controls. Concentrated sealed samples were sometimes stored for up to 7 days at room temperature, and, as long as there was no significant weight lost, sample behavior was studied over this period.

Despite the fact that water poses theoretical problems as a temperature and enthalpy standard, the fact that all biological samples were essentially aqueous solutions required the use of double-distilled water as a standard. The problems involved with that are discussed in Materials and Methods Section (A).

If the samples used were dilute polymer solutions and it was desired to measure highly concentrated solutions, an aliquot of dilute solution was loaded in an open sample pan and allowed to evaporate water

until the weight of remaining sample indicated that the proper concentration had been attained. The samples were then rapidly sealed and subjected to the normal weighing procedure.

If the samples were unfrozen wood, they were treated as if they were aqueous solutions of dilute polymer except that they were blotted dry of adhering water before weighing.

If samples were frozen (stored) wood they were treated in two different ways. If it was desired to measure in a sealed sample pan, then the wood was fractured in a dry ice environment and loaded in a sealable pan sitting in a small concavity of a block of dry ice taking care to exclude dry ice from the pan. Then the top of the pan was put in place and the pan was transferred to the precooled base of the crimper. Dry ice was then piled over the covered pan and crimper base so that the sealing plunger would contact the sample lid by passing through dry ice. Thus, warming of the sample was minimized. If it was desired to measure large samples of wood, larger, unsealable aluminum pans were used (P.N. 0219-0048 Perkin Elmer Corp.). These were loaded in a dry ice environment and unsealed aluminum covers were placed over the wood samples. The samples were subsequently held in the DSC at $-50^{\circ}C$ or $-30^{\circ}C$ to drive off traces of dry ice. All sample pans containing frozen wood were transferred to the DSC-4 sample pan holders in blocks of dry ice.

The DSC was often used as a drying oven for the biological samples at the end of a set of experiments. This was possible because the machine is easily capable of attaining temperatures in excess of $500^{\circ}C$ even with the heat sink at $-196^{\circ}C$. Thus, curves of the samples as completely dry samples could be recorded shortly after the experiments on live tissue. This could even be done on sealed samples by poking a

pin hole in the aluminum cap.

If biological samples were initially frozen they were generally weighed quickly after thawing at the end of an experimental sequence. There exists a supplement to the TADS software that allows one to change the stored weight of the sample after a permanent record of the run has been made, so this proved to be a reasonable, if inconvenient, procedure. On many records, however, this weight has not been recorded. Those records are identifiable by a default weight of 1.00 mg. Thus, calculations done on those curves include implicit division by a normalizing factor of 1.00 mg and, therefore, yield absolute energy or heat capacity changes.

Materials and Methods for Light Microscopy

Light microscope studies were performed on a Bausch and Lomb 'Dyna Zoom' microscope equipped with a cold stage or a perfusion stage and having an 'ultraplane' projection eyepiece. This latter eyepiece allowed the taking of photographs with a Nikon F-2 using Kodak 24-15 technical Pan Film; or of videotapes using a Sony video camera ABC 345 O, and a Sony Betamax SLO-123 videocassette recorder with an 1111 Sony black and white T.V.

Tissue samples for light microscope viewing were cut by hand with a surgical scalpel under a dissecting microscope, or, in early experiments, twig samples were mounted on a small block of wood with Cyanoacrylate glue and 30-50 micron thick strips were cut with a microtome. Hand cutting under the dissection microscope gave more reliable results. Except in one or two experiments cutting was always done longitudinally along the twig and not across the wood fibrils.

The light microscope studies primarily involved placing the slices on the aforementioned perfusion stage and treating them with progressively more concentrated $CaCl_2$ solutions, followed by stepwise reductions in concentration to distilled water again. This was generally recorded on film or videotape. Often the sequence was repeated twice, or large concentration jumps were made to test the compliance limits of the cell membranes.

Populus cells were also stressed by air drying at room temperature. This was accomplished by placing the wet sample slice in the perfusion stage and sucking room air past it while monitoring the drying on videotape. Thus liquid phase plasmolysis versus air drying at room temperature, as alternative models of the loss of water to ice, could be compared.

Materials and Methods for Freeze Fracture Freeze Etch Electron Microscopy

Samples were prepared in several different ways for freeze fracture-freeze etch studies. The traditional method (33) is to cut pieces of plant tissue into small parallelopipeds approximately 1mm x .5mm x .5mm and insert these into gold holders such that fracturing occurs across the wood fibers. We used the holders many times but there was a severe problem associated with them when wood was used as the tissue. The problem was that when fracturing was attempted the deeply frozen wood often did not crack but simply carried the ice that it was imbedded in with it and resided afterwards in one or the other tooth of the holder. Even if the wood did crack, as much as 90% of the time the cracked surface was a microscopic alpine nightmare of jagged wood fibers that produced immensely distorted replicas which subsequently disintegrated during acid cleaning.

Thus in most early runs material was cracked in the open air at a controlled temperature (using ice or dry ice) and large fractured surfaces of many square mM were produced in this way. These were then placed face up in a melted pool of ammonium acetate (freezing pt.= $-60^{o}C$), 40% glycerol-water solution (freezing pt=$-44^{o}C$), or, most recently, 57% glycerol-water solution (freezing at $-80^{o}C$) and surrounded by dry ice (or liquid nitrogen in the case of the 57% glycerol solution). The sample was allowed to freeze in place and etched at temperatures between $-110^{o}C$ and $-80^{o}C$. This produced relatively clean replicas uncontaminated by sublimed ammonium acetate or condensed volatiles of unknown composition. In later runs with 57% glycerol, samples were often cracked under LN_2, then transferred to the freeze etch unit and held at $-110^{o}C$ until a good vacuum was achieved.

Whether samples were cooled at $\leq 1^{\circ}C$/min in the fracturing holders in vials in alcohol baths or quenched to low temperature at several thousand degrees per minute in the holders, if they were in holders fracturing was done in vacuo in a shrouded chamber in the modified Denton D7-3. In the shrouded chamber the estimated vacuum for H_2O is 10^{-9}torr when the external vacuum is 5×10^{-7}torr because the shroud has liquid nitrogen circulating through it and thus acts as a trap for volatiles (33).

Previous to replication samples were usually etched. This was accomplished by raising the temperature of the sample from $-110^{\circ}C$ to between $-80^{\circ}C$ and $-98^{\circ}C$ while maintaining a pressure of 5×10^{-7} torr external to the shroud and allowing any ice to sublime (the rate increases exponentially with temperature because of Clapeyron's relation).

After a period of time varying from 1 minute to 15 minutes the temperature was dropped to $-196^{\circ}C$ and the sample was replicated. Replication was accomplished by evaporating platinum from carbon tip guns, with the evaporation controlled by a resistance monitor which measures the amount of platinum accumulating on a control surface. The resultant Pt replica films were in the order of 2 nm thick and membrane associated particles 5-10 nm in diameter could clearly be seen at high magnification. The platinum films were backed by about 20 nm of carbon evaporated from a second gun, the evaporation being visually monitored on sheets of white paper. The carbon is not electron dense and is added for structural support.

After replication, the chamber was allowed to fill with dry nitrogen gas and the tissue with replica on it was removed to distilled

H_2O, then dilute chromic-sulphuric acid and, finally, after 5 to 10 minutes in dilute acid the wood was dissolved in concentrated acid. Generally the ferocity of the acid hydrolysis broke the replicas into such small pieces that almost all replica surface was lost. Since most replica surface is of cell wall this meant that there was high probability that whatever was salvaged was uninteresting. Until recently only those fortuitous runs in which a large area of cellular cross-fracturing occurred were likely to give good replicas.

Very recently Eric Erbe has perfected a new technique that has allowed us to obtain large sheets of replica of wood routinely (87). Basically the technique consists of coating the newly made replica with 2% lexan,a polycarbonate plastic dissolved in ethylene dichloride, immediately after each replica is made, then allowing the ethylene dichloride to evaporate in a small freezer at about $-10^{o}C$. The replica, now held together by acid resistant plastic, is then run through the acid digestion process to remove the subtending wood.

Once replicas are cleaned in acid and washed in distilled water they are placed on small copper grids with the electron clear plastic collodion stretched over them. These are then placed in a cleaning solution of ethylene dichloride to remove the lexan (collodion is resistant to this solvent).

After mounting on the copper grids all replicas were then placed in a Hitachi HU-12 electron microscope (operated at 80 kev) and examined. If an area was found to be of interest it was photographed at one or more appropriate magnifications. Most of the time the photographs were made in stereo pairs, with one photograph rocked 10^{o} with respect to the other by use of a goniometer stage in the microscope. Photographs were imprinted on Kodak glass electron image plates and are here reproduced

such that all shadows are black, as in nature, and shadows point down to give proper stereo.

Since the primary goal of the electron microscope study was to acertain whether evidence of ice could be seen as a result of a particular freezing stress of the tissue, it is important to state what the criteria were for claiming that there was or was not evidence of ice formation. Essentially the evidence for ice formation is the presence of clustered holes in the replicas which indicate that ice crystals have sublimed away leaving ridges of solidified glassy solution in between them (these have an effective aqueous vapor pressure in the time frame of the etching process many orders of magnitude lower than the pure ice). This has been discussed in detail in the literature (18,53,90).

Biological Results

Figures I and II show the effects on tender and superhardy cells, respectively, of an increasing osmotic stress due to immersion in $CaCl_2$ solutions at room temperature. Note the striking difference in minimum volume between the cells in these two states: <10% $V_{initial}$ for tender cells, 30-40% $V_{initial}$ for hardy cells. This shows that the hardy cells have a far larger volume of solute in the cytoplasm/vacuoloplasm than the tender cells.

Tender cells collapsed upon reimbibing water (deplasmolysis) after exposure to high osmolality indicating destabilization of the plasma membrane. Thus volume information could not be obtained on deplasmolysis of tender cells. The superhardy cells showed no such instability, but they did return to a smaller final volume, indicating a measurable plastic deformation of the cell wall.

Figures III and IV illustrate key results of quenching experiments on partially superhardy Populus (Tq about -30°C) and fully superhardy Populus, respectively. In these experiments, twigs were cooled at 3°C/hr (always referred to as slow cooling) to the desired quenching temperature (where each curve begins on the T axis). Quench cooling (~1200°C/min) was effected by immersion in liquid nitrogen. Controls remained unimmersed and were held at the quenching temperature or were slowly frozen to temperatures $\leq$-50°C. Warming of quench cooled samples was by insertion of the centrifuge tubes into a temperature bath. As can be seen, it was much slower than cooling (~10°C/min). The mortality was complete in partially superhardy twigs (Figure III) if quenching commenced at -20°C. Mortality was 75% but not complete (and marginally distinguishable (P=.045) from the the 45% mortality of control c) when

quenching was from -25°C. Mortality in fully superhardy twigs (Figure IV) with quenching from -20°C was 23% vs. 7% for controls (control b, thawed at 3°C/hr from -70°C after being plunged into dry ice from -20°C) with a P of .35 (not distinguishable). When the quenching temperature of fully superhardy twigs was -15°C, the difference was dramatic with mortality at 100% and $P = 10^{-16}$. This may imply a very large change in the glass forming and ice forming characteristics of the fully superhardy intracellular medium when the equilibrium temperature of the intracellular solutions is shifted from -15°C to -20°C. The probabilities reported here (in both Figures III and IV) are for live twigs versus dead twigs. Comparing partially superhardy twigs showing cell reproduction (callosing/bud break) after quenching from -60°C to those showing cell reproduction after quenching from -25°C (see expt. 11 and 16 in Appendix I), one finds $-25°C \geq Tq \geq -60°C$ for these late autumn twigs.

The results clearly support a Tq of $\geq$-20°C for fully superhardy twigs. If callosing and/or bud break after quenching from $\leq$-20°C is compared with total mortality after quenching from $\leq$-20°C, they are both found indistinquishable from controls and thus the Tq's are the same and probabilities do not support different conclusions as to whether experimental and control groups differ by either criterion. Thus no evidence was seen for an increase in damage (after extreme freezing stress) interfering with cell reproduction as opposed to cell survival.

Another important point is that the fully superhardy material showed no difference in mortality when 10°C/min warming continued from -196°C to the original quenching temperature as opposed to very slow warming after reinsertion at a much lower temperature (such as -70°C). This is illustrated by the P = .81 and P = .35 curves (quench from

$-20^{\circ}C$) on Figure IV. Thus there was no evidence of a warming rate effect at $\leq Tq$.

Tender cells were not examined as discussed above because they exhibit 100% mortality by $-2^{\circ}C$.

A detailed summary of each treatment is given in Appendix I.

Figure I AUGUST 26, 1980

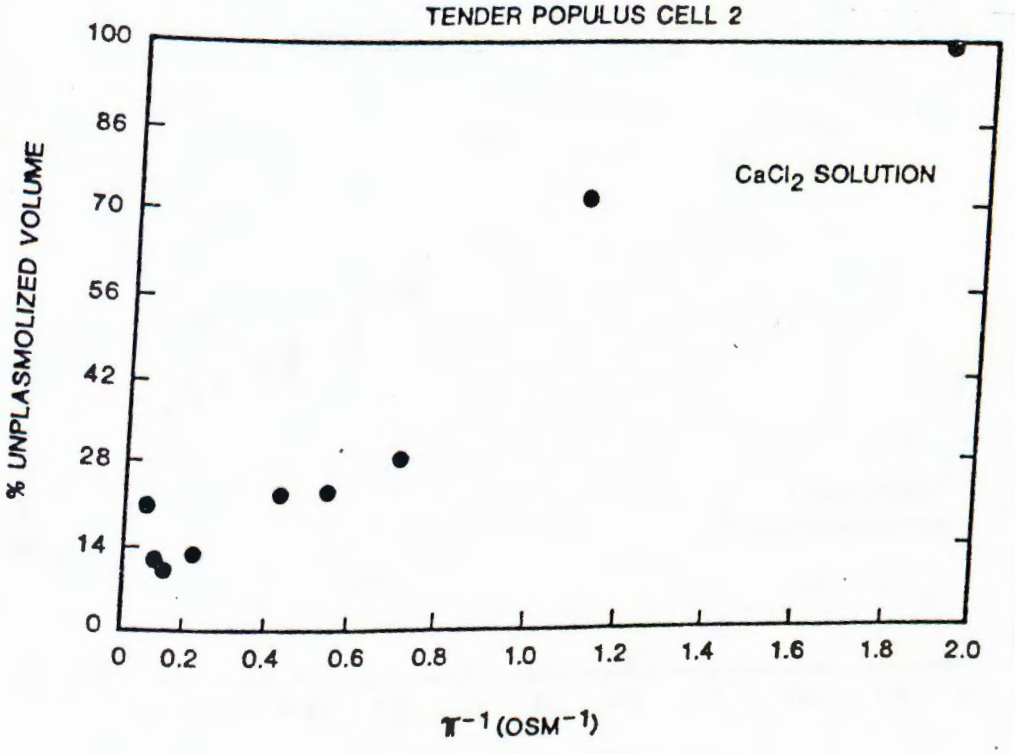

Figure I Biological Results Captions

Plasmolysis in calcium chloride brine of a completely tender cell. Relative volume was determined by measuring area on a photograph and raising it to the 2/3 power. The small rise in the last two points is seen repeatedly in records of this type and indicates loss of semi-permeability (and concurrent expansion).

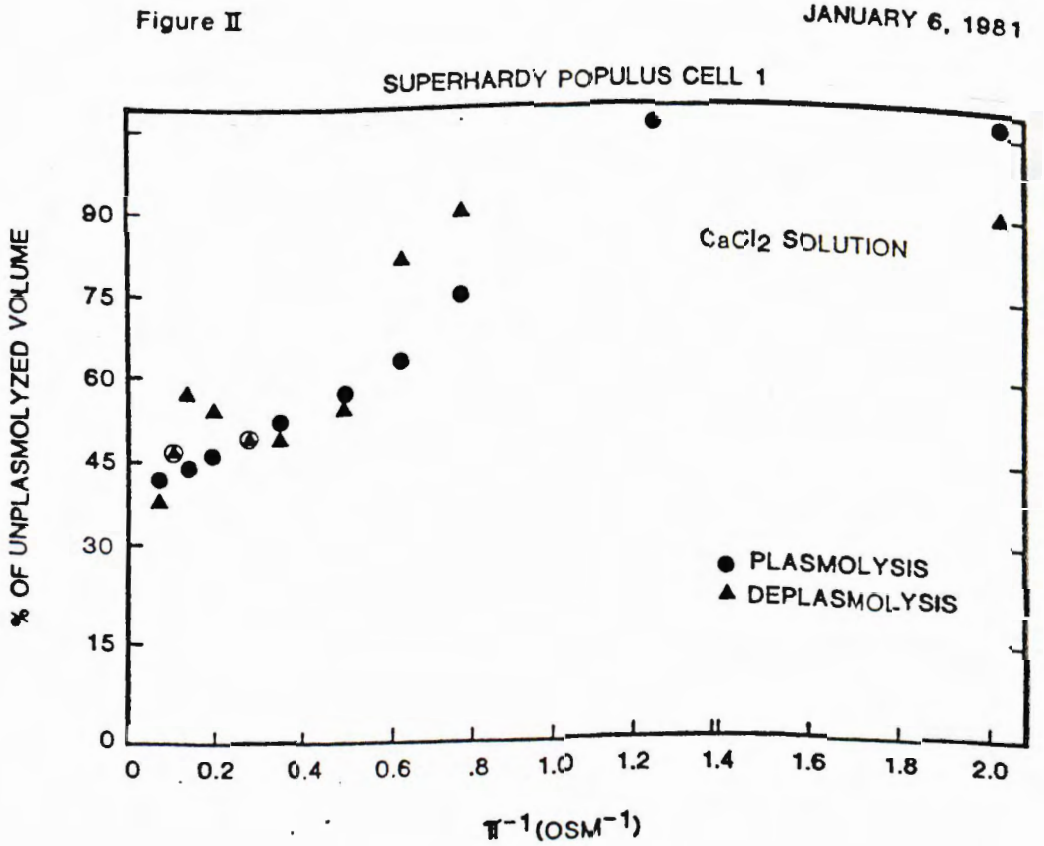

Figure II Biological Results

This is a record of the plasmolysis of a superhardy cell in calcium chloride brine. Volume determined as in Figure I. Note that the asymptote is to a minimum volume value of about 40%. In the tender cell the intercept is to a value of about 5% or less. Also important is the fact that the final deplasmolysis volume is always smaller than the initial volume. This is due to the fact that the cell has pulled the cell wall in during plasmolysis and at the time of the last measurement full relaxation back to the resting volume, even with turgor pressure operating, has not occurred.

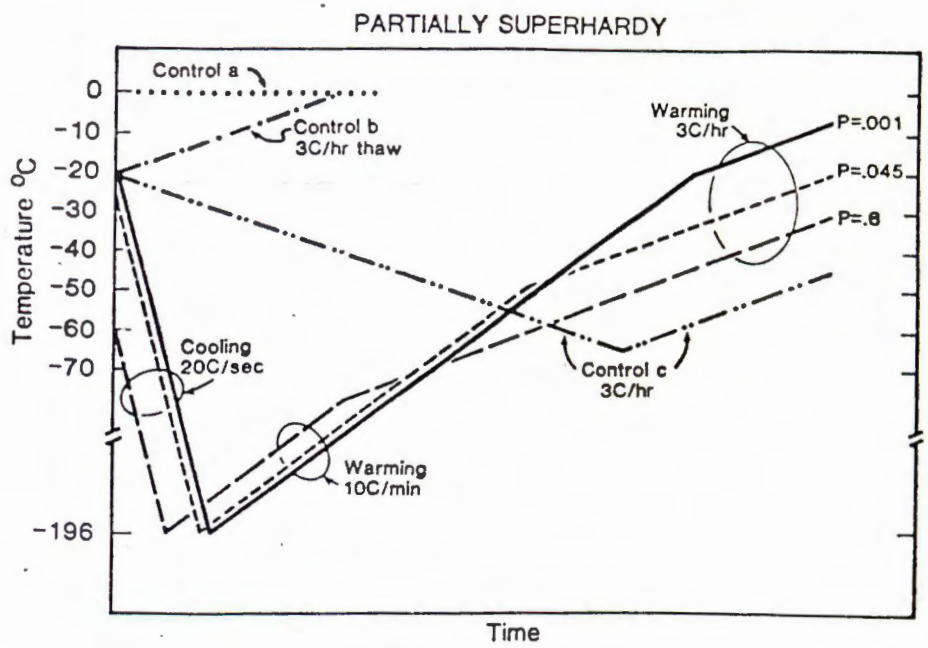

Figure III Partially Superhardy Populus.

The point of origin on the left hand axis indicates to what temperature the tissue was frozen at 3°C/hr. The initial segments of the lines then descend, the slope indicating the rate of cooling to liquid nitrogen. The first set of ascending lines indicates the rate of warming in the alcohol bath. The break in slope in the ascending lines indicates at what temperature 3°C/hr warming recommenced.

The material analyzed here is partially superhardy because when it was quenched from -50°C and reinserted at -80°C then warmed slowly to thaw (long dash line) it showed no increase in mortality above control (P=.6, null hypothesis = no significant difference in mortality between control and experimental samples). When the twigs were quenched from -25°C and reinserted at -50°C for slow warming, the difference between the experimental survival and control was barely significant (P=.045). This is despite the fact that the time allowed for possible devitrification between -50°C and -25°C was 8 hrs. When the material was quenched from -20°C, then warmed so that the total elapsed time allowed for devitrification for the entire range -135°C to -20°C was only 11 minutes, a significant difference in mortality was nevertheless observed (P=.001).

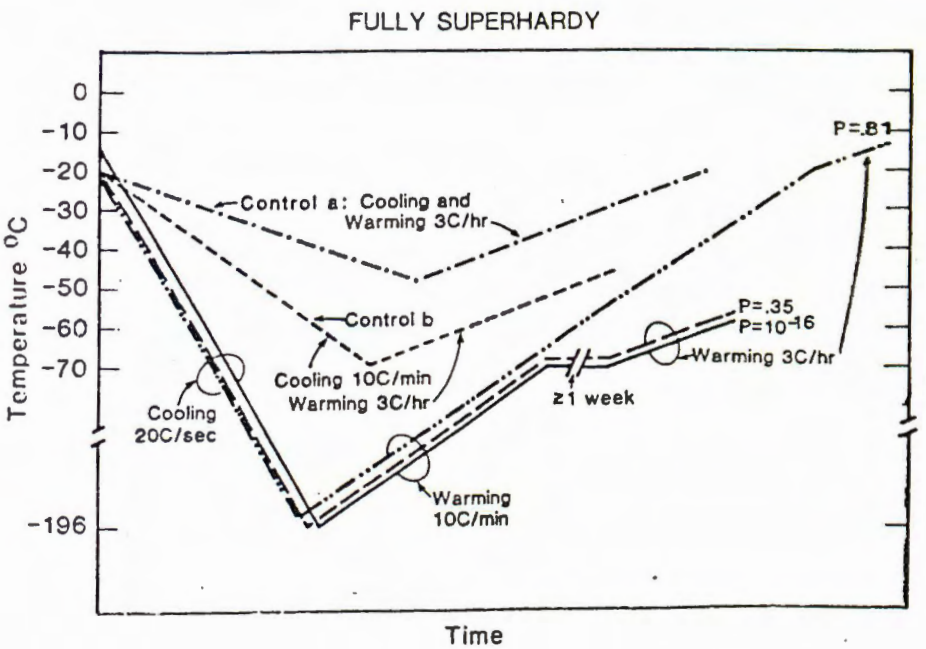

Figure IV Fully Superhardy Populus

The point at which descending curves begin on the left hand axis indicates the quenching temperature: the temperature at which quick cooling began after 3°C/hr cooling. In this case, the dash and double dot dash curves shown material quenched into liquid nitrogen from -20°C while the solid curve shows material quenched from -15°C. The -15°C material was warmed at 10°C/min to -70°C, stored 1 week, then thawed at 3°C/hr. Mortality was complete and highly significant ($P=10^{-16}$). Material quenched from -20°C but otherwise treated identically (dashed curve) had no significant increase in mortality over control (P=.35). Material quenched from -20°C and warmed relatively rapidly back to -20°C also showed no significant damage (P=.81). Thus the instability to devitrification of the intracellular glassy melt begins when the melt composition is in equilibrium with ice at between -15 and -20°C.

Light Microscope Results

Light micrographs (A-E) demonstrate the fundamentally different behavior of the superhardy cells when dehydrated in liquid solution as opposed to vapor phase removal of water. Micrographs (A and B) show that, in both longitudinal and transverse dimensions, cells in osmotically concentrated solutions plasmolyze away from the cell wall. Micrograph (C) shows that vapor phase loss of water causes the plasmalemma to stick to the cell wall and causes the latter's collapse in the center of the cell. Micrograph (D) makes this clearer by showing the vapor phase water depleted cells in a highly concentrated $CaCl_2$ solution. Since no water re-enters the cells in such a solution, the arrangement of the cytoplasm does not change and the tonoplast remains collapsed (presumably with the cell wall no longer stuck to the plasmalemma). Micrograph (E) shows that as water re-enters the cells in a more dilute $CaCl_2$ solution the tonoplast returns to its spherical shape, i.e. reimbibes water. This is followed by immediate lysis of the cells, which does not occur when the cells reimbibe water subsequent to removal by concentrated $CaCl_2$ solution.

Micrograph A

1000x Superhardy Populus cell from a section cut across the grain of the wood (transverse) in osmolal calcium chloride solution. Oval outline is cell wall (cw), arrow shaped outline is plasma membrane (p). Dark mass is clumped chloroplasts (ch), typical of winter hardy cells.

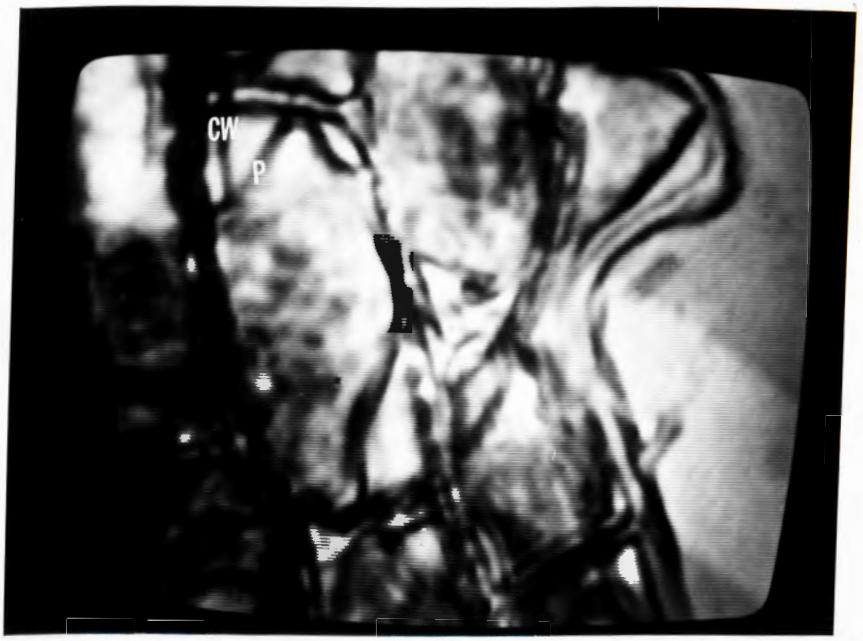

Micrograph B

1000x Superhardy Populus cell from a section cut parallel to the grain of the wood (longitudinal). The rectangular outline is the cell wall (cw), irregular 'hot water bottle' outline is plasma membrane (p). The plasmolyzing solution is 2.3 osmolal calcium chloride. Thus in both transverse (Micrograph (A)) and longitudinal directions removal of water from cells in hypertonic solutions plasmolyzes them away from the cell wall.

Micrograph C

1000x Hardy cells air dried for about two minutes. Ring-like structures are both cytoplasm (c) and vacuole (v). Window-like structures in center appear to contain little cell sap, perhaps they are mostly membranous: tonoplast and plasmalemma.

Micrograph D

Hardy cells air dried (as in (C)) then perfused with concentrated calcium chloride brine (freezing point -17°C). Note that the ring-like accretion of cytoplasm (c) and vacuolar contents (v) has not changed. Note also that the wavy section of cell wall (cw) corresponds to the plasmadesmata invaginations shown in the electron micrographs (Plate series (3)). Thus, when water is not removed by a large volume of hypertonic solution, but by vapor phase loss, the plasma membrane of the hardy cells appear to collapse in one dimension and stick to the cell wall.

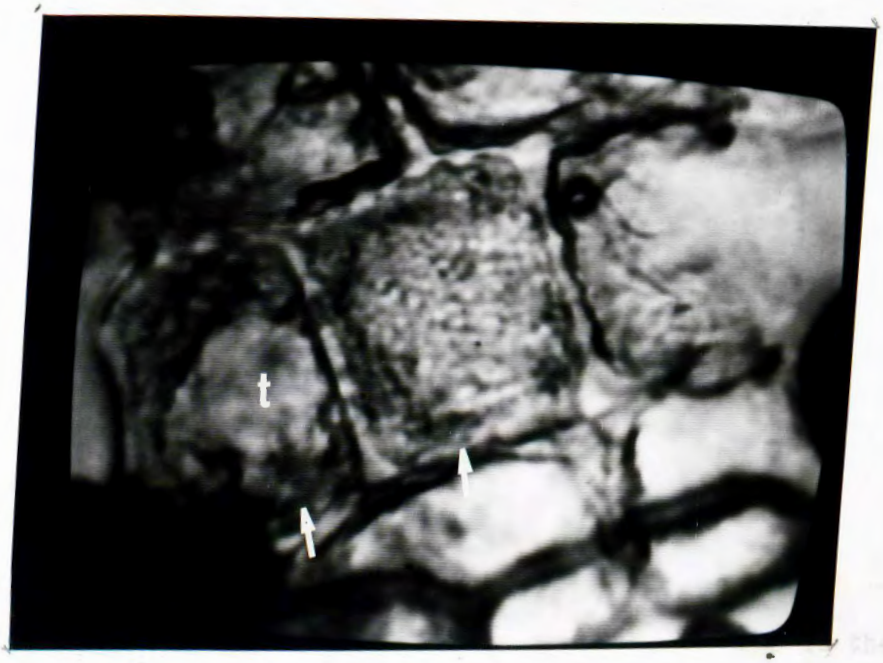

Micrograph E

1000x Hardy cells dried in air (same cells as (C) and (D)), perfused with concentrated calcium chloride brine, now shown in 6% calcium chloride (freezing point -3°C) such that water has re-entered the cells and they have rearranged their internal contents. Cell on far left shows spherical tonoplast (t) again. Both cells (arrows) lysed within one minute, but cells that survive rearrange themselves into shapes like those that have simply plasmolyzed in hypertonic solution. Thus the surface energy relationship between cell membrane and cell wall is deeply modified by the presence of bulk extracellular solution.

Electron Microscope Results

The primary goal of the electron microscope study was to directly assess the presence or absence of ice crystals in tissues, both superhardy and tender, during various cooling and warming regimens. With that goal in mind, Figure set 1 consists of (1) tissue frozen quickly after slow warming to a high subzero temperature: tender vs. hardy; and (2) tissue frozen quickly after slow warming to a low subzero temperature: tender vs. hardy.

Plate (1a) shows tender Populus quenched in LN_2 from 0°C. Since there was no initial extracellular ice, these cells were initially unplasmolyzed. Note that all intracellular compartments are massively frozen. Note especially that the vacuolar ice is coarser, indicating a faster rate of ice growth in the vacuoles during the cooling.

Plate (1b) shows tender Populus quenched in LN_2 from 0°C after infiltration by the cryoprotective solution 25% sucrose/25% glycerol/50% H_2O w/v/v. The magnification is the same as in Plate (1a), but the replica is remarkably different. Note the complete lack of evidence of etching in this sample (no ice crystals large enough to be observed). The proof that this is not due to surface contamination is the crispness of the membrane associated particles, about 10 nm in diameter (30).

Plates (1c) and (1d) show superhardy Populus cooled at 3°C/hr to -6°C, then quenched in LN_2. Slow warming after such a treatment is 100% lethal. Also, thermal evidence (see DSC Thermogram 23) indicates intracellular freezing during fast cooling from -6°C (100°C/min) with additional intracellular freezing during fast warming (50°C/min) from -160°C after fast cooling from -6°C occurring only above -98°C. Thus it is not surprising that the cells represented by Plates (1c) and (1d),

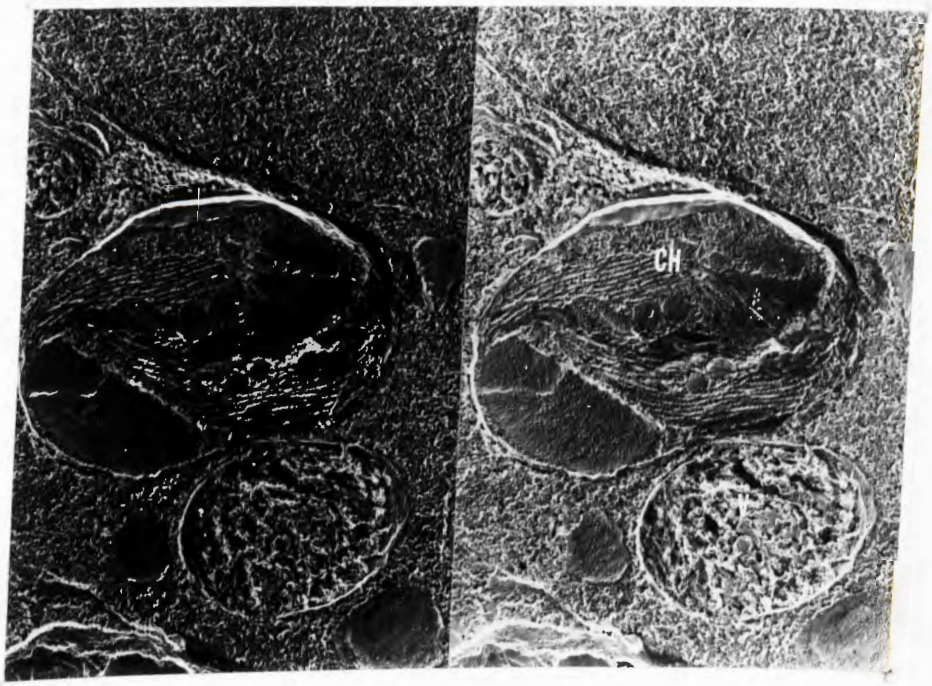

Plate 1a

10,000 X A fully tender Populus cell from approx. 1 mm^3 of tissue plunged into liquid nitrogen from 0°C, then fractured and etched. The cell is frozen throughout. Large elliptic organelle in center of photograph is a chloroplast (ch) fractured perpendicular to its long axis. Immediately below and to the right of the chloroplast is a vacuole (v). Note that the vacuolar contents are much coarser indicating significantly larger ice crystals formed in the vacuole. The size of the ice crystals is 25-50 nm in the cytoplasm and 100-200 nm in the vacuole. This corrugated appearance would not be seen if the sample had not been etched because then the ice would not have sublimed away.

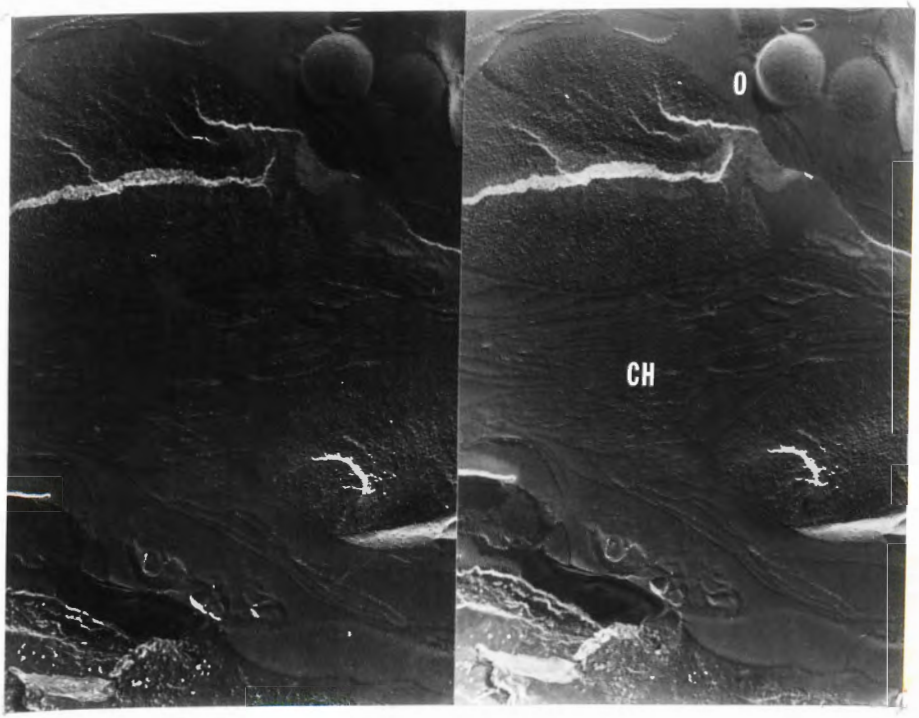

Plate 1b

10,000 X A fully tender Populus cell from a 1 mm^3 sample loaded with a cryoprotective solution of 25% glycerol/25% glucose/50% H_2O v/w/v, then plunged into liquid nitrogen followed by fracturing and etching. The center of the micrograph is a crossfractured chloroplast (ch) with cytoplasm containing organelles (o) at the top of the picture. Note that membrane associated particles are crisp indicating that the failure to observe the corrugated structure seen in Plate (1a) is not due to contamination. The cryoprotective solution plus the normal intracellular contents is either glassy or contains ice crystals so small that the holes they leave when they sublime away during etching are smaller than the 2-3 nm resolution of the microscope.

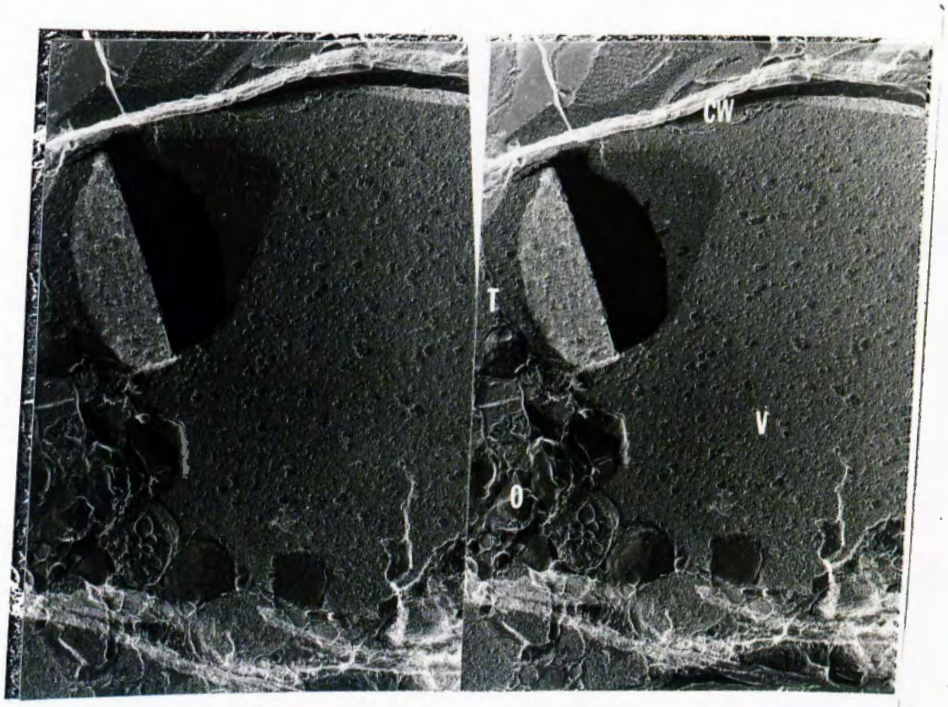

Plate 1c

5000 X A fully superhardy Populus cell from a twig prefrozen slowly to -6°C then plunged into liquid nitrogen for cooling at about 1200°C/min. Here fractured and etched the region on the right of the cell appears to be vacuolar (v) due to the lack of organelles (o). The latter are dense in the lower left of the micrograph indicating a cytoplasmic region there. Cell wall (cw) is evident at both the top and bottom of the micrograph. Along the boundary between the organellar region and the vacuole is the tonoplast, the vacuolar membrane (t). The corrugated texture of the cellular contents indicates extensive freezing. This is shown in more detail in plate (1d).

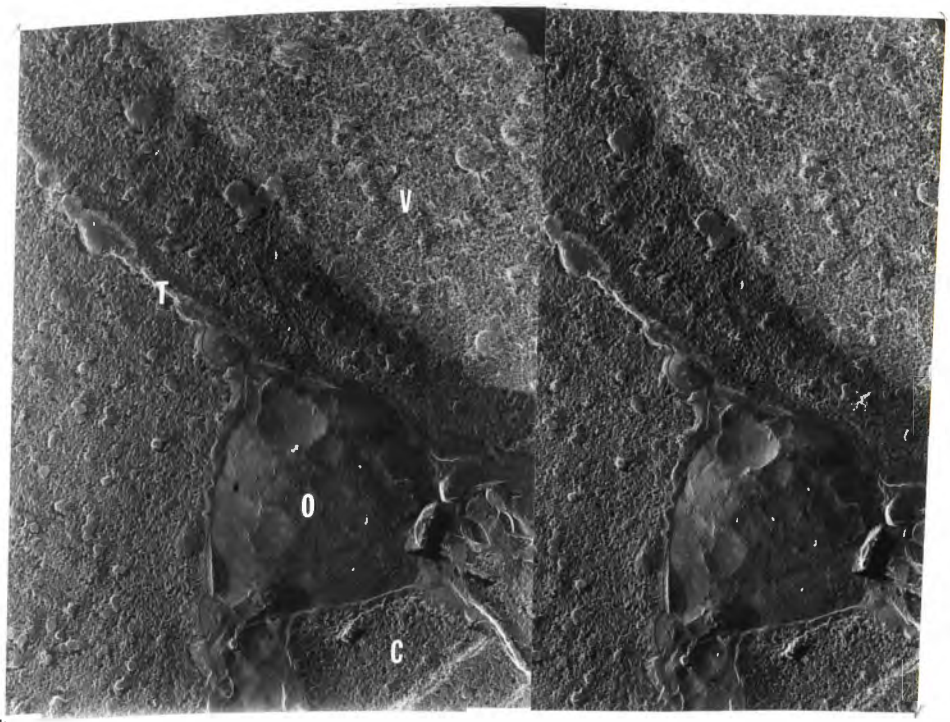

Plate 1d

10,000 X Superhardy Populus cell quench cooled from -6°C (same as micrograph (1c)), then fractured and etched without the temperature ever rising above -70°C. Running diagonally across the plate is the vacuolar membrane, the tonoplast (t). It is in contact with an organelle (o) in the lower right center. Thus the region in the upper right is presumed to be vacuolar (v) and in the lower center cytoplasmic (c). Both areas have the characteristic corrugated appearance of etched solutions full of ice crystals. There appears to be little difference in crystal size between the cytoplasmic and vacuolar compartments.

though never warmed above -98°C during replication, show intracellular ice. Note that Plate (1d) is the same magnification as Plates (1a) and (1b), the quick cooled tender Populus. One can see that the ice crystals in the hardy material are smaller, but not excessively so (~20nm for the hardy vs. ~20-50nm for tender). Thus there is no evidence here that the superhardy cells' cytoplasm is unusually resistant to homogeneous nucleation during quench cooling when initially in equilibrium with ice at -6°C.

Plate (1e) illustrates that extreme resistance to homogeneous nucleation can be achieved by drying fully superhardy Populus at -6°C in drierite (dry $CaCl_2$) until nearly half of the tissue water is removed (50% initial H_2O content to 36% final H_2O content). The material so dried callosed when it reimbibed water (without freezing below -6°C). The material pictured here was quenched in LN_2 from 0°C and never warmed above -98°C. Note the lack of evidence of ice crystals larger than 10 nm either in the cytoplasm or the vacuole. Thus, with about 40% of the water removed from this twig, the equilibrium freezing temperature of this cell appeared to be significantly lower than -6°C and homogeneous nucleation was suppressed.

The second series of micrographs, Plates (2a-i) show tender and hardy material slowly frozen to temperatures $\leq$-50°C, or plunged into dry ice and then held between -70°C and -110°C.

The most important result demonstrated by all of the Plates 2(a-i) is that neither in tender nor superhardy material does one see evidence of intracellular ice. This despite the fact that the tender material is killed after exposure to -2°C.

This is especially evident in the high magnification plate of tender cytoplasm (2c) and the plates of superhardy material (2d) and

(2e, high magnification).

Other notable results in the series 2 plates are (1) the contrast between the amounts of observable extracellular ice in tender vs. superhardy material; and (2) the differences in gross membrane morphology following slow freezing of the two tissue types. Plate (2b) shows in the lower right of the micrograph a section of cell wall in slowly frozen tender Populus. Since the 'lizard skin' appearance is typical of eutectic ridging, and since it does not extend across the adjacent membrane surface (ruling out contamination), it is assumed to be evidence of a high cell wall water content (while in the frozen state). This can be contrasted with Plate (2i) which portrays a similar picture of fractured-through membrane and cell wall in the superhardy tissue. Note the sparseness of eutectic ridging of a sharp, elevated nature on the cell wall. This implies that the amount of extracellular ice is far less, as one would expect of tissue with 4x less water to start with on a gram per gram dry wt. basis.

The matter of plasmalemma configuration is crucial in providing (1) a possible estimate of loss of cell volume during freezing; (2) a picture of differential membrane responses to osmotic stress; and (3) information as to whether the cells stick to the cell wall, causing it to undergo viscoelastic collapse during freezing. Thus Plates (2a) and (2b) clearly show a pattern of deep plasma membrane wrinkling in the deeply frozen tender tissue. It is difficult to ascertain whether the cells stuck to the cell wall in the direction perpendicular to the fracture, but it is clear that they did so completely in the plane of the fracture. It is not possible to estimate cell volume loss from these photographs alone. In addition to the wrinkling which is a sign

of strain in the membranes of tender Populus, one sees a significant occurrence of particle free patches in the membranes (Plate (2c)).

Cell surface configuration in the superhardy cells after slow freezing is illustrated by Plates (2f), which is looking into a cell, and (2g), which is looking from inside the cell out. In both cases the cell membrane is invaginated inward between the plasmadesmata fields, as is the membrane of deeply frozen tender cells, illustrated in Plate (2b). The question is whether this invagination is deeper than the natural invagination of the fields in the unstressed cells (note cell wall edges in light micrographs (D) and (E)). The light micrographs indicate a depth of about 1 micrometer and that is about the depth indicated by the magnification in Plates (2f) and (2g). This shows that the cell membrane is sticking to the cell wall and the whole structure is collapsing in, as is also seen in the light micrographs of air dried material. In other words, if the plasma membrane moved away from the cell wall the part of the membrane still attached to the plasmadesmata would be a deep funnel shape. This evidence is further corroborated by Plate (2h) which again illustrates two completely superhardy cells, slowly cooled to -70°C, showing no detachment from the cell wall in the plane of fracture.

To summarize: Plate series 1 and 2 show that (1) quench cooling of hardy and tender cells from temperatures $\geq$-6°C produces massive intracellular freezing, with ice crystals larger in vacuolar structures; (2) slow freezing to temperatures $\leq$-50°C produces no intracellular freezing in either tender or superhardy material, despite death of the tender material by -2°C; (3) some cells of the superhardy material are resistant to the formation of intracellular ice by fast freezing (without subsequent warming above -70°C) from 0°C when about half the

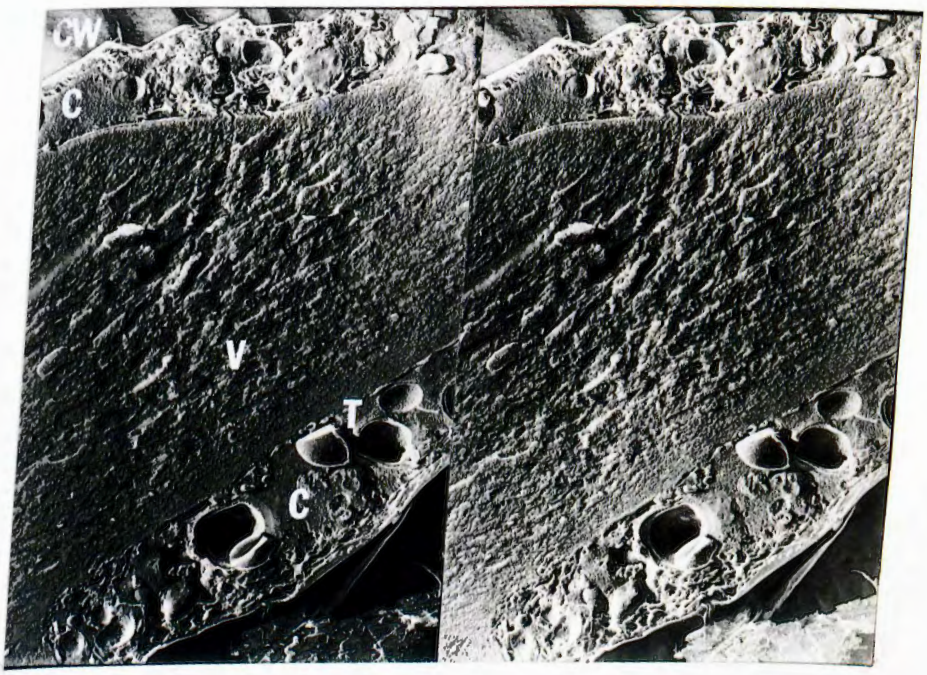

Plate 1e

12,500 X A cross fractured superhardy Populus cell from a twig held 3 weeks in dry calcium chloride at -6°C. The water content of the twig fell from 50% to 36%. Sample was loaded into gold holders in mineral oil to prevent rapid uptake of water before immersion in liquid nitrogen directly from 0°C. The unquenched section of twig reimbibed water and survived. The central region is vacuole (v) surrounded by tonoplast (t). Between the tonoplast and the cell wall (cw) is the cytoplasm region (c) rich in organelles. The cytoplasm appears to be free of ice. The vacuolar contents may have ice in the 5-10 nm crystal size. Certainly any ice crystals are much smaller than any in the cell sap of the normally hydrated cell precooled to -6°C (micrograph (1c,d). Thus this cell was probably in equilibrium with ice at <-6°C.

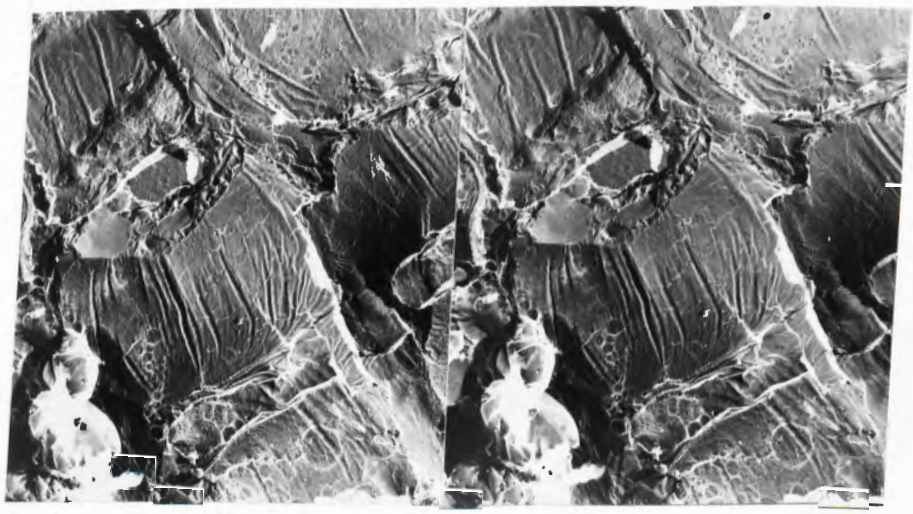

Plate 2a

2000 X Fully tender Populus cells frozen slowly to -50°C before plunging into dry ice. Cell in the center is fractured through at upper right exposing the cytoplasm (c). Note the wrinkled surface of the plasma membranes indicating significant osmomechanical strain. Cells along the top of the micrograph show wrinkling of opposite parity because we are seeing E face i.e. in those cells we are looking from inside the cell at the inner (cytoplasmic) surface of the outer leaflet of the plasma membrane. In this plane of fracture cell membranes have clearly stuck to the cell wall.

Plate 2b

4000 X E face of crossfractured tender Populus cells frozen slowly to -50°C and processed as described previously. Area in lower right is cell wall (cw) covered with what appears to be large amounts of eutectic ridging (er) indicating a high ice content previous to fracture (because the ridging does not extend across the membrane surfaces, contamination can be ruled out). The large pit-like depressions are plasmadesmata fields (p) and the fact that they are the same depth as the complementary cell wall depressions in light micrographs (see Micrograph d) implies that these membranes have stuck to the cell wall. Wrinkling (w) of the membranes under severe osmotic stress is evident.

Plate 2c

25,000x Completely tender Populus (same cells as (2a,b)) frozen slowly to -50°C before plunging into dry ice and later fractured and etched below -70°C. The lower right of the micrograph is the P-face of the plasma membrane (p). Immediately to the left is cytoplasm (c) and organelles (o). Arrows point to regions devoid of membrane associated particles that have presumably formed from slow freezing. Such particle free patches appear to be far more uncommon in the superhardy cells. No evidence of cytoplasmic ice can be seen.

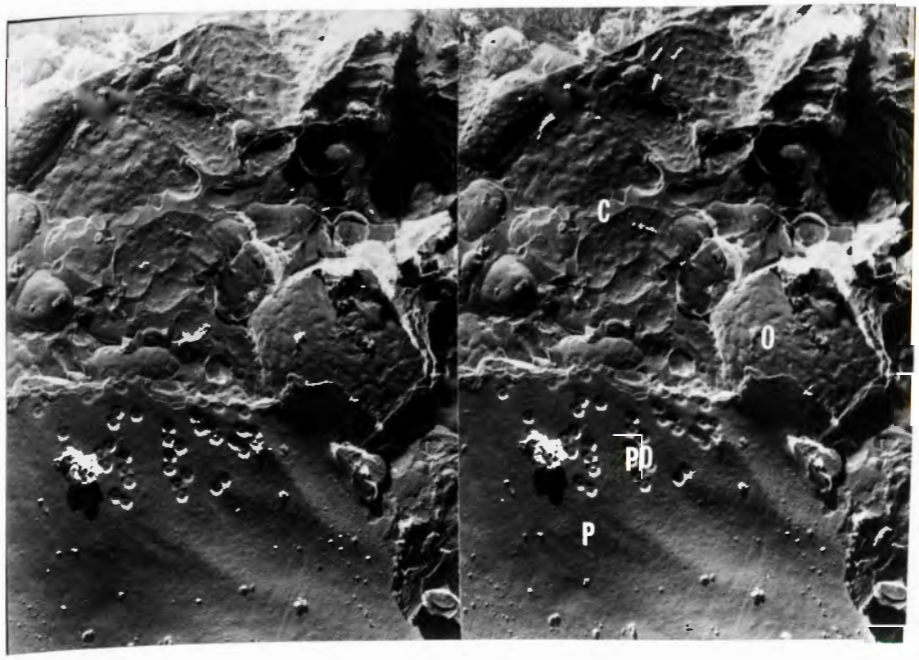

Plate 2d

10,000x Meristematic tissue from completely superhardy Populus frozen slowly to -70°C and stored in dry ice 3 months. This twig survived upon slow warming. Here we see the results of fracturing in air at -70°C followed by 15 min of etching at a relatively high temperature (-80°C). The region in the lower left is P-face of plasmalemma (p) with a plasmadesmata field showing (pd). Note the appearance of the plasmadesmata as pits. Since the region at the top of the micrograph is cytoplasm (c) containing organelles (o), this tells us that the plasmadesmata can be used as orientation devices (looking into to or out of the cell). Note that there is no evidence of etching in the cytoplasm and both the plasmalemma and organellar membranes appear largely unstrained. There appears to be less evidence of membrane associated particle clumping than in slowly frozen tender material (see plates 2a-c).

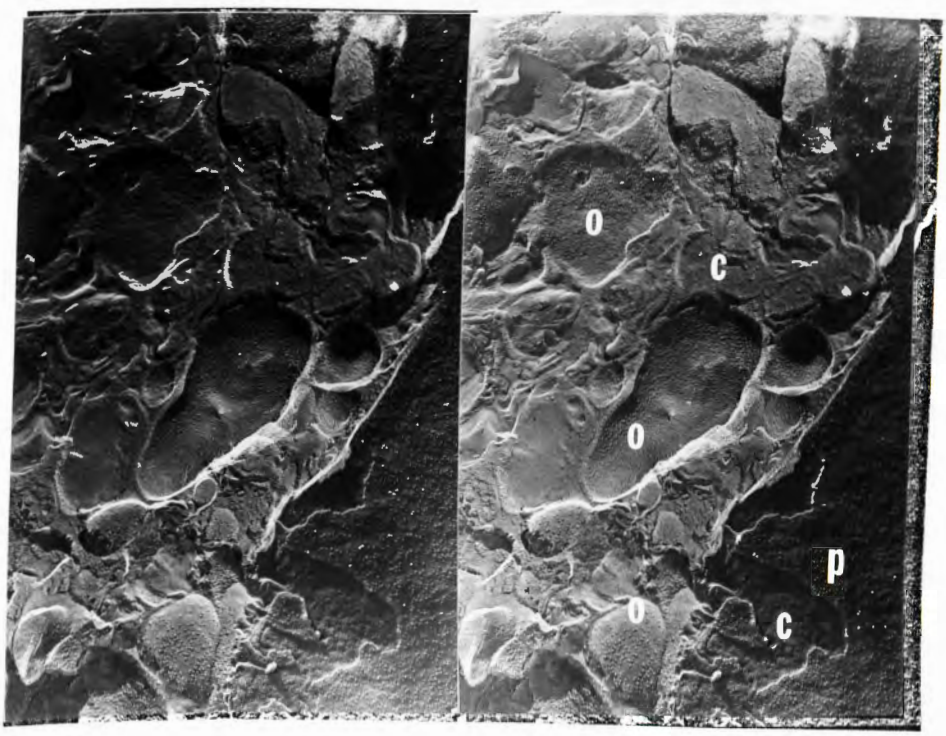

Plate 2e

25,000x Superhardy Populus frozen slowly to -70°C and stored in dry ice for 3 months (from same twig as (2d)). It was fractured in air at -70°C and etched 10 min at -80°C. P-face of plasma membrane (p) is to the right with membrane associated particles clearly not clumped. There is little evidence for such clumping in the organellar membranes (o) and all membrane surfaces appear unstrained. No evidence for etching (ice) in the cytoplasm (c) can be seen.

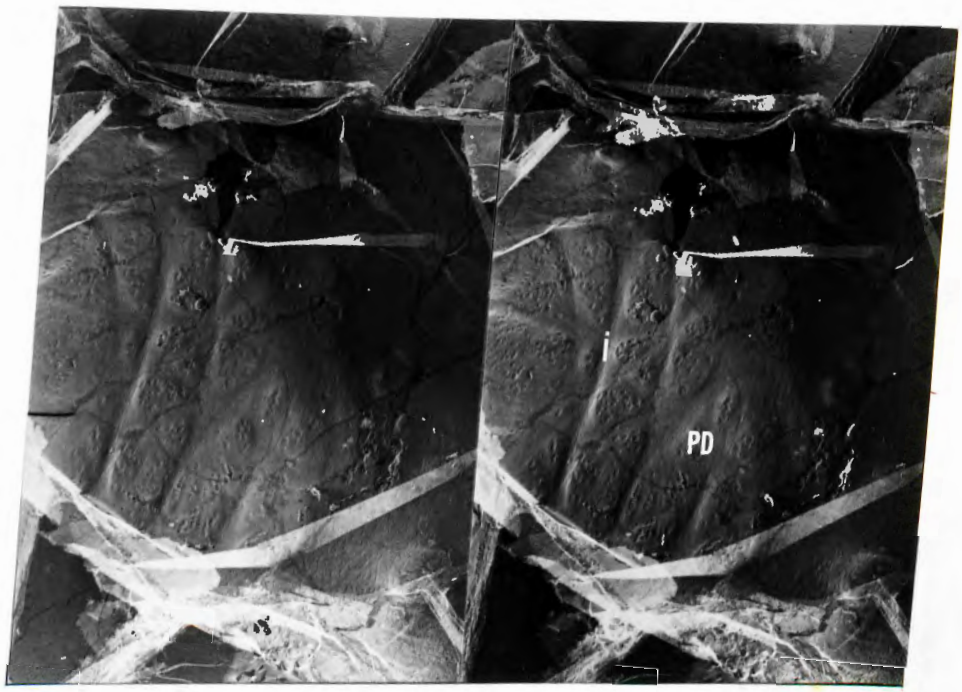

Plate 2f

5000x View of most of a superhardy cell slowly frozen to -70°C. This is plasmalemma showing extensive plasmadesmata fields. The direction is looking into the cell (P-face). Note that the depth of the invagination (i) between the plasmadesmata fields (pd) is not greater than indicated by the light micrographs of unstressed cells. This implies that the cell membrane has stuck to the cell wall during collapse.

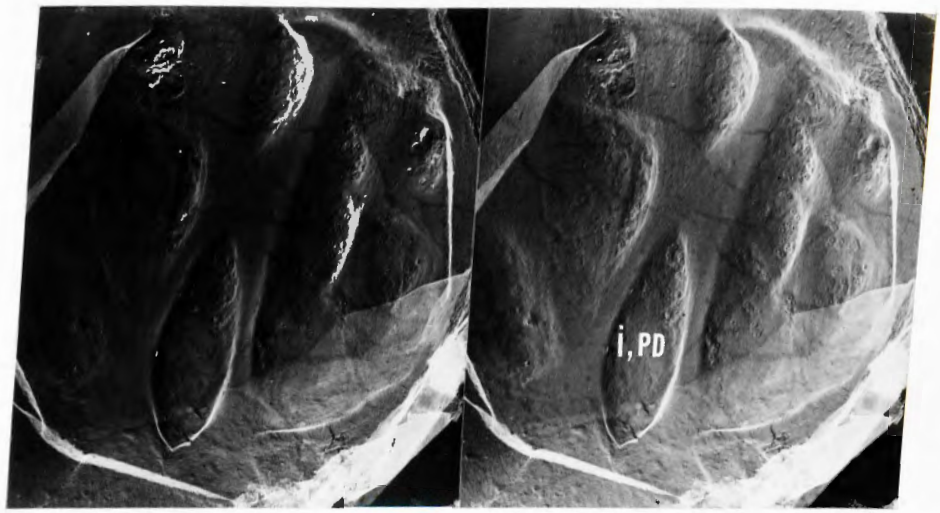

Plate 2g

8,500x Superhardy Populus slowly frozen to -70°C. As in Plate (2f) we see a large section of plasmalemma, but here we are looking from inside the cell out (E-face). Again the depth of invagination (i) of the plasmadesmata fields (pd) implies the underlying membrane was sticking to the cell wall.

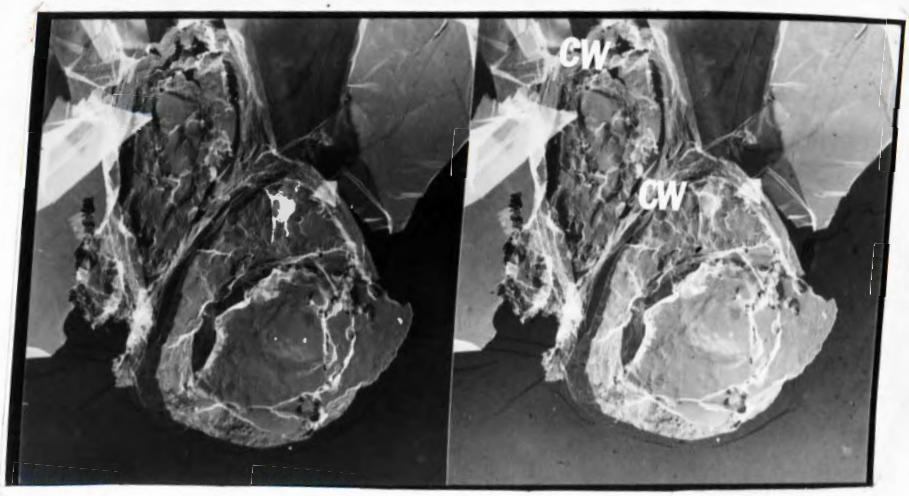

Plate 2h

5000x Completely superhardy Populus slowly frozen to -70°C, then fractured and etched at -80°C for 10 minutes. Two whole cells are illustrated. Note that the cell membranes seem wholly attached to cell wall (cw) in this plane of fracture. This is further illustrated in Plates (2f,g).

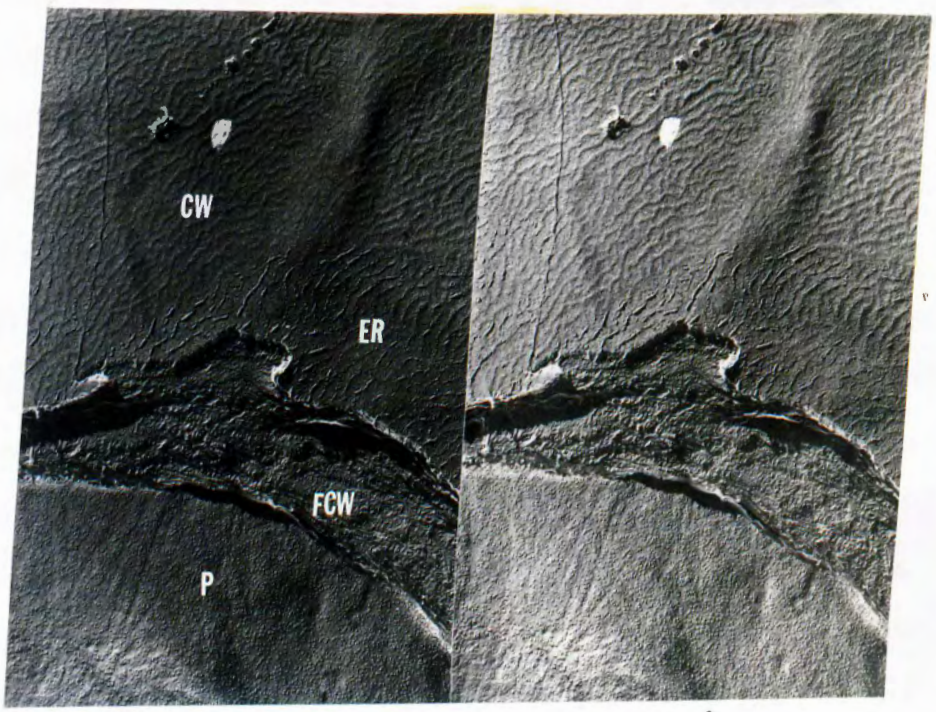

Plate 21

20,000x Slowly frozen superhardy Populus fractured in air at -70°C and extensively etched at -80°C the same as in plates (2e,d). The upper part of the plate is the outer surface of cell wall (cw). The middle band is cell wall fractured through (fcw) and the lower part is P-face of plasmalemma (p). The absence of the eutectic ridge (er) type formations on the plasma membrane surface implies they were deposited before fracturing. Thus they are probably the non-aqueous portion of the extracellular solution. Their sparseness indicates the fact that there is a large extracellular space mostly filled with air in superhardy material, so that when the cellular water diffuses to extracellular ice there is much less ice formed/unit volume than in the tender material.

cellular water has been removed from the tissue as measured on whole twigs; (4) both tender and superhardy Populus appear to pull the cell wall along with the cell membrane during loss of cell volume during freezing; (5) tender cells show cell surface wrinkling during freezing stress while hardy cells do not; and (6) extracellular water content after slow freezing can be visualized, and is higher in tender Populus than superhardy Populus.

Plate series 3 is confined to examination of superhardy Populus where, as shown in biological results, a very sharp mortality difference can be demonstrated between fully superhardy Populus quench frozen from -20°C (mortality indistinguishable from controls on slow warming) and -15°C (100% mortality upon slow warming).

Plate series 3 examines the ice forming behavior after quenching from these two temperatures and subsequent warming. Plate (3a) shows fully superhardy material slowly frozen to -15°C, then quenched in LN_2 and replicated below -70°C. Note the lack of evidence of any etching, i.e. observable ice crystals. This sample died upon slow warming. Similarly Plate (3b) shows fully superhardy material quenched from -20°C, reinserted at -27°C, then recooled by insertion into dry ice and replicated at below -70°C. Note the lack of observable ice crystals in this preparation as well, despite the long annealing time (12 hours) at -27°C to allow devitrification to proceed. This sample survived on slow warming. In contrast, Plate (3c) shows a partially superhardy sample quench cooled from -20°C in LN_2, reinserted in a -25°C cooling bath for 12 hrs, stored in dry ice, then replicated below -70°C. The sample showed 100% mortality on slow warming. Note that the cytoplasm is free of observable ice, whereas the vacuole shows extensive ice formation.

This indicates that the freezing of the vacuolar compartment alone is sufficient to kill the cell.

Plate (3d) shows fully superhardy (T_q = -30°C) Populus cooled to -15°C, plunged into LN_2, then reinserted at -25°C for 12 hrs before being plunged into dry ice followed by replication at -70°C. Note the ice clusters throughout the cytoplasm. Thus the evidence is that the cytoplasm of fully superhardy material is not stabilized against devitrification upon slow warming until it reaches equilibrium with ice at about -20°C.

Plate (4) shows massive intracellular ice formation in fully superhardy Populus that had been cooled to -35°C then quenched in LN_2 and replicated below -80°C after having been loaded with H_2O under reduced pressure at 0 C. This latter procedure increased tissue water content by 100 to 150%, thus demonstrating that the space external to the cell membrane is as large as or larger than the intracellular space in these tissues and is mostly air filled. Unfrozen controls survived, but these micrographs demonstrate the massive intracellular freezing that results in 100% mortality in the frozen twigs under these conditions. This means that ice penetrates the cells during slow cooling at temperatures above -35°C when the tissue is artifically loaded with pure water.

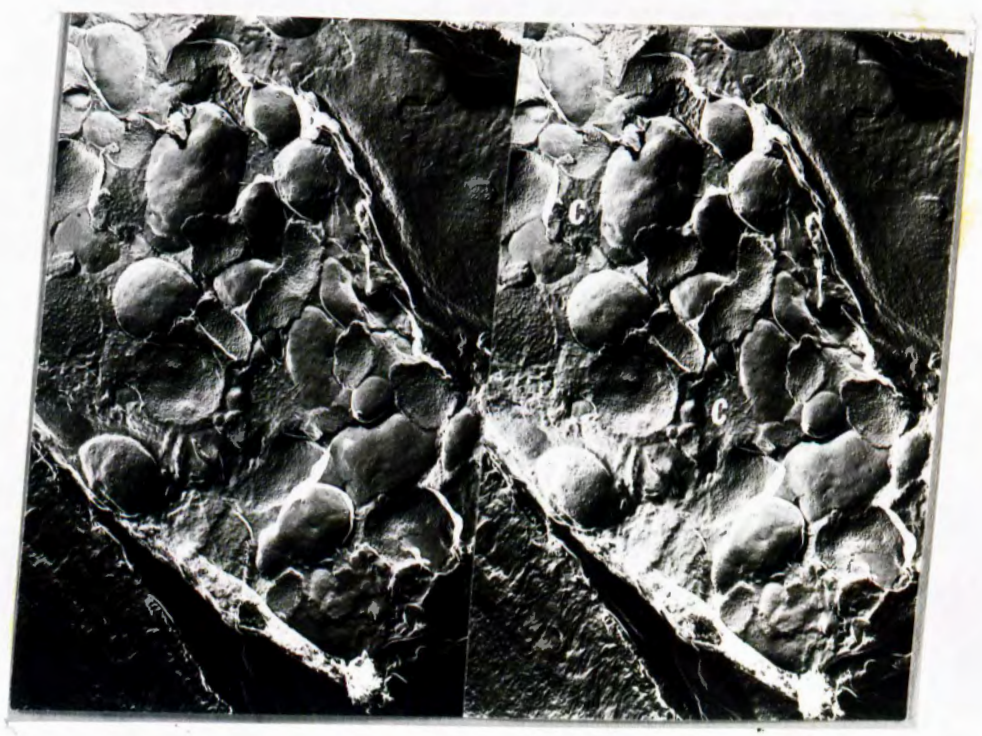

Plate 3a

25,000x Completely superhardy Populus cooled slowly to -15°C then plunged into liquid nitrogen (cooling 1200°C/min). The twig was fractured at -70°C in air then etched for >10 min at -80°C. Note the lack of any evidence of ice in the cytoplasm (c). This is despite the fact that the cytoplasm was in contact with ice crystals at -70°C for at least 1/2 hour before all contaminating ice could be removed in vacuo. Thus the cytoplasm, when in equilibrium with ice at -15°C is highly resistant to ice crystal growth at or below -70°C.

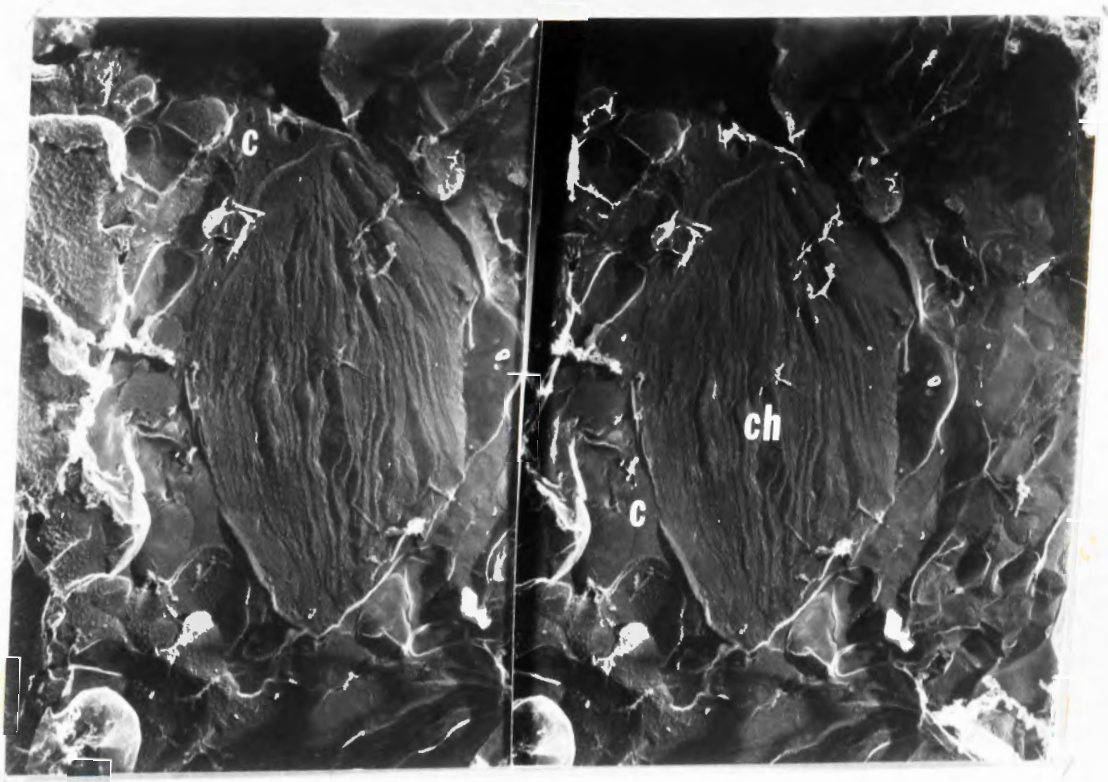

Plate 3b

20,000x Completely superhardy Populus cooled slowly to -20°C then plunged into liquid nitrogen, reinserted at -27°C for 12 hrs then inserted in dry ice for storage. These twigs survived the treatment upon later slow warming from dry ice storage. The material was fractured under liquid nitrogen and etched at -90°C. Note the lack of evidence of ice either in the cytoplasm (c) or the interior of the chloroplast (ch). DSC records indicate that any devitrification under these circumstances will proceed fastest at ~-30°C, thus this is strong proof of the stability of the intracellular solution in equilibrium at -20°C.

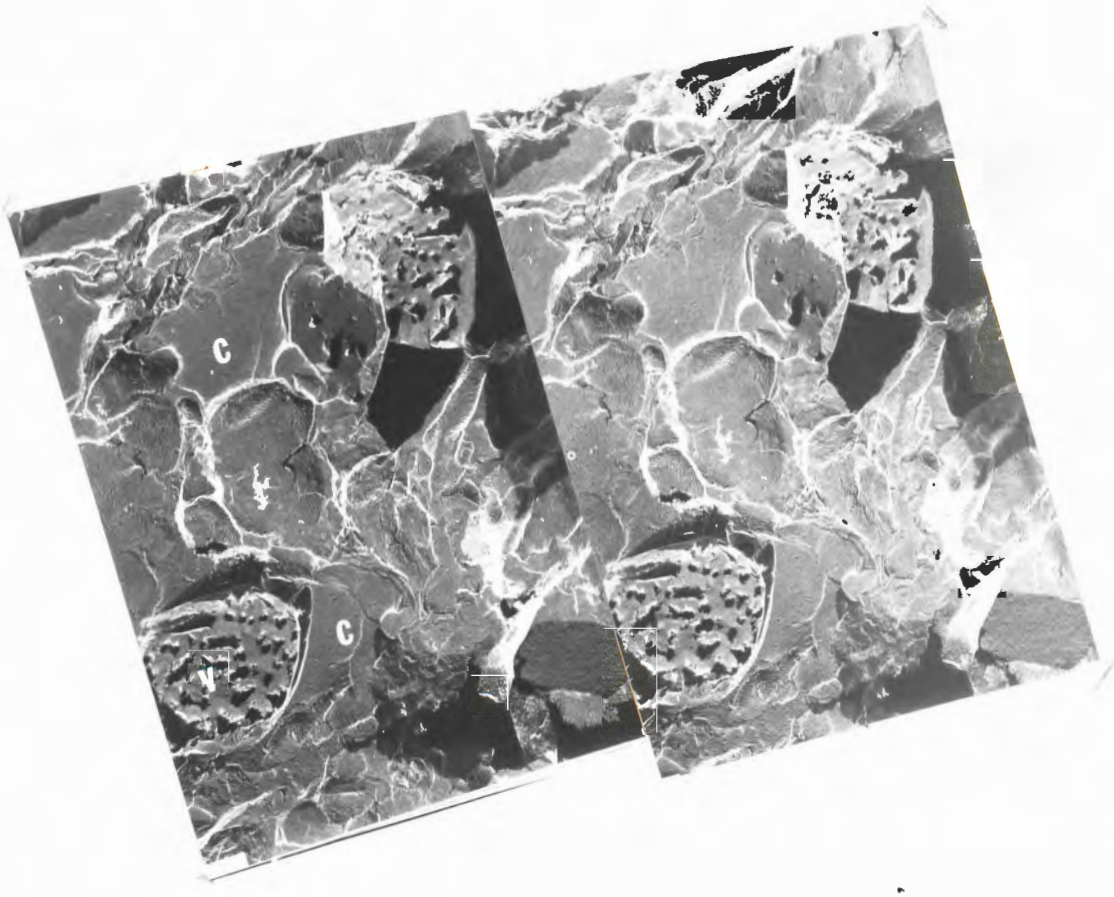

Plate 3c

25,000x Partially superhardy Populus (Tq not known) frozen slowly to -20°C, quenched in liquid nitrogen, reinserted for 12 hrs at -27°C, then fstored in dry ice (1°C/min cooling to -70°C). The sample was fractured under liquid nitrogen and etched at -90°C. The cytoplasm (c) appears free of ice crystals, but the vacuoles (v) are heavily frozen. Subsequent warming showed that these twigs experienced 100% mortality, implying that vacuolar freezing is sufficient to cause death.

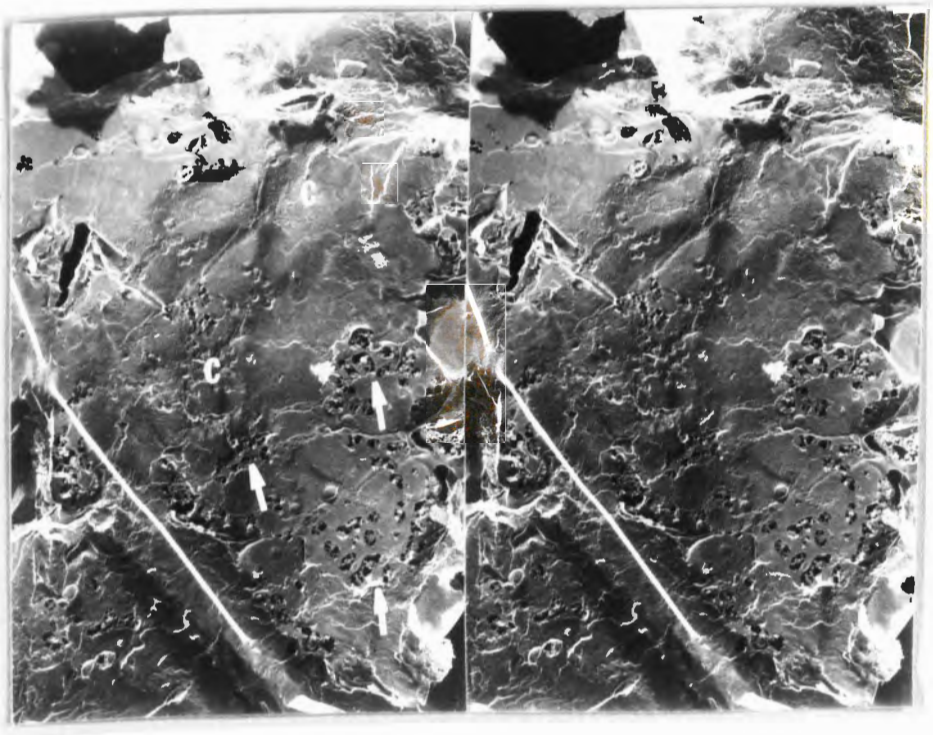

Plate 3d

10,000x Fully superhardy Populus cooled slowly to -15°C, then quenched in liquid nitrogen, reinserted for 12 hrs at -27°C, stored in dry ice and replicated by fracturing under liquid nitrogen and etching at -90°C. This is plasmalemma (P-face). Note the clusters of holes (arrows) indicating areas of exposed cytoplasm where subliming ice tore the plasma membrane away. Other areas of cytoplasm (c) appear to be ice-free. Thus the double quench induced observable cytoplasmic ice, but not massive freezing of the cytoplasm. Nevertheless mortality is 100% after this treatment.

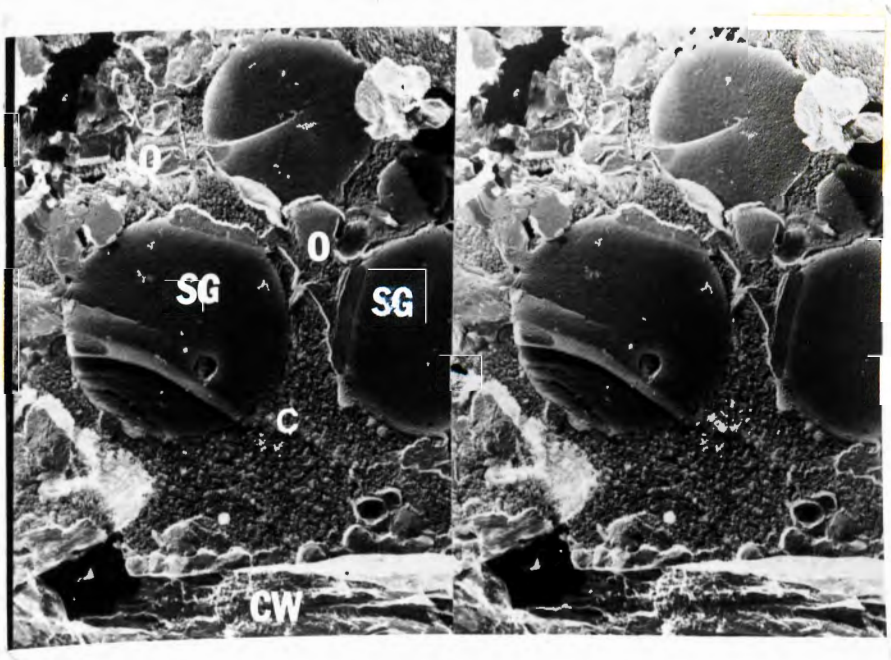

Plate 4

17,500x Completely superhardy Populus water loaded and frozen slowly to -35°C then fractured and etched at -98°C. Here we see what may be starch granules (sg), an organelle with membrane associated particles (o), cell wall (cw) and massively frozen cytoplasm (c). Thus slow freezing of water loaded tissue appears to allow ice to enter the superhardy cells and freeze them throughout.

DSC Results

To estimate the amount of glass forming solute in the unstressed superhardy cells, one needs to know how much water has left the cells to freeze as extracellular ice as a function of temperature below 0°C, and how water is partitioned between intracellular and extracellular compartments in the unstressed state. Thermogram (1) shows two tender wood samples cooled at 1°C/min to -9°C then warmed at 6°C/hr to thaw. The higher temperature peaks represent the melting of the nearly pure extracellular water (note the apparent inaccuracy of the machine's temperature scale due in part to low heat conductance of the frozen wood), while the larger low temperature peaks show the melting of the intracellular water. The distance between the peaks gives an estimate of the equilibrium freezing point of the water in the unstressed cells. It is 600-700 mOsm (~-1°C), in good agreement with the 500-600 mOsm estimated from light microscope observations (incipient plasmolysis point). Integration of the peaks shows that by -5.3°C (adjusted by high temperature endotherm) at least 75% of the total tissue water has frozen in the completely tender Populus. Furthermore, 90% of the water is initially intracellular, calculated as the ratio of the integral of the large peak to the sum [integral of large peak plus integral of small peak]. The curve with almost no extracellular water also showed an even higher percentage of water freezing by -5.3°C, about 90%. Since this is even more than for an ideal solution, it should be assumed that in this sample heat transfer from sample to sensor encountered significant resistance.

Thermogram (2) shows the same analysis for a superhardy twig. Note that a much higher proportion, 11%, of the water appears to be extra-

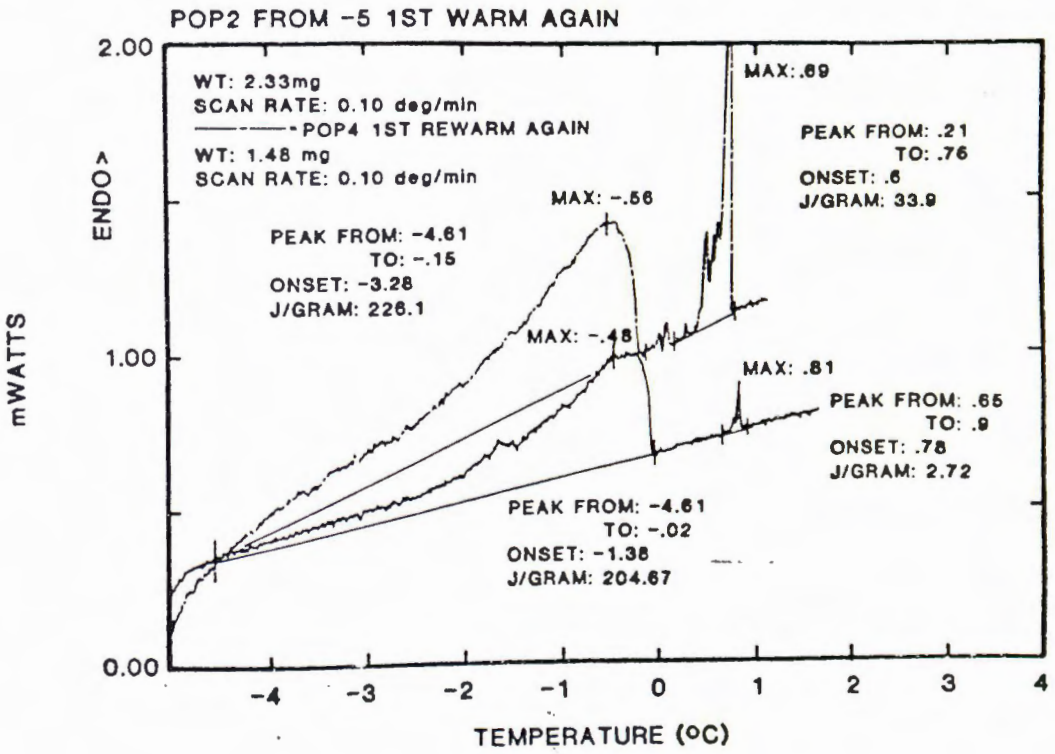

Thermogram 1

Thermal records of two completely tender twigs cooled at 1°C/min to -9°C then warmed at 6°C/hr to thaw. The broad, low temperature peaks represent the intracellular contents reimbibing water from melting extracellular ice as the temperature rises. Their maximum is a good estimate of the mean freezing point depression of the cellular contents, if the maximum of the smaller peaks is taken as 0°C. Thus the internal osmolality of both samples appears to be 600-700 mosm. The area under each peak can be used to estimate the water content of either the intracellular (broad, low temperature peak) or extracellular (narrow, high temperature peak) compartments. The results clearly show most water is intracellular (>90%). The reason for the disparity in extracellular water content between samples is not clear.

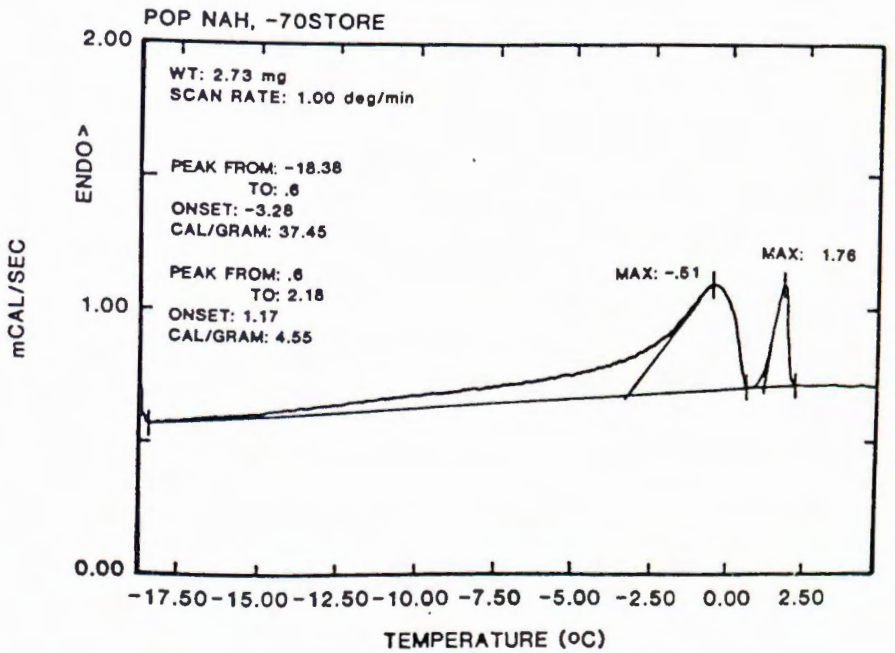

Thermogram 2

Partially superhardy twig (water content 55%) cooled at 1°C/min to -20°C then warmed at 1°C/min to thaw. At most 11% of the water was extracellular, intracellular osmolality was 1200 mosm (by the difference in the two peak maxima). Since the estimated percent of intracellular water freezing by -20°C is 95.5%, and since ideal behavior of a solution starting with 1.3 osm would be ~90% of water frozen by -20°C, the machine appears to have overestimated the enthalpy of melting. This is discussed in DSC Materials and Methods.

cellular. Note that the distance between peaks corresponds to an intracellular solution of about 1200 mOsm, in excellent agreement with light microscope studies indicating incipient plasmolysis in 5% $CaCl_2$ solution (freezing point $-2.3^{\circ}C$, 1300 mOsm).

In these twigs about 94% (water content 55%) of the total water and about 95.5% of the intracellular water had frozen by $-20^{\circ}C$. Thus the cells behaved almost ideally to $-20^{\circ}C$ even though most of the cytoplasmic contents of these partially superhardy twigs appear to become glasses by $-50^{\circ}C$. Ideal behavior was calculated by the classic equation (92)

$$\ln X_w = \left[\frac{H(273.15) - Cp\ 273.15}{R}\right] x \left[\frac{1}{273.15} - \frac{1}{T}\right] + \frac{\Delta Cp}{R} \ln \frac{T}{273.15}$$

where: X_w = mole fraction of water

$H\ (273.15)$ = heat of fusion of water at $0^{\circ}C$

T = temperature of system

R = gas law constant

ΔCp = heat capacity difference: water - ice

Since this was partially superhardy wood and since an ideal system would lose 89% of its H_2O from a starting concentration of 1.3 osmoles, we should assume again that the DSC somewhat overestimated the enthalpy of melting.

Thermogram (3) shows the behavior of a model glass forming system PEG:H_2O 1.0:3.3 w/w. The solid curve shows that warming after $100^{\circ}C$/min cooling (from $0^{\circ}C$) gave a glass transition at $-70^{\circ}C$ followed by a large two peaked devitrification between $-30^{\circ}C$ and $-50^{\circ}C$ (solid line). The dashed line was made after warming to and annealing at $-15^{\circ}C$ then

recooling at 100°C/min to -160°C. This allowed devitrification to proceed completely and thus produced a stable, more concentrated glass with a lower water content. In the latter case the glass transition began at a higher temperature and was smaller in magnitude with no subsequent devitrification. All of these characteristics are what one would expect of a binary aqueous glass forming solution.

Thermogram (4) shows glass formation in slowly cooled, tender Populus. The dashed line indicates that a stable glass, probably an equilibrium glass, with a transition at about -80°C was formed. Subsequent annealing at -22°C followed by 100 C/min cooling to -160°C yielded a slightly different warming curve with evidence of devitrification at -85°C followed by glass transition at -80°C and a major devitrification commencing at -40°C. Thus the water content of the intracellular medium at an equilibrium temperature of -22°C was not very much greater than at equilibrium with ice at -70°C (indicated by the slight change in T_g), but the resistance to ice formation on warming (devitrification) was significantly less.

In contrast, Thermogram (5) shows the same tender sample (dashed curve) as in Thermogram (4) compared to a superhardy sample quench cooled from -25°C after slow cooling to -25°C (solid curve). The superhardy sample showed a much higher specific heat capacity above -100°C, indicating an increase in liquid content relative to the tender sample, but unlike the -22°C annealed tender sample there was no devitrification on warming, indicating that the low temperature glassy intracellular solution was not homogeneously nucleated by quench cooling from -25°C in the superhardy sample.

Biological microscope results (see Figures I and II) indicate that the tender cells plasmolyze to a much smaller final volume (<10% of

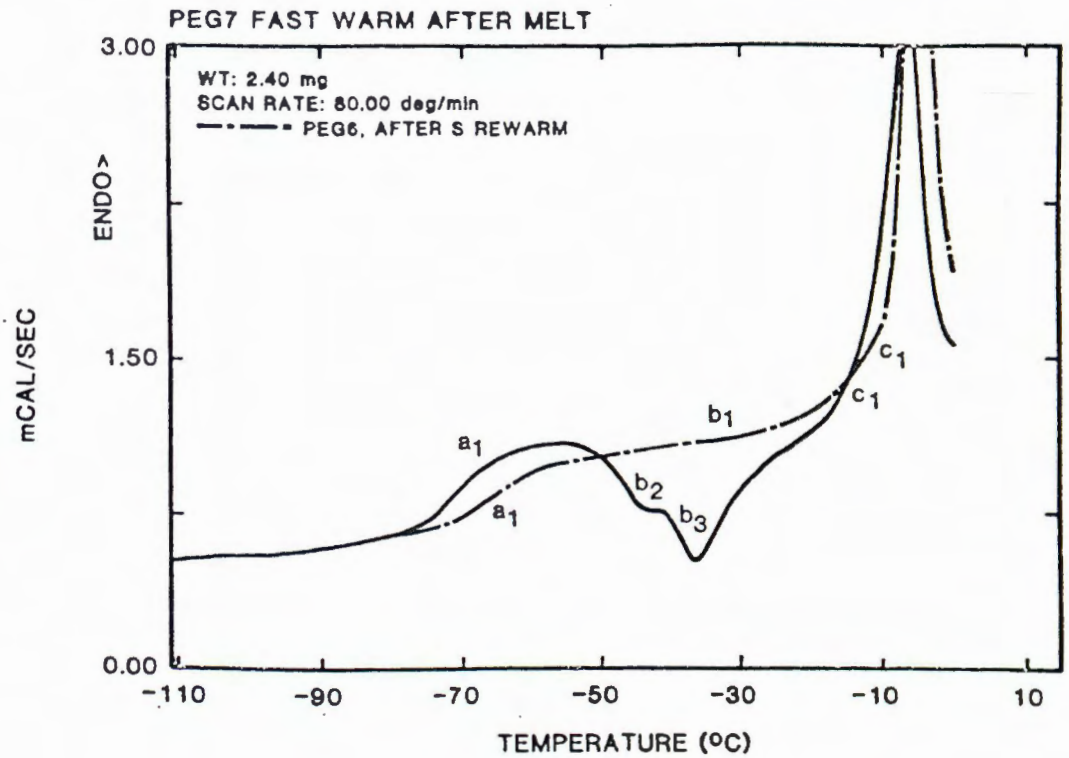

Thermogram 3

A 1.0:3.3 H_2O-polyethylene glycol (PEG MW 8000) solution, w/w, was cooled at 100°C/min to -160°C then warmed at 5°C/min to -15°C, recooled at 100°C/min to -160°C, and finally warmed at 80°C/min to thaw as shown by the dashed line. On the dashed line (a_1) represents the glass transition, (b_1) the very slight devitrification, and (c_1) the equilibrium melting of the ice in the system. The solid line is the same sample after cooling 100°C/min to -160°C from the thawed state. The (a_1) transition is the glass transition. Note that it is at a lower temperature and involves a larger change of heat capacity than the recooled material. This indicates a more dilute aqueous glass. Note also the large devitrification ($(b_2,b_3)\equiv b_1$), also an expected result of increased water content. The melt (c_1) is virtually the same as in the first run; the slight shift in the onset of melting is unexplained.

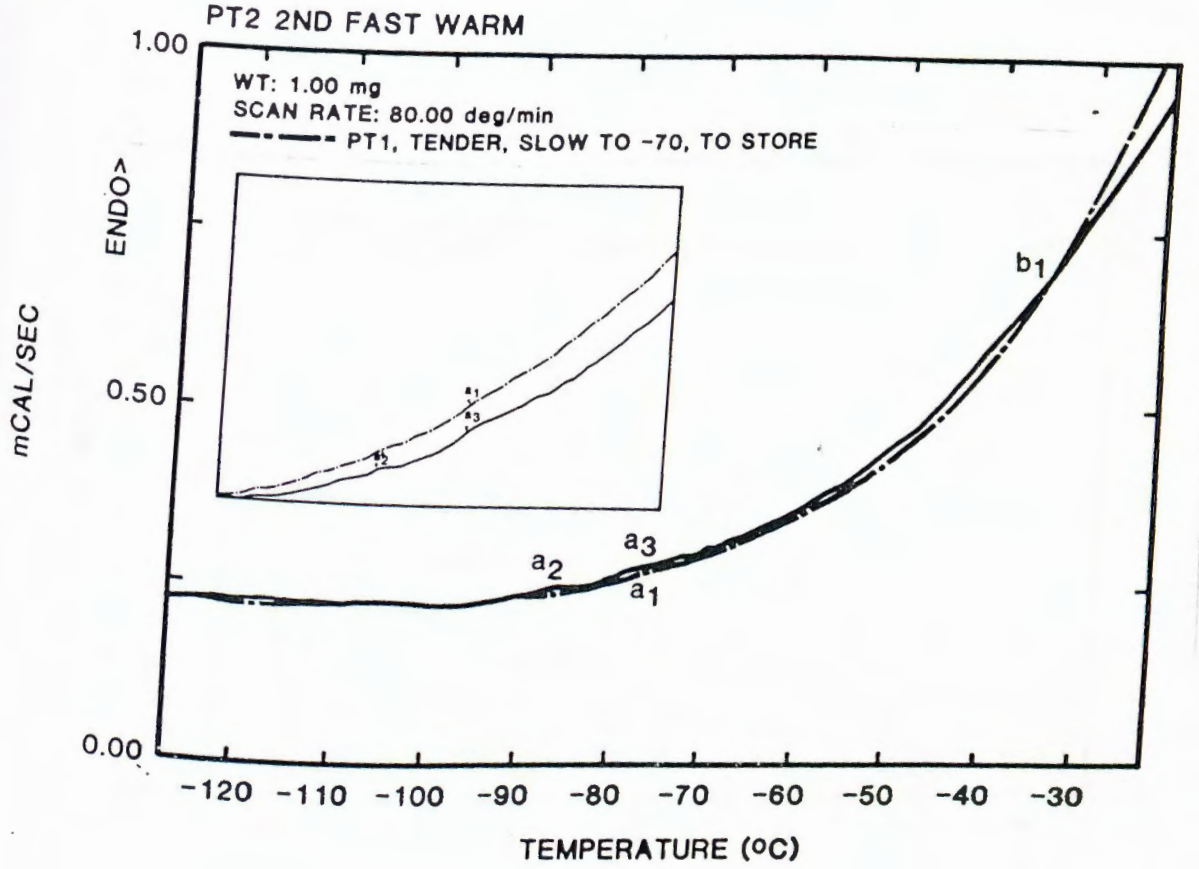

Thermogram 4

A tender Populus sample cooled at 3°C/hr to -70°C, then stored. The dashed line shows the first fast warm at 80°C/min to -22°C after cooling to -160°C where the sample was annealed for 10 min. Transition (a_1) appears to be a small glass transition, perhaps that of the normal intracellular salt, small organic molecule, protein solution. There is no apparent devitrification. The solid curve shows the warming of the same sample after recooling to -160°C at 100°C/min from -22°C. Note the increased size of the low temperature glass transitions (a_2,a_3) followed by a marked devitrification starting at (b_1). This shows that, even though very little water remains in the tender cells at equilibrium at -22°C due to the initially low intracellular osmolality, what does remain produces an unstable glass upon quick cooling; so unstable as to devitrify below -40°C even when warming is at 80°C/min. This is in sharp contrast to quenched superhardy material (Thermogram (5)). Insert shows transitions in more detail. They are at the limit of machine's resolution.

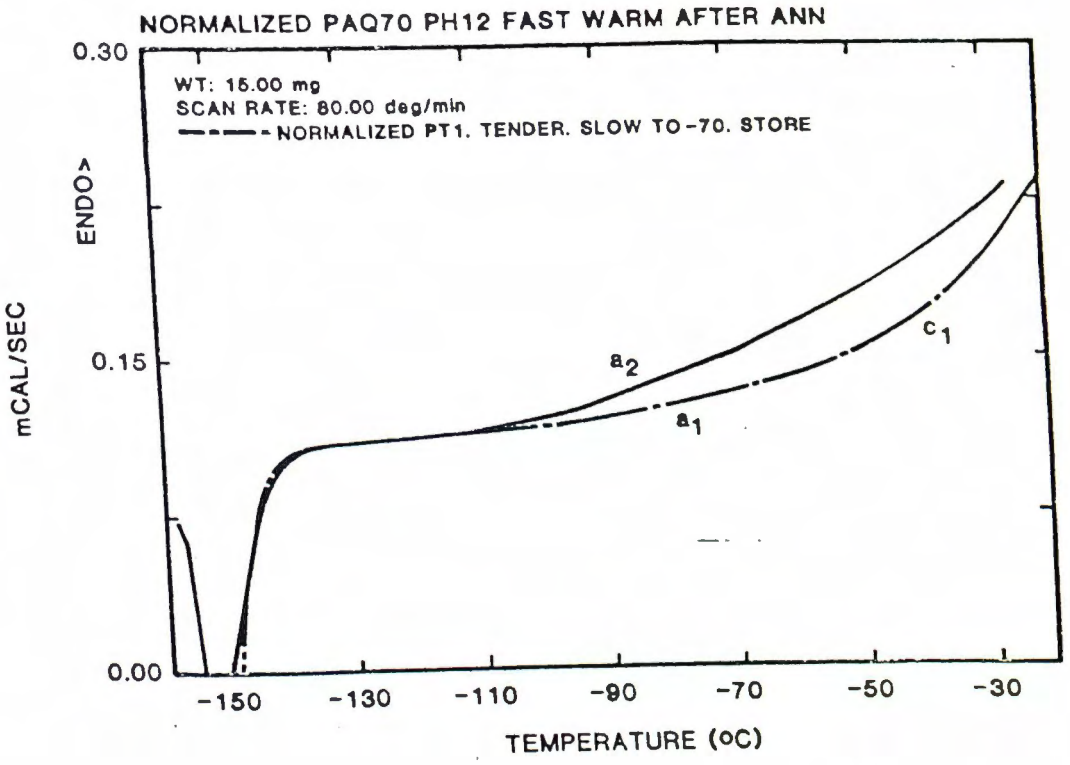

Thermogram 5

This graph compares the fast warming (solid curve) of a fully superhardy twig slowly cooled to -25°C, quench cooled in liquid nitrogen then stored in dry ice to the fast warming (dashed curve) of a fully tender sample cooled slowly to -70°C. The records have been normalized to a per gram basis. Note that the glass transition in the hardy material is perhaps 10x larger (a_2) than in the tender sample (a_1), yet there is no devitrification as in the warming after -22°C annealing of this same sample as shown in Thermogram (4). Note also that the melt in the tender sample begins at (c_1), much earlier than in the hardy sample. In general this is to be expected of more dilute solutions: that more ice melts by a given temperature as they are warmed. The broadness of the transitions is most likely due to both the poor heat conductance and the chemical heterogeneity of the tissue.

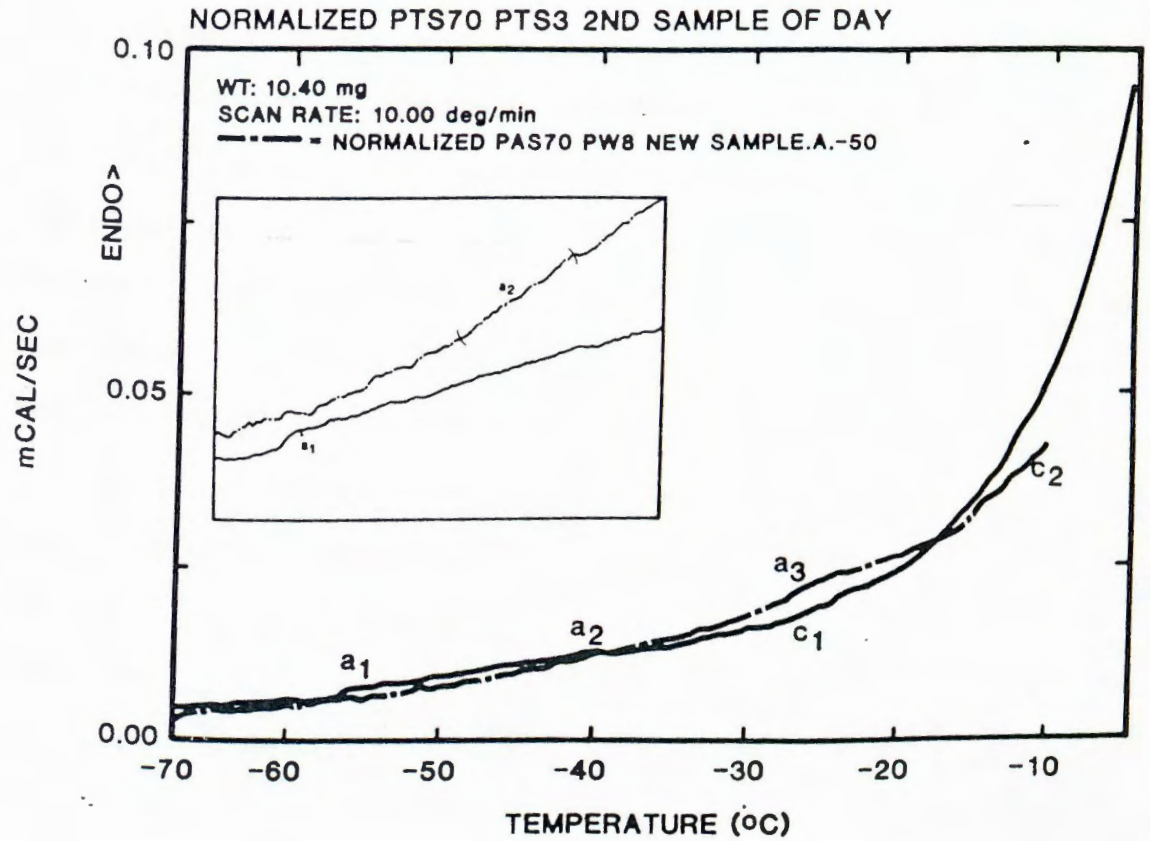

Thermogram 6

This graph shows the warming of fully superhardy wood cooled slowly (dashed curve) and tender wood cooled slowly (solid curve). Again results are on a per gram basis. The tender wood was cooled slowly to $-50^{\circ}C$, stored in dry ice, and here warmed at the intermediate rate of $10^{\circ}C$/min. It shows a glass transition at about $-55^{\circ}C$ (a_1) and what appears to be a smooth melt begins at (c_1). In contrast the dashed curve shows the superhardy wood cooled slowly to $-50^{\circ}C$ then stored in dry ice. Note that the first significant glass transition is at $-45^{\circ}C$ (a_2), with the major one at $-32^{\circ}C$ (a_3), and the main ice melt (c_2) at about $-17^{\circ}C$. Note that the sum total Cp of [(a_2) + (a_3)] is many times larger than (a_1), yet once the melting begins again (as in Thermogram (5)), the tender sample is endothermic with respect to the hardy sample, due to an increased volume of ice melting to the more dilute cell contents of the tender material. The insert shows the unnormalized graphs, at high resolution. Note that (a_1) and (a_2) are well above noise level, but this is near the limit of machine resolution.

initial volume) than that of superhardy cells (≈40% of initial volume). Thus one would expect that the glass transitions of the superhardy cells would be considerably larger because of the much greater volume of glassy material in the cells. This is born out by Thermograph (6) which shows tender Populus cooled slowly to -50°C at 3°C/hr then stored at -70°C (solid curve) compared to superhardy Populus cooled slowly to -50°C and stored at -70°C (dashed curve). Note that the main glass transition in the superhardy wood at (a_3) was much larger than that in the tender wood at (a_1) but also note that at high temperatures much more water is melting in the tender wood. This is indirect evidence that the initial osmolality of the tender cells was significantly lower.

The proof that the S shaped transitions so far referred to are really glass transitions is based on the fact that the higher the water content of an aqueous glass forming solution the lower will be the Tg (glass transition temperature), the larger the ΔCp of transition, and the larger the devitrification upon warming (all as illustrated by the control solution PEG:H_2O in Thermogram (3)). Since the plant cells are enclosed in semipermeable membranes, it is a simple matter to vary their intracellular water content by annealing the wood at various subzero temperatures. This then effectively alters the glass transitions as just described, if such glasses are present, and this can be observed by cooling rapidly from the annealing temperature to below the glass transition temperature of the annealed system, then warming again to record glass transitions and devitrifications.

This is illustrated in detail in Thermographs (7-12) inclusive. These graphs are all from the same sample cooled and warmed repeatedly.

The sample was partially superhardy and the twigs were cooled at 3°C/hr to -20°C then plunged into dry ice several months before this

run. Twigs that were subsequently warmed slowly from -70°C survived.

Thermogram (7) shows (solid line) the first warm after annealing 10 min at -30°C to drive off any excess CO_2 then 100°C/min recooling to -70°C. A glass transition is labeled (a_1) and a small devitrification (b_1). The dashed line shows the warming of the sample after 11 min annealing at -5°C followed by 100°C/min cooling to -160°C. Equivalent peaks are so labeled: a's = glass transitions, b's = devitrifications.

Note the very large temperature shift in (a_1) and (b_1) and the presence of a very low temperature glass transition-devitrification labeled (a_2, b_2). Note also the increase in amplitude of both the glass melt and devitrification after annealing at -5°C.

Thermogram (8) shows the same -5°C annealed record (solid curve) versus the sample after annealing at -10°C for 3 min (dashed curve). The latter time is insufficient for the cells to reach full equilibrium on warming so the mean equilibrium freezing point of the cellular solutions is <-10°C. Note that (a_1) and (b_1) are intermediate in all respects to the two sets of (a_1, b_1) in Thermogram (7). Note that (a_2, b_2) are barely discernible on the dashed curve but still temperature shifted about the same amount relative to (a_1, b_1) in both curves. Note also that the -10°C annealed specimen displays a small set of very low temperature events (a_3, b_3).

Thermogram (9) again shows the -5°C anneal for 10 min record (solid curve) versus the -10°C anneal for 10 min record (dashed curve). Now the longer annealing at -10°C (after warming) allows more water to re-enter the cells (virtual equilibrium) and thus the glass transitions are shifted to lower temperature and increased in amplitude, as are the devitrifications. This is made clearer by the direct comparison of the

$-10^{o}C$ for 10 min anneal (solid curve) versus the $-10^{o}C$ for 3 min anneal (dashed curve) in Thermogram (10).

Thermogram (11) indicates what happens when one tries to re-establish low temperature equilibrium below the major equilibrium glass transition of the intracellular solution ($\sim -28^{o}C$). The solid curve is the sample after 10 min at $-5^{o}C$ followed by $100^{o}C$/min cool to $-160^{o}C$ as before. The dashed curve shows what happened when the wood was annealed 10 min at $-5^{o}C$, then cooled at $100^{o}C$/min to $-30^{o}C$, held 18 min at that temperature, then cooled at $100^{o}C$/min to $-160^{o}C$. That the cellular solutions could not quickly attain equilibrium with ice is shown in the dashed curve. Note that (a_1 b_1) are labelled as occurring at two places on the dashed curve. This is because it is clear from the overall comparative pattern between the two curves that some of the cells (and/or compartments in groups of cells) attained equilibrium very slowly at $-30^{o}C$, thus they retained essentially the same composition as they had after the 10 minutes at $-5^{o}C$ and the transitions they showed are the same as in the solid curve. The higher temperature (a_1, b_1) transitions are almost at the same composition as in the original $-30^{o}C$ annealed state (immediately after removal to the DSC from $-70^{o}C$ storage, solid curve Thermogram (7)). This is further illustrated by Thermograph (12). The solid curve is immediately after storage at $-70^{o}C$ and 10 min annealing at $-30^{o}C$, the dashed curve is the same as the dashed curve thermograph (11).

In summary, Thermograms (7-12) show that there are at least 3 major glass transitions in the whole, living twig tissue. They all behave as the transitions of classic aqueous glass forming solutions do as the water composition of the solutions is varied. The cells can be annealed so as to vary these compositions in a systematic way (because they

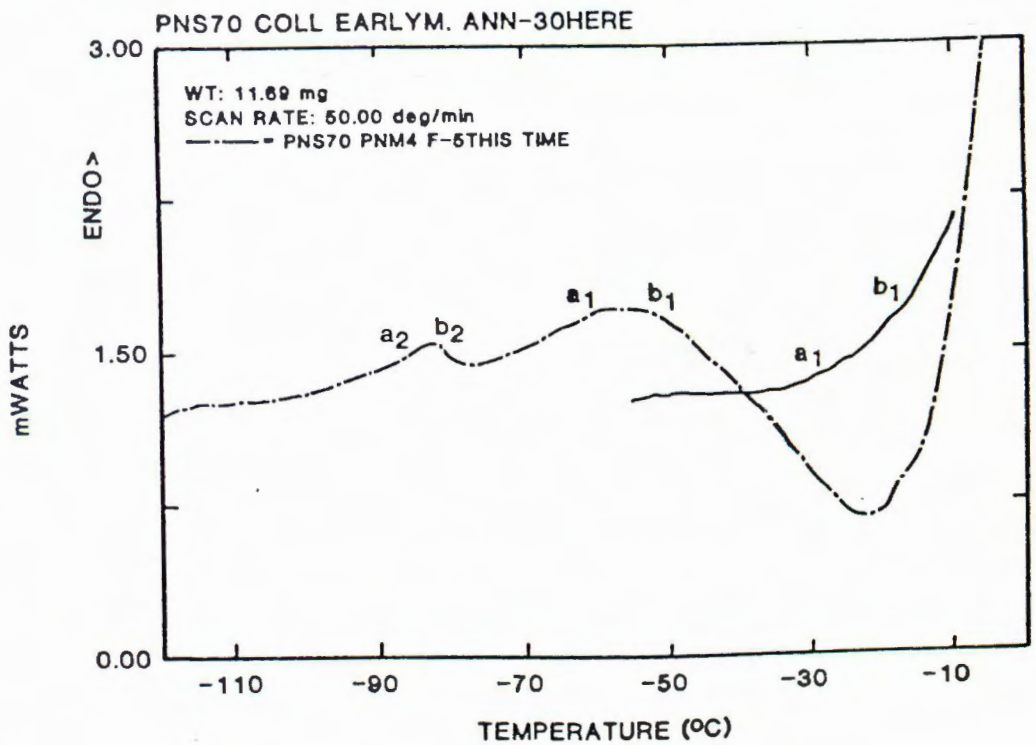

Thermogram 7

This is the first of a series of thermographs showing a partially superhardy sample that was initially cooled slowly to -20°C then plunged into dry ice for several months. The solid curve in this graph shows the first 50°C/min warm of the sample (after annealing at -30°C to sublime dry ice). Note a complex glass transition at (a_1) and a slight devitrification at (b_1). Since the twigs of this sample subsequently survived slow warming from -70°C, (b_1) on the solid curve could not be a lethal event in a significant number of cells. This curve is in contrast to the dashed curve which shows the warming of the same sample after 10 min annealing at -5°C followed by 100°C/min cooling to -160°C. Equivalent events (to those on the solid curve) are so labeled. Note that (a_1) is much larger as is the devitrification (b_1) and both occur at a much lower temperature. Note that another glass transition-devitrification (a_2, b_2) is now evident at about -80°C.

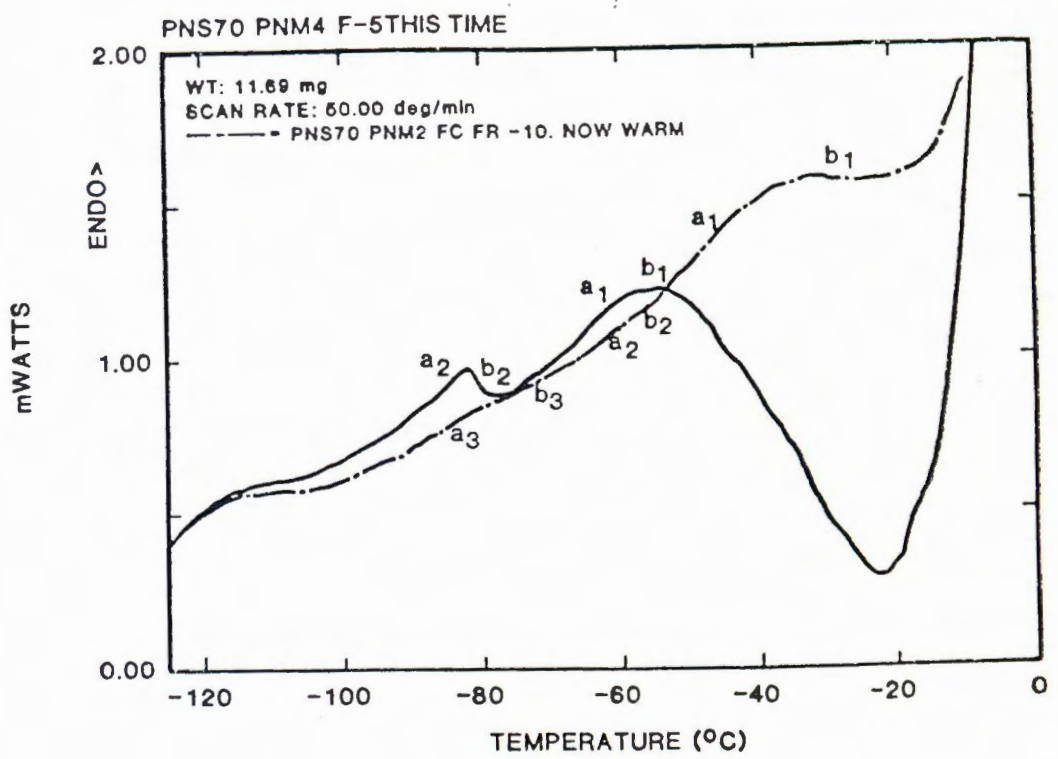

Thermogram 8

The same partially superhardy sample as in graphs (7-12). The solid curve represents the fast warming of the sample after 10 min annealing at -5°C followed by 100°C/min cooling to -160°C. The dashed curve shows the 50°C/min warming of the sample after 3 min annealing at -10°C, an insufficient time to come to equilibrium with extracellular ice. Thus the intracellular contents were in equilibrium between -10°C and -20°C under these circumstances. The major high temperature glass transition-devitrification is at (a_1,b_1) on both curves. Note that it is at lower temperature and larger on the solid curve, as expected, but is considerably larger on the dashed curve than the transitions of the -70°C stored wood (in equilibrium at -20°C to -30°C) shown on the solid curve of graph (7). The intermediate glass transition-devitrification that is invisible on the solid curve of Thermograph (7) is here small but discernible (a_2,b_2) on the curve of -10°C annealed wood (dashed curve) and it too has gotten larger and shifted to lower temperature after -5°C annealing (a_2,b_2 (as shown on the solid curve)). A third very low temperature transition (a_3,b_3) appears in the -10°C annealed wood, but is invisible on the record of -5°C annealed wood. This is presumed to be the normal background components of the cytosol (glycolytic enzymes, salts, organic acids, etc) which may play a role in limiting the upper temperature limits of intracellular stability to quench cooling by seeding the solution when the quenching temperature is too high. The (a_3,b_3) transition is presumed absent in the -5°C annealed material because significant homogeneous nucleation occurs during cooling at 100°C/min from -5°C and thus the dilute glass (a_3) is assumed to be concentrated by that event.

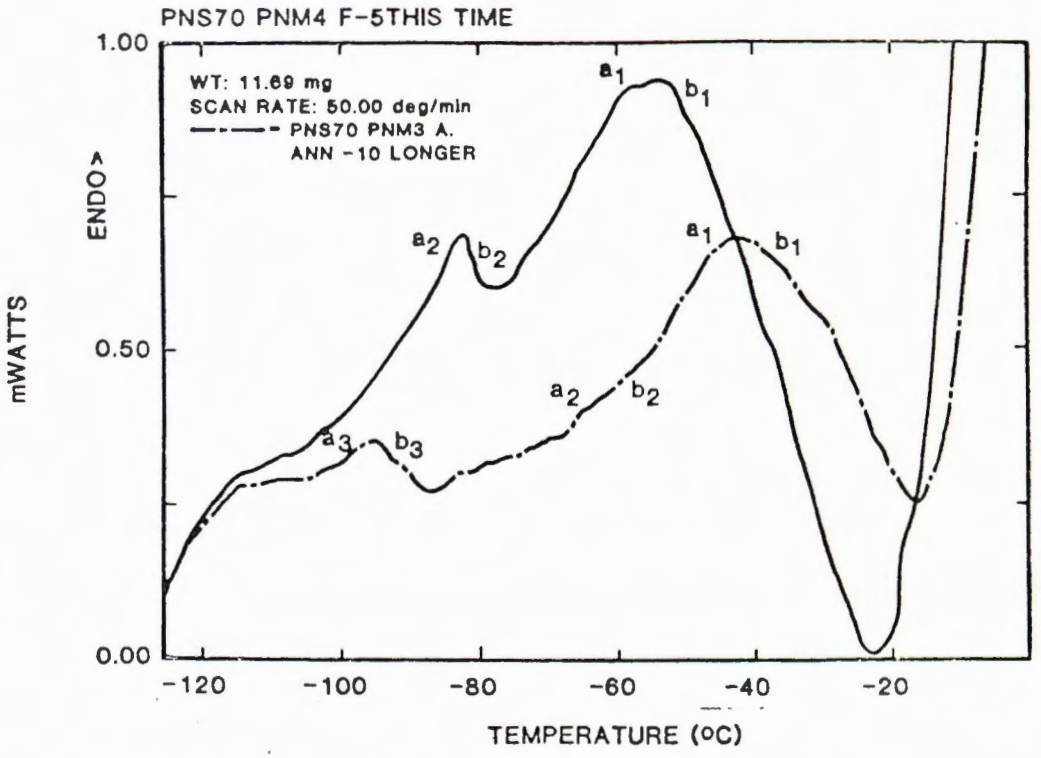

Thermogram 9

The fast warming of the partially superhardy sample is shown after 100°C/min cooling following 10 min annealing at -5°C (solid curve) versus the 50°C/min warming of the sample after 100°C/min cooling from 10 min annealing at -10°C (dashed curve). Thus this graph differs from graph (8) in that the annealing at -10°C is more than 3x as long and the intracellular solution was represented by the dashed curve much closer to equilibrium with ice at -10°C. The results are fully consistant with the patterns in graph (8). The highest glass transition devitrification (a_1,b_1) has again moved to a lower temperature and gotten larger in magnitude (increased water content due to higher equilibrium temperature of intracellular contents). Likewise, the intermediate glass transition-devitrification (a_2,b_2) is also larger and at a lower temperature. The same holds for the lowest temperature glass transition devitrification (a_3,b_3). Note the contribution (a_2,b_2) appears to make to the seeding of the intracellular medium. The glass transition (a_1) and (a_2) are at or above the temperature of any events seen on cooling at only 50°C/min in cooling records of wood annealed at -10°C (graph (21)), thus if this (a_3) component were not present it would be hard to understand why devitrification would occur on fast warming.

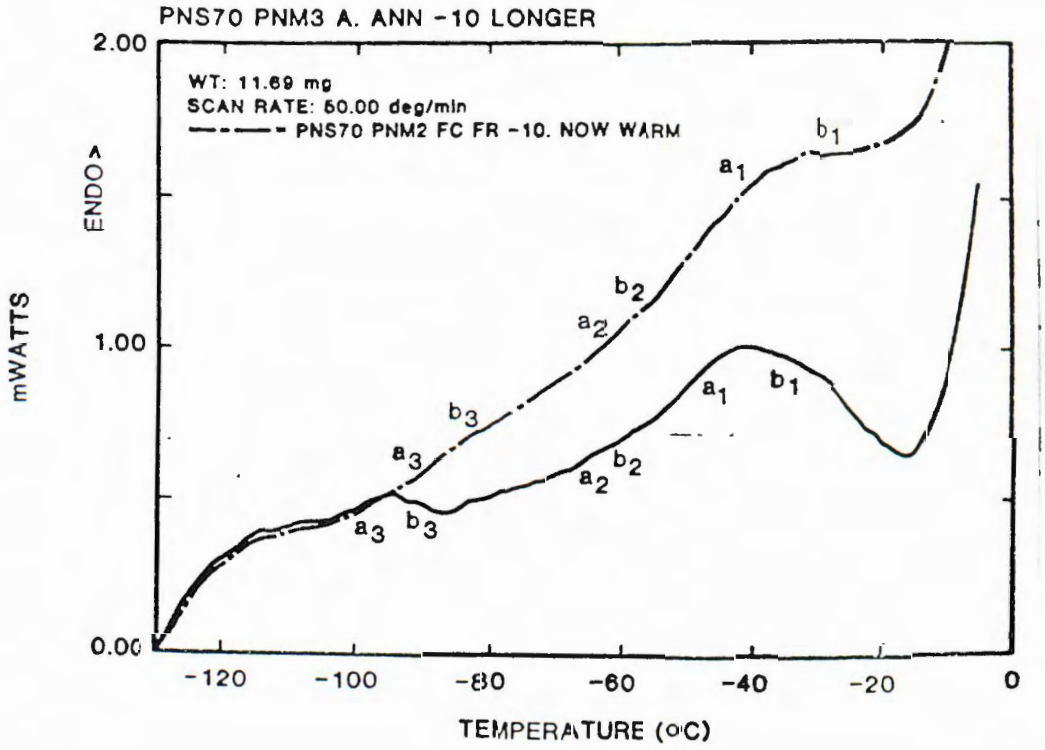

Thermogram 10

Direct comparison of 50°C/min warming of the sample after 100°C/min cooling from 3 min at -10°C (dashed curve) and 10 min at -10°C (solid curve). Equivalent glass transition-devitrifications (a's and b's respectively) are so labeled. Note that all transitions have moved to a lower temperature and have a larger amplitude in the wood annealed longer at high temperatures.

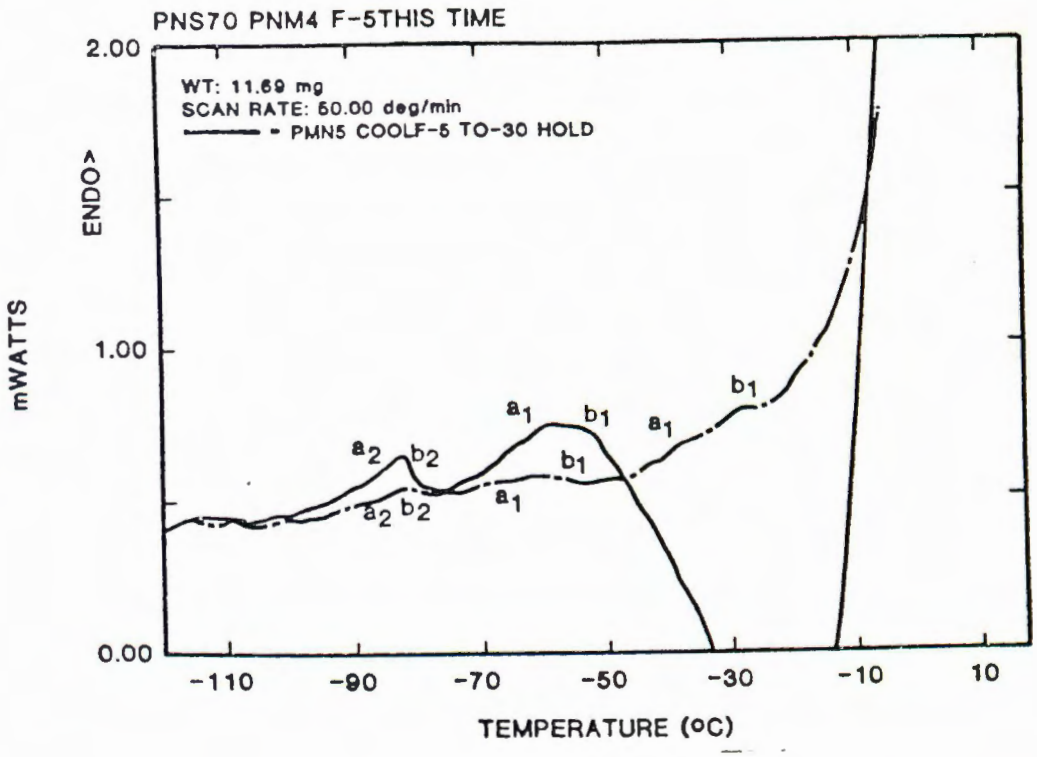

Thermogram 11

This comparison of fast warming curves shows what happens when one tries to re-establish equilibrium in the neighborhood of the equilibrium glass transition of the major high temperature glass forming component. The solid curve is the 50°C/min warming of the sample after 100°C/min cooling to -160°C from 10 min annealing at -5°C. The dashed curve is the 50°C/min warming of the sample after it was annealed 10 min at -5°C, cooled at 100°C/min to -30°C, held at that temperature for 18 min, then cooled at 100°C/min to -160°C. The 3 glass model (see Discussion) predicts that if a solution is in equilibrium with ice at a temperature above the glass transition point, and it is then cooled to a point below that temperature quickly enough so its composition remains essentially unchanged during cooling, then it will lose water to ice until it approaches a composition whose glass transition is at that lower temperature, a composition more dilute than the equilibrium glass transition composition.

Thus one would expect that a jump cooling experiment such as shown here would yield a composition of less stability than one slow cooled to the high temperature glass transition, and we would expect that the dynamics of re-equilibrating this tissue at temperatures such as -30°C would be much slower because of the high viscosity associated with formation of an aqueous glass. These expectations are born out by the dashed curve. Notice that some cells have apparently hardly changed their composition in the 18 min annealing, thus the lower temperature (a_1,b_1) and (a_2,b_2) match those on the -5°C curve well. Other cells have moved towards equilibrium at -30°C and thus the high temperature (a_1,b_1) is seen as well.

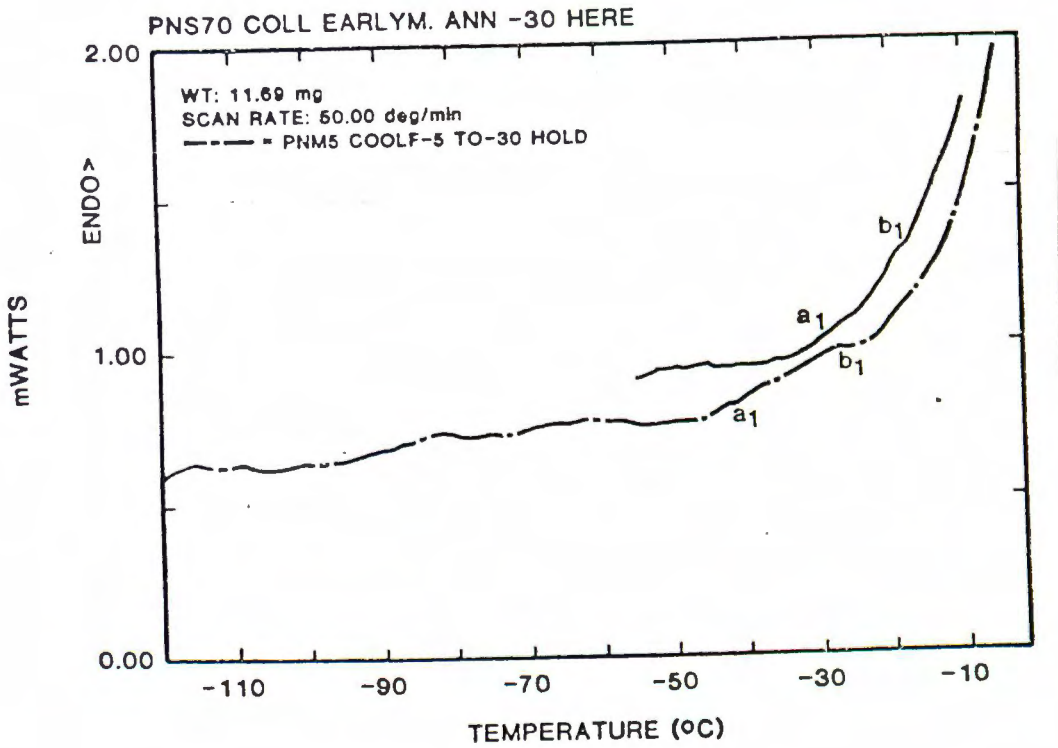

Thermogram 12

A continued examination of the double jump cooling of graph (11). Here the fast warming curve of the initial run is shown (solid curve, also solid curve of graph (7)). This material was slowly cooled to -20°C then plunged into dry ice storage for several months, then warmed to -30°C for 10 min annealing to remove dry ice then recooled at 100°C/min to -70°C before 50°C/min warming as shown by the solid curve. The dashed curve is the 50°C/min warming of the sample after annealing 10 min at -5°C, 100°C/min cooling to -30°C, 18 min annealing there, then 100°C/min to -160°C. As explained in DSC Results and Thermogram (11), the slow cooling to -20°C allows the sample to concentrate further than fast cooling to a temperature below the equilibrium glass transition followed by annealing at that low temperature. This is because the highest glass transition temperature that can be attained after fast cooling to a temperature below the equilibrium glass transition is the new, low annealing temperature. Since -30°C is actually about equal to the equilibrium glass transition, the fact that the glass transition-devitrification (a_1,b_1) shown in the dashed curve is at a lower temperature and greater in amplitude then the corresponding transitions on the solid curve is probably due mostly to the kinetics of cell water loss in such viscous intracellular solutions. Nevertheless, the movement of (a_1,b_1) back towards the original position and size as shown on the solid curve, but the failure to attain it during the double jump cooling is further proof of the glass transition model.

possess semipermeable membranes), increasing and then decreasing the magnitude of both the transitions and their associated devitrifications, and simultaneously decreasing and then increasing the temperature of occurrence of these transitions, as one anneals at higher temperatures followed by reannealing at lower temperatures again. This can be done even though the first devitrifications that occur are completely lethal to the cells by long term mortality measurements ($\geq$10 days).

To further assure that the events seen were glass transition-devitrifications, the warming experiments were repeated at the slower warming rate of 10°C/min on completely superhardy wood previously slowly cooled to -70°C, then stored.

The patterns observed, shown in Thermograms (13-17) are essentially the same as shown by the 50°C/min warm. Here all annealing was always for 10 min. Note that the records are far simpler than the 50°C/min records because the smaller amplitude glass transitions can no longer be distinguished from noise.

In Thermogram (13) the major glass transition (a_1) has moved from ~-28°C (dashed curve is sample immediately after slow cool to and storage at -70°C) to ~-50°C (solid curve is after annealing at -20°C followed by 100°C/min cooling to -160°C) and gotten much larger, but no associated devitrification is seen. This corresponds well with the biological data indicating no mortality after quenching from -20°C followed by very slow warming. This changes dramatically in Thermogram (14) showing what happened after annealing at -10°C (solid curve). The glass transition continued to increase in magnitude and moved to -70°C, but is now associated with a large devitrification (b_1). In Thermogram (15), after annealing at -5°C, the glass transition moved to ~-90°C (solid curve). However, as emphasized in Thermograph (16), which compares the -5°C

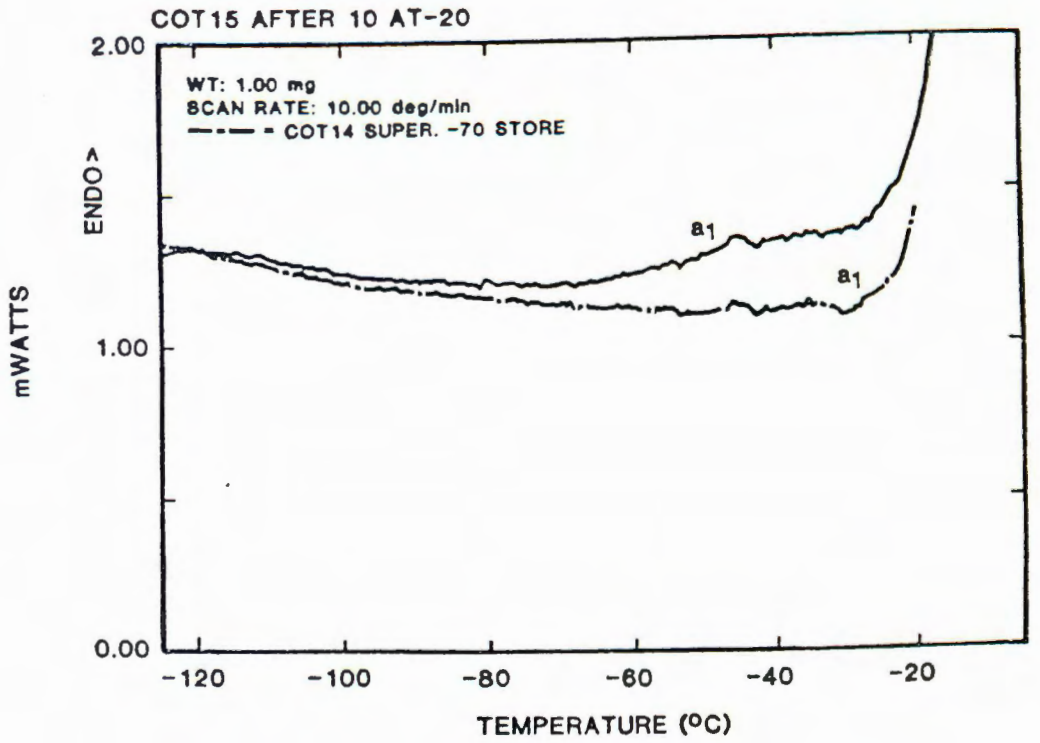

Thermogram 13

Completely superhardy Populus cooled slowly to -70°C, here warmed at 10°C/min from -160°C (after 10 min at -30°C to eliminate dry ice) to -20°C (dashed curve) where it was held for 10 min then recooled at 100°C/min to -160°C and rewarmed at 10°C/min (solid curve) to -10°C. All the smaller events visible in the 50°C/min runs of graphs (7-12) are invisible here. Since the power input necessary to maintain isothermality between sample and control is linearly proportional to the Cp of a glass transition, it is to be expected that curve simplification as a result of a slower rate would result. One sees that the equilibrium glass transition at (a_1) has moved from -28°C to about -60°C and gotten larger. But there is no evidence of devitrification. This is of course consistent with the notion that the intracellular glass melt must be stable to ice formation during warming after quench cooling to avoid injury-and we know the tissue resists quenching from -20°C.

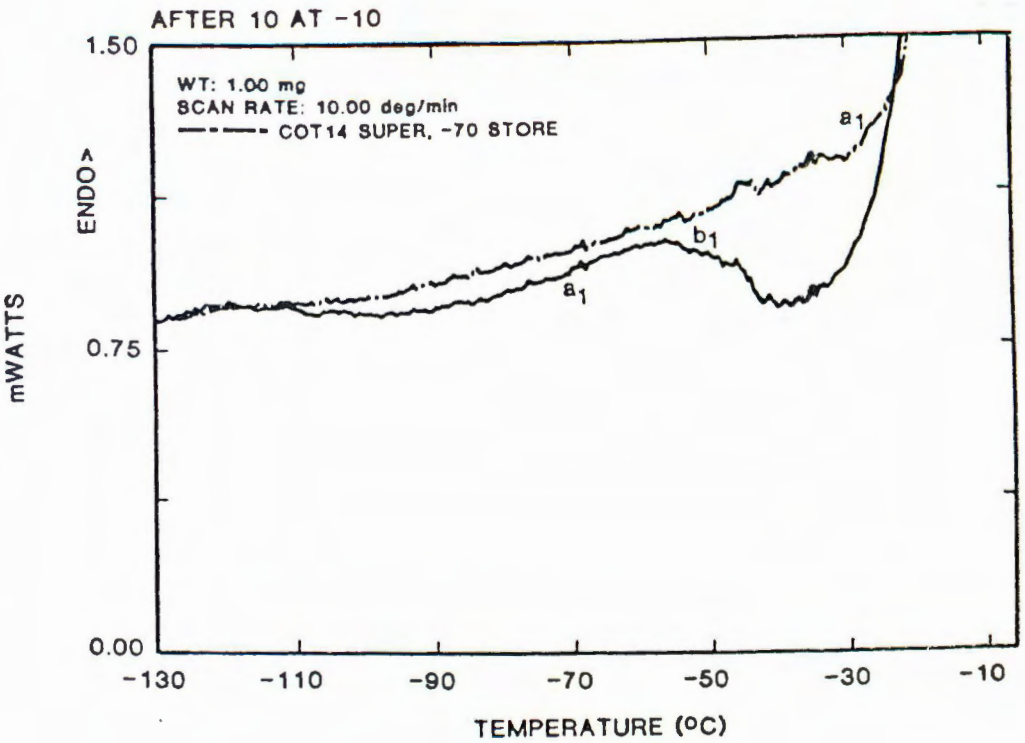

Thermogram 14

The same sample as graphs (13-17). The dashed curve represents 10°C/min warming after removal from storage. Note that there appears to be an equilibrium glass transition at (a_1). The solid curve is 10°C/min warm after 10 min annealing at -10°C followed by 100°C/min cooling to -160°C. The glass transition is much larger and at a much lower temperature (~-75°C) and it is followed by a marked devitrification (b_1). This is consistent with the idea of the instability of the intracellular glasses after quenching from -10°C as well as electron microscope data and biological data (see Biological Results Figure IV and Electron Microscope Results Plate series 3) indicating that the instability first appears at quenching temperatures between -10°C and -20°C.

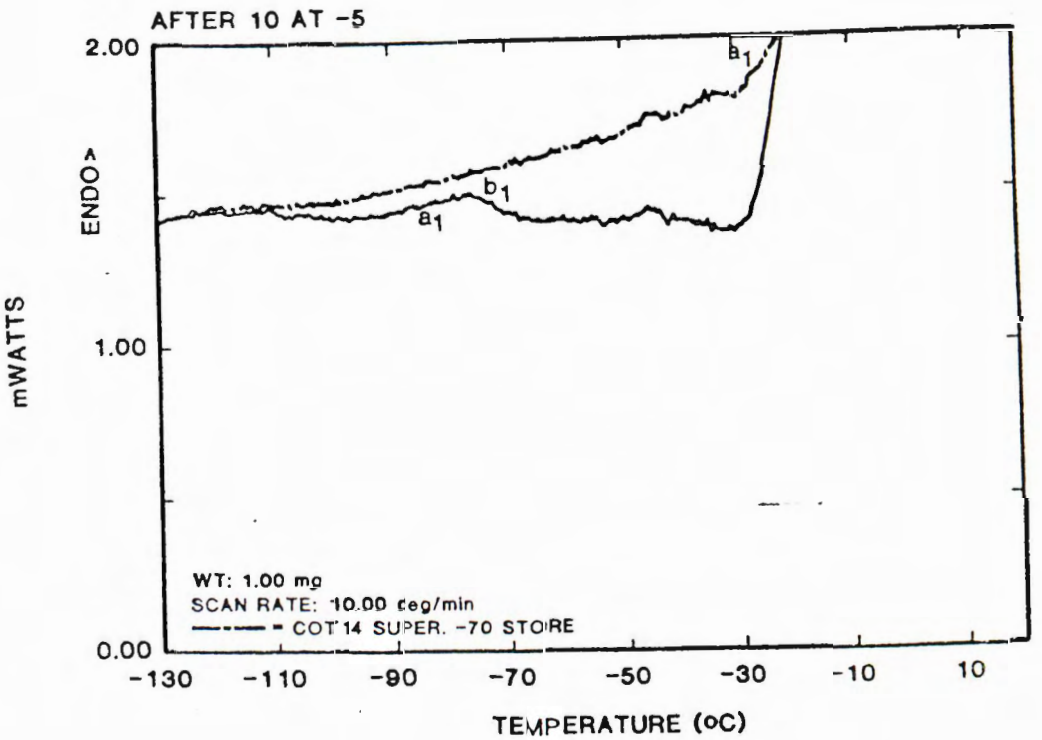

Thermogram 15

The dashed curve represents the warming of the slowly cooled, fully superhardy sample after storage at -70°C. The solid curve shows what happens to the warming curve after 10 min annealing at -5°C, followed by 100°C/min cooling to -160°C. Note that the glass transition (a_1) in the -5°C annealed run is at a lower temperature (~-95°C) than after annealing at -10°C (graph (14)) but is not as large. The latter is probably due to the larger devitrification (b_1) in the -5°C sample obscuring the increase in heat capacity due to glass melting by emission of latent heat of freezing. See graph (16) for direct comparison.

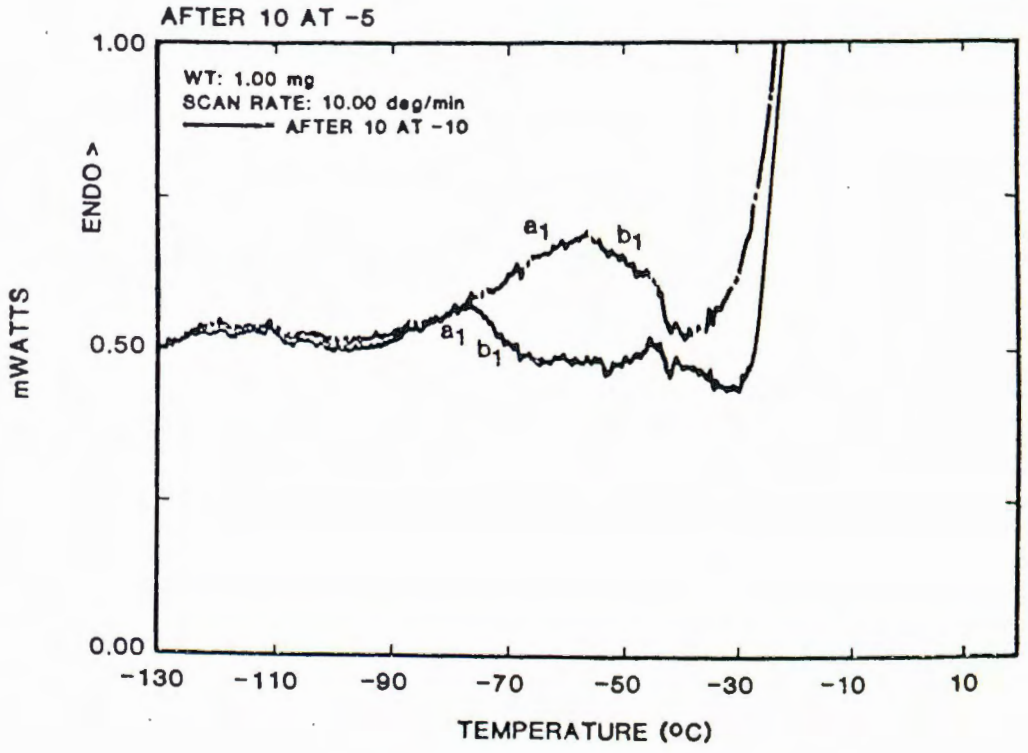

Thermogram 16

This graph shows the 10°C/min warming of the superhardy material annealed 10 min at -10°C then quick cooled to -160°C (dashed curve) vs. -5°C annealing followed by quick cooling to -160°C. The decrease in temperature of the glass transition-devitrification (a_1,b_1) and the larger devitrification (b_1) in the -5°C sample are clearly shown.

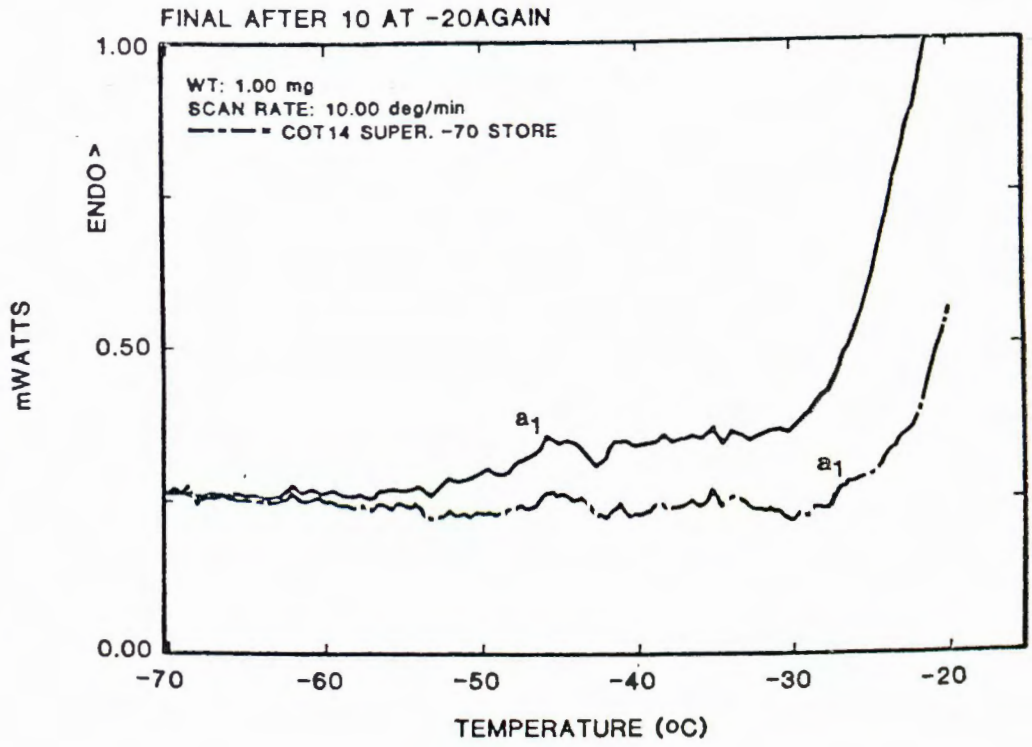

Thermogram 17

If the cellular system is acting as a nearly perfect osmometer at temperatures >-28°C then reannealing the sample initially equilibrated at a high temperature at a lower temperature (but still >-28°C) should restore the thermal characteristics of equilibrium at the lower temperature. This shows the 10°C/min warming of the sample after 100°C/min cooling from -5°C to -20°C then 10 min annealing there followed by 100°C/min cooling to -160°C. Note that once again only stable glass transitions (a_1) are seen, no devitrification are seen. Not only does this fit the 3' glass model, but it also shows that, despite repeated lethal intracellular freezes (Thermograms (14-16)) there is no immediate loss of: (1) the ability of the cells to act as osmometers; (2) the ability of the plasmalemma to resist penetration by extracellular ice; and (3) the ability of the cells to avoid heterogenously nucleating intracellular ice during deep supercooling. Since the cells are definitely lethally injured this degree of intactness is remarkable.

anneal (solid curve) to the -10°C anneal (dashed curve) the amplitude of the glass transition appeared to grow smaller after -5°C annealing, although the devitrification was apparently larger. Since the devitrification may simply have overwhelmed the glass transition, this is not too surprising. Thermogram (17) shows that reannealing at -20°C (solid curve) returns the record to virtually the same form as the first annealing at -20°C (Thermogram (13)), again demonstrating the continued capability of the overstressed cells to act as osmometers.

The last set of Thermograms (18-26) illustrates the supercooling behavior of the fully superhardy wood. The fact that the intracellular solutions, if sufficiently dilute to begin with, can experience freezing during cooling at $\geq$50°C/min (homogeneous nucleation) is of great importance to the interpretation of the warming and mortality data as well as the microscopic results. Here samples were annealed for 10 min at temperatures ranging from -25°C to thaw, then cooled at 50°C/min to -140°C, the thermal behavior being recorded during the cooling. After each cooling, the samples were rewarmed at 100°C/min to the staring temperature of the next run. Since each succeeding run for temperatures above -15°C was annealed at a higher temperature, any ice that did form intracellularly was melted before cooling commenced again. Throughout this set of records the solid curve represents fast cooling from -15°C.

In Thermograms (18) and (19), quench from -25°C and -20°C respectively, very little in the way of events can be discerned. Area (a_1) on the solid curve may be slightly exothermic (indicating some homogeneous nucleation) but the evidence is weak. It should be noted that the order of these records is -15°C, first quenching temperature, -20°C next,

-25°C third. Thus if intracellular freezing occurred during the first fast freeze from -15°C, the intracellular ice may not have melted upon rewarming to -20°C. This would then preclude the observation of further supercooling events upon recooling. However, the electron microscope results (which see) indicate only a small amount of ice formation upon warming after a -15°C quench at 24x this cooling rate and a 10x slower warming rate. Also, Thermogram (5) clearly demonstrates that at equilibrium at -25°C a significant fraction of the intracellular medium has a low glass transition temperature, below -50°C. Thus, cooling at 50°C per minute may well have allowed enough water to escape from the cells such that no homogeneous nucleation took place in the -15 quenched run. Certainly that is consistent with Thermograms (18) and (19), which show, to very low temperatures, a general endotherm of the -20°C and -25°C quenches with respect to the -15°C quench. The lack of a sudden increase (localized at a certain temperature) in the relative endotherm Y (increase in the distance between the curves) appears to argue in favor of simple increased availability of diffusible water in the -20°C quenched run as opposed to the -25°C quenched run.

Thermogram (20) further emphasizes the likelihood that little homogeneous nucleation occurred in the -15°C quench run (solid curve). There is increased continuous freezing of water (general exothermy of dashed curve (-12 quench) with respect to the solid curve). The high temperature homogeneous nucleation at (a_1) is hardly more noticeable and an apparently significant low temperature freeze at ~-120°C (a_2) is in fact an artifact which appears as a dip in the control curve for the run (empty aluminum pan vs. empty aluminum pan). Due to a technical error the control run was only automatically subtracted from the runs with annealing temperatures $\geq$-15°C.

Thermogram (21) shows quenching from $-10^{o}C$ (dashed curve) with event (a_1) slightly larger.

Thermograms (22) through (26) show that at quenching temperatures $\geq -8^{o}C$ there are two relatively high temperature homogeneous nucleations (a_1) and (a_3). Again, (a_2) is artifactual in Thermograms (21) through (26).

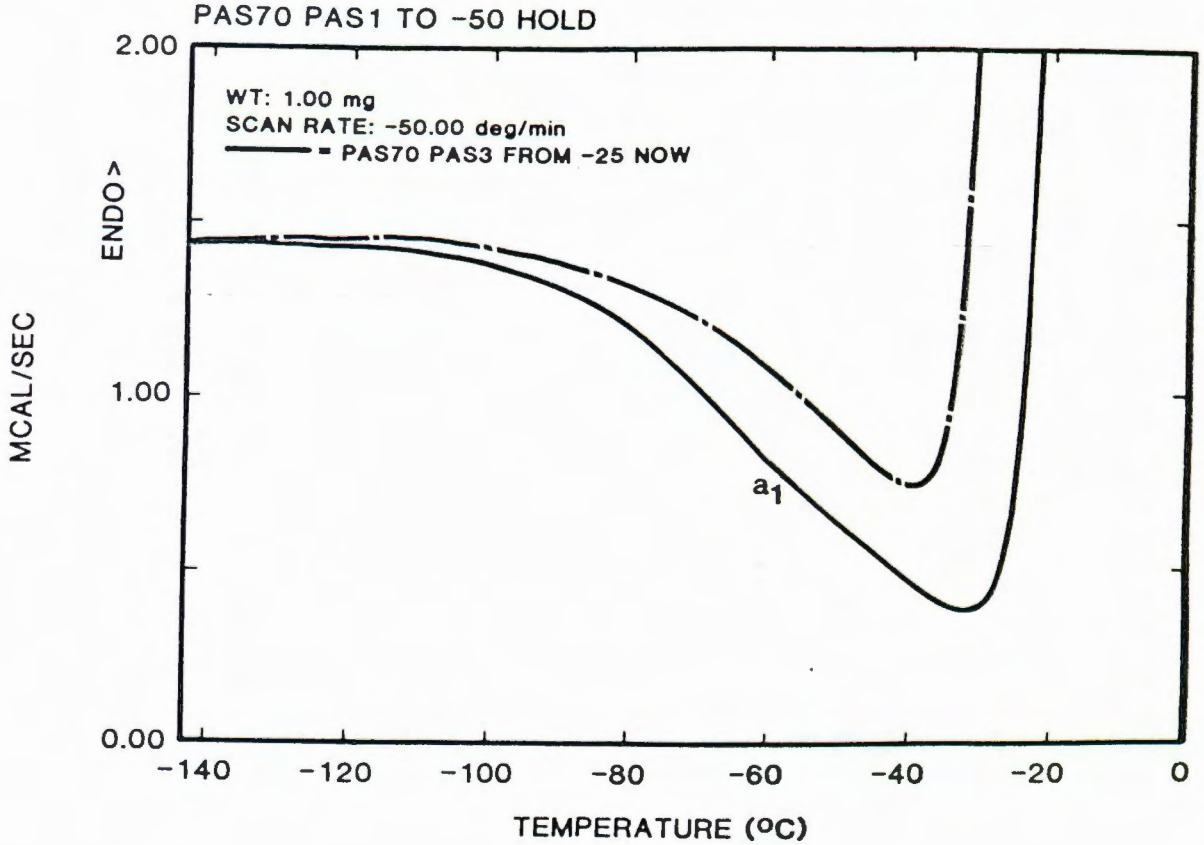

Thermogram 18*

These nine graphs show the thermal behavior of the fully superhardy wood during 50°C/min cooling. The solid curve in all records represents cooling from 10 min annealing at -15°C. The annealing temperature of the other curves is shown on each graph and varies from -25°C to >0°C. Note that the curves of -25°C (graph (18)) and -20°C (graph (19)) annealing are generally endothermic with respect to the -15°C run whereas the runs commencing from -12°C to thaw are progressively more exothermic. This is due to the progressively larger amount of water diffusing out of the cells to ice with consequent increases in self generated heat of fusion during cooling as the annealing temperature is raised. Since "event" (a_2) is an artifact, actual intracellular freezing events are not easy to discern until the event (a_1) appears at -60°C in the -10°C annealed run (graph (21)). Certainly the events (a_1) and (a_3) are not apparent when annealing is carried out below -10°C. Thus the notion that lethal amounts of ice only form on warming after quench cooling from -15°C is supported. In fact, the graphs (20) and (21) suggest that significant intracellular ice may not form on cooling of fully superhardy material until the quenching temperature is -10°C or higher.

*The caption refers to all nine Thermograms, numbers 18-26 inclusive.

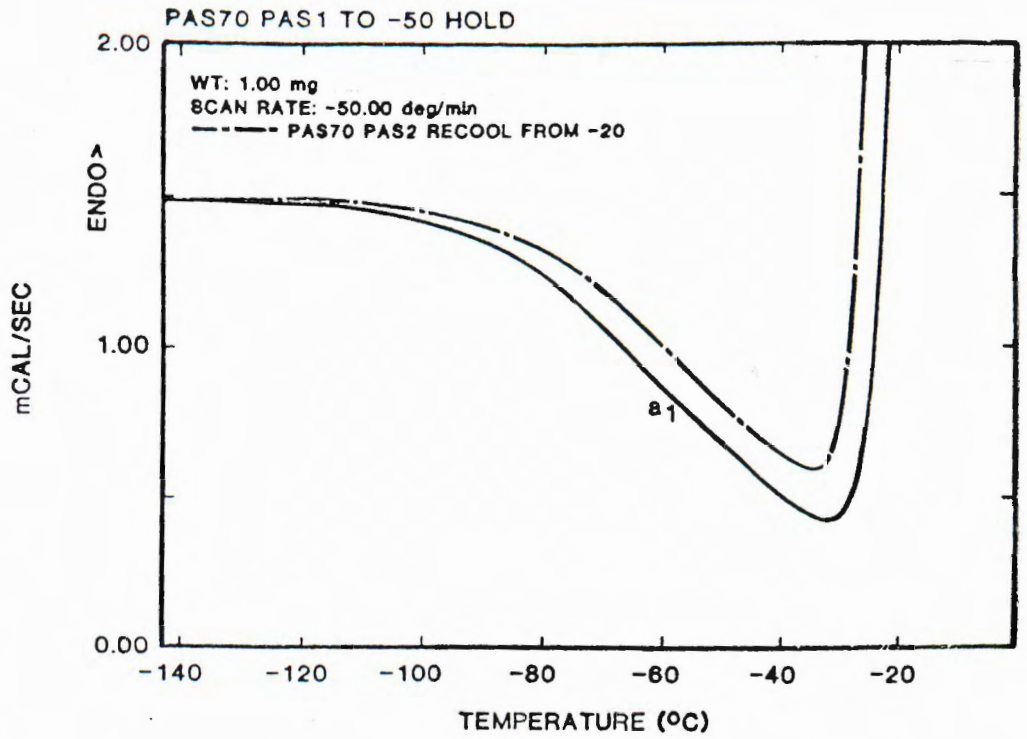

Thermogram 19

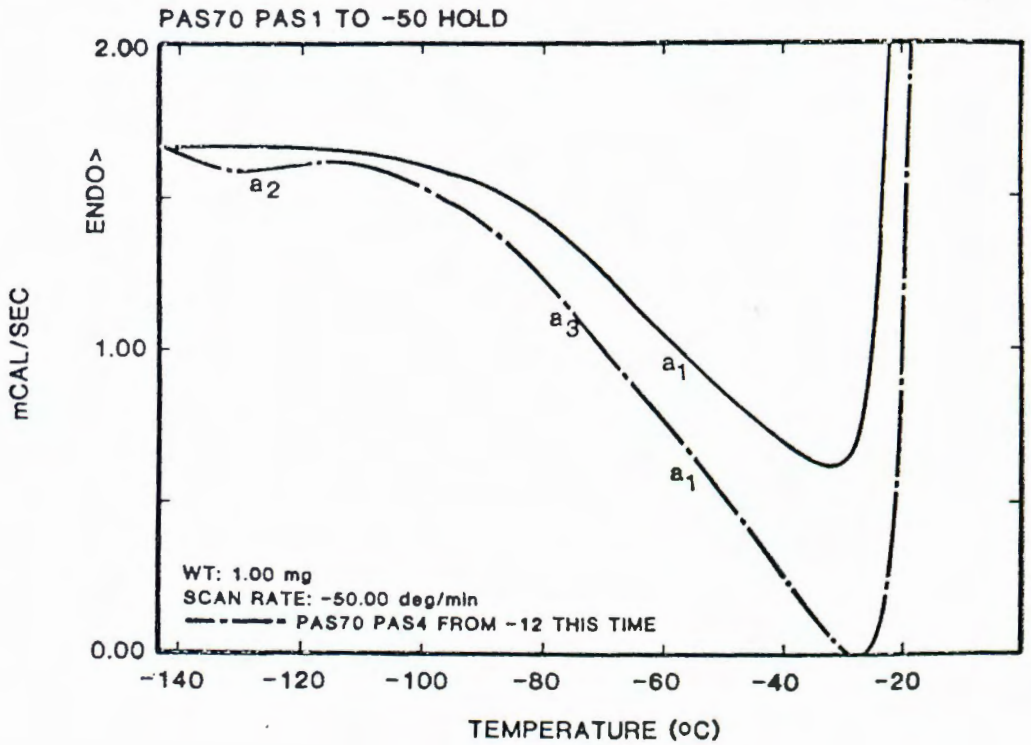

Thermogram 20

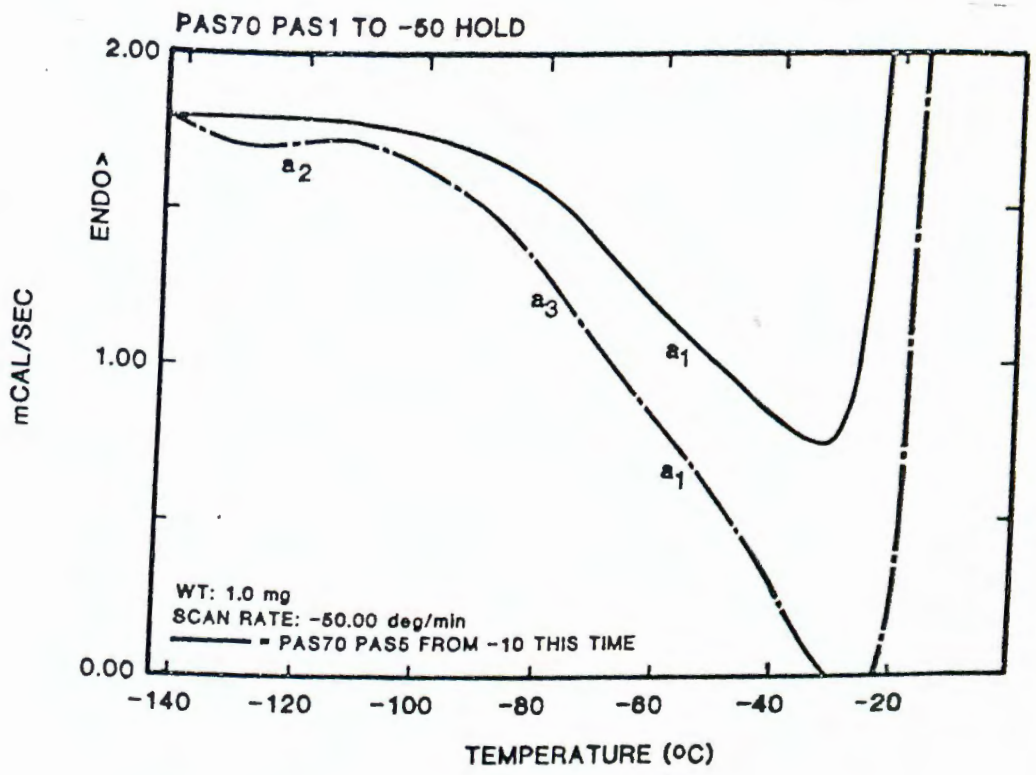

Thermogram 21

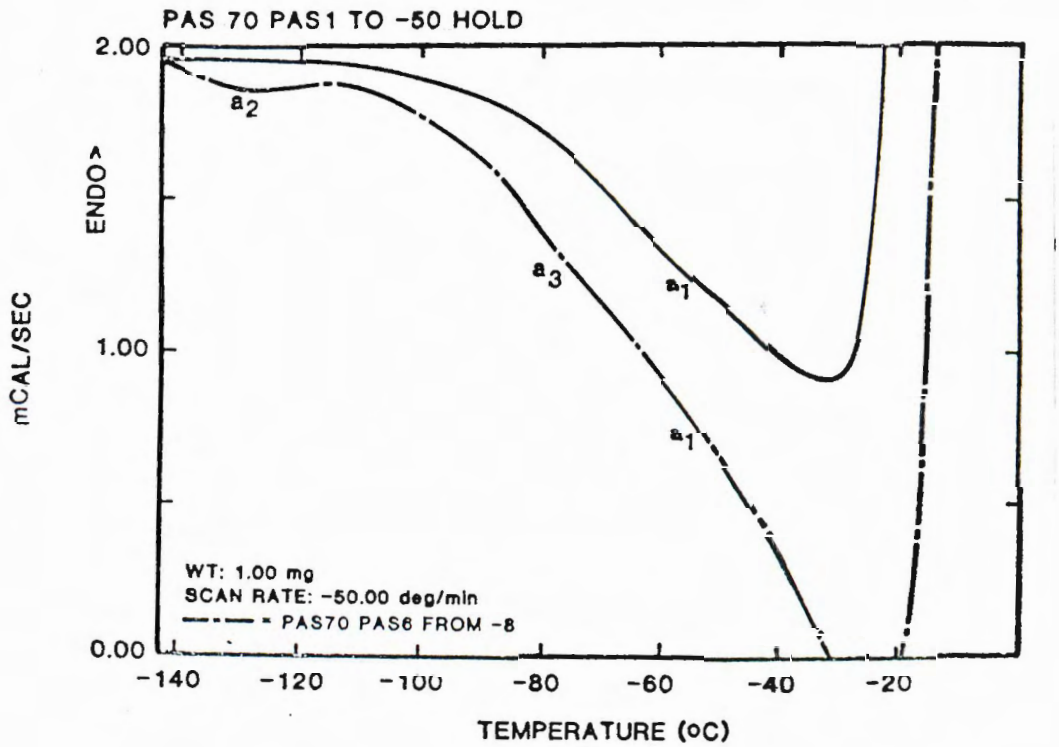

Thermogram 22

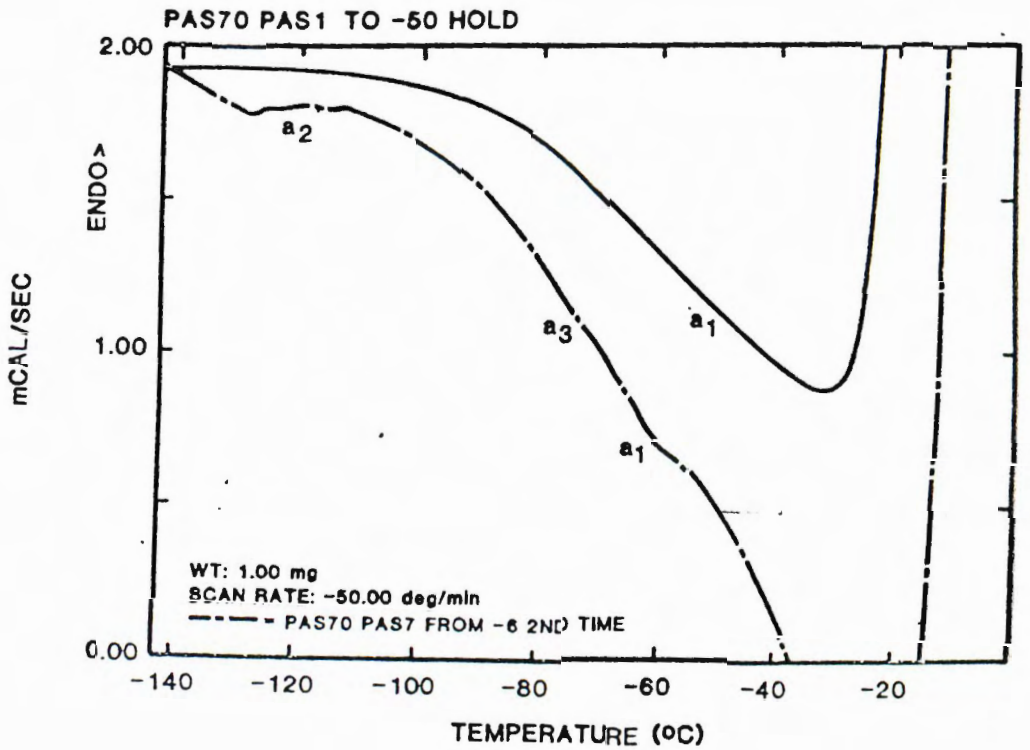

Thermogram 23

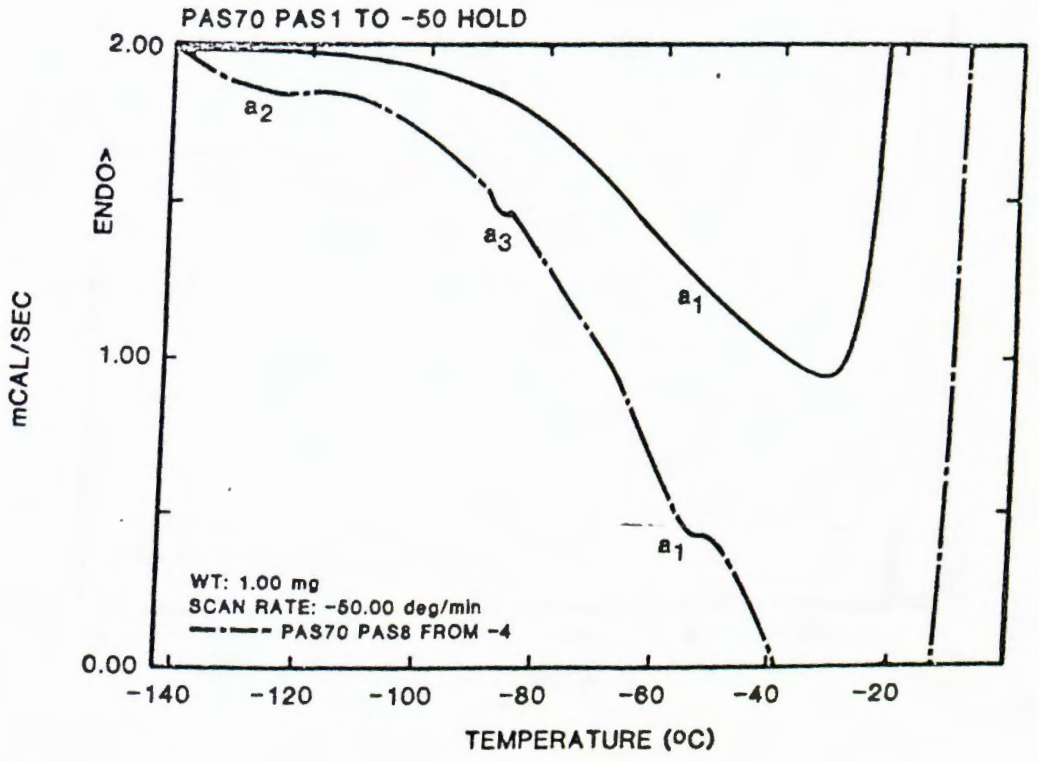

Thermogram 24

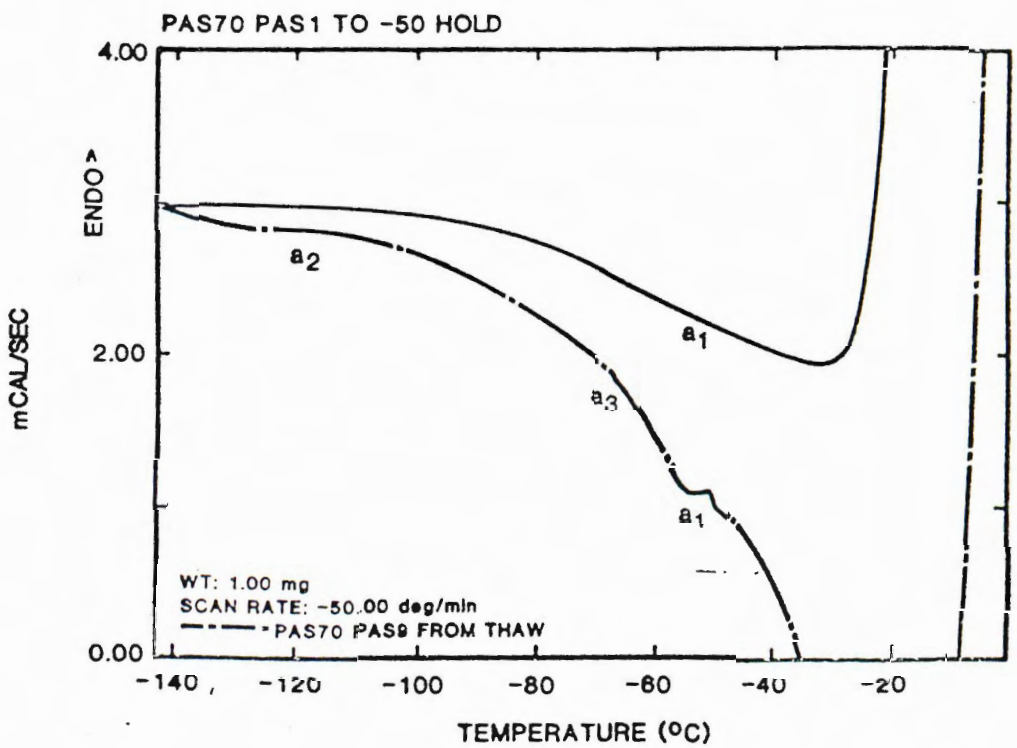

Thermogram 25

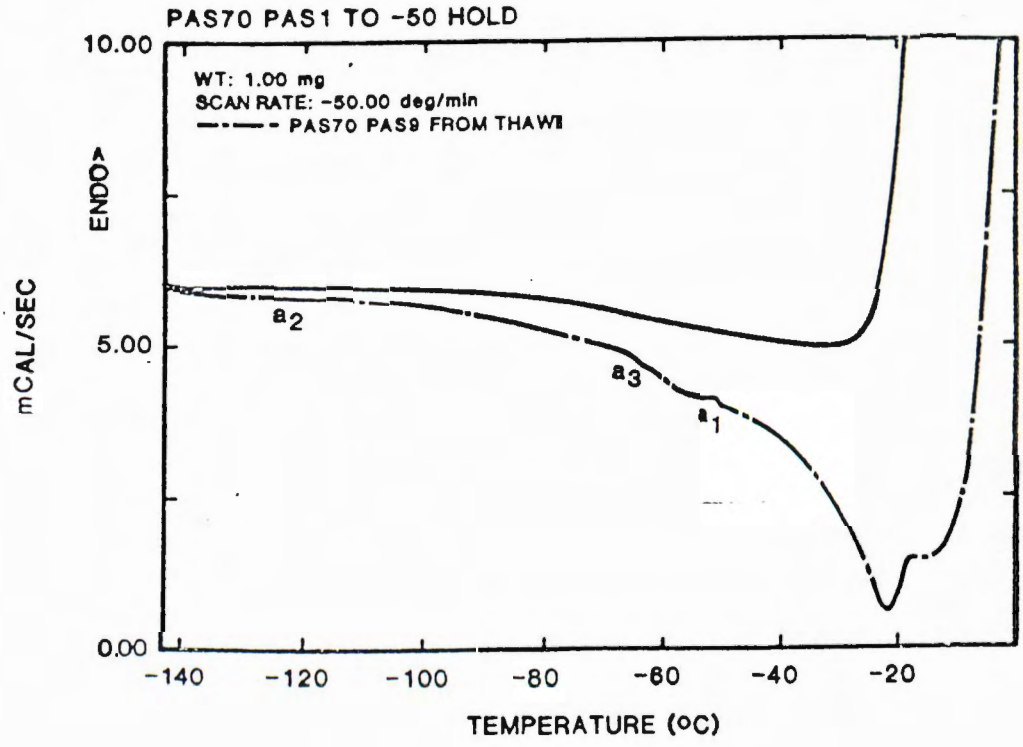

Thermogram 26

Discussion

It is model (3) that most closely fits the data. Thus, the essential assertion of this thesis is that the fully superhardy Populus cells elaborate one or more substances intracellularly during the autumnal 'hardening off' period to the extent that when the cells are in equilibrium with ice at about -28°C the bulk of the intracellular solutions becomes a glassy solid. To this model should be added two additional elements: (1) An unknown quantity of intracellular material and its associated water has a small equilibrium glass transition at -45°C, and (2) a second unknown quantity of intracellular material and its associated water has very small equilibrium glass transition below -70°C.

To analyze all the models in greater detail we shall re-examine them in light of the six questions posed in the overview.

Model (1)

Model 1 postulates that superhardiness is resistance to extreme dehydration and volume loss. It is addressed by answering Question (1).

Question (1) was: How is water partitioned between intracellular and extracellular spaces during freezing and what is the resultant cell volume as a function of temperature below 0°C? The data on cell volume obtained by light microscope observations of cells in $CaCl_2$ solutions clearly establish a minimum volume for the superhardy Populus cells of 35-40% of initial volume.

The tender cells, in contrast, manifest a minimum volume of <10% of initial volume. Thus modest loss of volume is correlated with the hardy state and this tends to rule out model 1. The calorimetric measurement of water partioning further corroborates this finding. Virtually all the water is initially intracellular in the superhardy wood. By -20°C at least 12% of this remains unfrozen, so extreme dehydration does not occur.

Model (2)

Model (2) postulates that the cells might elaborate a large quantity of hydrate forming material so as to mitigate cell volume loss and at the same time provide extreme dehydration resistance. The model's veracity is addressed by questions (4) and (5).

Question (4) is: During a two-step cooling procedure consisting of slow freezing to a high subzero temperature followed by fast cooling to the temperature of liquid nitrogen, how high does the lower limit of slow cooling have to be for there to be ice present in the intracellular fluids either during the cooling step or after slow warming? Question (4) addresses the resistance to freezing of the intracellular fluids as a function of water content. Question (5) is: How does intracellular ice formation correlate with mortality of the tissue after two step cooling? Together the answers to these questions delineate the extent to which the stability of the intracellular fluid correlates with tissue mortality. This correlation can then be used to infer whether superhardiness is limited by the appearance of intracellular ice and whether there is an intracellular composition which is both fluid and resistant to intracellular ice formation no matter what the cooling/warming regimen applied to that composition. If no such composition exists that implies that all fluid water must be removed from the cell (leaving only water of hydration) to achieve superhardiness. The data present a very clear answer to these two questions. The 10°C/min DSC warming data of fully superhardy Populus slowly cooled to -70°C, when compared to the 10°C/min warming data from the same sample after annealing at -20°C makes a clear case for the establishment of a stable intracellular glass forming solution by -20°C. The glass transition at equilibrium at -20°C appears to be about -50°C but no devitrification is seen on warming. This data is heavily augmented by the electron micrographs of fully superhardy material quenched in LN_2 from -20°C

then reinserted at -27°C recooled to -70°C then rewarmed at 3°C/hr with the same survival as controls (see Appendix for details). The cells showed no evidence of intracellular ice as seen in the relevant micrographs (Figure series 3, Results). Thus model (2) is eliminated from consideration because the combined DSC - LN_2 quench - mortality data indicate that when the fully superhardy Populus cells are in equilibrium at -20°C they go through a glass transition at about -50°C but they do not devitrify between -50°C and -20°C upon slow warming. This means that to achieve complete freezing resistance below -20°C, the cells are not filled with 'bound water' in a lower free energy state than ice. They are filled with a glassy melt. It should be noted that this is in sharp contrast to completely drought resistant mosses such as Tortula ruralis or brine shrimp eggs (6,16,75). When these organisms are drying out they have virtually no freezing resistance, but when all remaining intracellular water becomes thermally and spectroscopically silent water of hydration, they are completely resistant to freezing. This changes in the case of the moss during fall 'hardening off'. When dormancy is complete the drought resistant northern mosses are completely freezing resistant even when initially hydrated.

Model (4)

Question (2) asks whether the low extracellular water content present in the superhardy plant is necessary to survival. The affirmative answer proved surprising for several reasons. Not only were water loaded superhardy twigs killed completely by slow freezing to -35°C, but they froze intracellularly above that temperature. This is clear, since superhardy twigs in the normal dehydrated condition show no evidence of intracellular ice after cooling to -20° C or below at 3°C/hr followed by cooling at any rate to -196°C then slow warming. Thus the ice must have penetrated the water loaded cells during the

slow cool to -35°C. This is in agreement with a substantial body of work by Olien (55) which indicates that moderately hardy wheat cells adhere to extracellular ice if large amounts of it are present and are killed by it during osmotic stress. However, Olien did not unequivocally demonstrate that ice penetrated the cells under these conditions. Since model (4) postulates tolerance of intracellular ice as the key element in the superhardiness of the Populus, this observation is in sharp disagreement with that model.

Question (3) is: Are ice crystals present in the intracellular fluids of slowly frozen Populus? This question is the converse of question (2) from the experimental point of view. That is, when observable ice is present throughout the cell, as in the water loaded material, massive injury results and model (4) is put in doubt, but one could assume that under conditions of slow cooling to a very low temperature non-lethal ice crystals too small to be observed in the electron micrographs (<10 nm) might form in tissue that is in the normal extracellular dehydrated state.

This is a much harder question to answer definitively. In the non-water loaded wood if the ice forms slowly above -35°C there is no reason to believe the crystals would be smaller than the ice that formed in that temperature range during slow cooling subsequent to water loading. Thus the evidence compels us to consider only ice formation below -35°C during slow cooling of normally dehydrated wood. This might produce an exothermic event at the freezing point upon fast cooling from -35°C in the DSC, but no such exotherm is observed for material cooled to -20°C or below slowly, then quick cooled. If one argues instead that the ice can only grow slowly at its nucleation point, so that quick cooling allows nuclei to form but no significant ice growth (and therefore no detectable DSC signal), then slow warming after quick cooling should still produce an identifiable devitrification event. The

10°C/min warming scans of material quick cooled from -20°C or below show no such event. The fact that they clearly show a lower temperature glass transition and a higher heat capacity below -30°C than when slow cooling continued below -35°C clearly indicates that the cells are not yet at minimum water content at -20°C and the intracellular contents are still fluid. The only other alternative would be to postulate that the rate of homogeneous nucleation and the rate of crystal growth are both very slow at the temperature ($\leq$-100°C, see 47,61) at which ice would be expected to form from homogeneous nucleation in cells in equilibrium with ice at or below -35°C. Thus only slow cooling below -110°C would produce ice in the cytoplasm. Early biological experiments in this study included slow cooling to -160°C and slow warming with no mortality, but the direct thermal measurements are lacking. However, if the intracellular solution is fluid below -110°C (freezing can only occur in the melt) when it is in equilibrium at $\leq$-35°C, it surely will not display large glass transitions well above -110 C when in equilibrium at temperatures $>$ -35°C. Nevertheless, that is what the DSC records show in great detail. Thus model (4), tolerance of intracellular freezing is completely ruled out, and the likelihood of submicroscopic ice crystals in the slowly frozen cells is likewise very low.

Model (5)

Only two models are left for consideration: (3) the high temperature intracellular glass formation hypothesis, and (5) the extreme depression of homogeneous nucleation, low temperature intracellular glass formation model. Since the intracellular equilibrium glass transitions appear to be at about -45°C and -28°C model (5) can be discarded.

Comparison of Superhardy Wood to Aqueous Glass Forming Solutions

Figure (1) shows the supplemented phase diagram of aqueous 30,000 MW PVP (from 21,47). This highly soluble polymer has an equilibrium glass transition at about -35°C (where the Tg-Tm curves cross) and is thus a suitable model for the major glass former in the Populus.

Note that in MacKenzie's measurements detection of homogeneous nucleation (the T_h curve) is confined to the range -40 to -60°C and compositions in equilibrium with ice at ≥-5°C or higher. An examination of the Populus data (Thermograms (18-26)) shows that at cooling rates as slow as 50°C/min one of the detectable homogeneous nucleations appears to occur at -100°C. Furthermore, as long as MacKenzie was able to detect homogeneous nucleation in the PVP solutions he was unable to simultaneously detect devitrification (the composition range sets of the two phenomena are mutually exclusive). In the Populus, 50°C/min cooling from ≥-10°C yields both cooling exotherms indicative of homogeneous nucleation and large devitrifications in the DSC warming data (Thermograms (7-12)).

Part of the discrepancy between the biological and the PVP model system data can be attributed to MacKenzie's slow rates: 1.5°C/min cooling and 2-3°C/min warming. Thus one might argue that in Populus at equilibrium with ice at -5°C the homogeneous nucleation and subsequent ice growth rate is fairly slow between -40 and -60°C so that at 50°C/min cooling the intracellular composition is not fully concentrated to its glass transition composition point by the homogeneous nucleation process (dotted horizontal arrows in Figure (1)). At 1.3°C/min this appears to have occurred in the aqueous PVP system - leading to a composition stable to devitrification upon warming. Obviously an analogous supercooling would not occur at 1.3°C/min in the Populus because in that case most water molecules would have sufficient time to diffuse to extracellular ice and the cells would stay close to

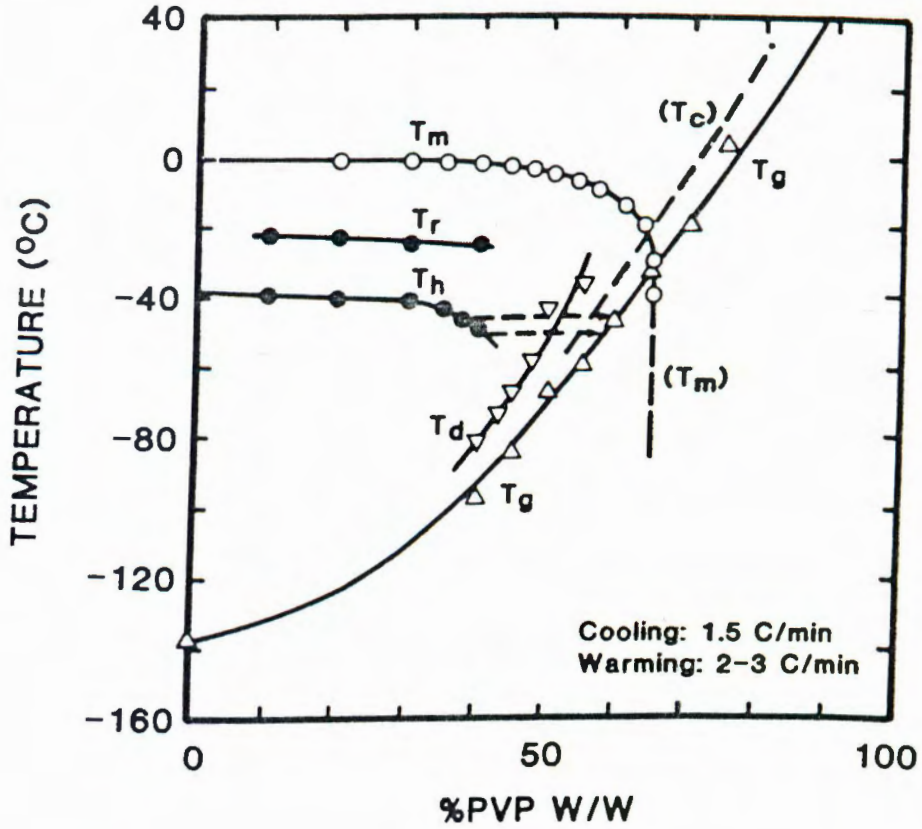

Figure 1

This is the supplemented phase diagram of aqueous, 30,000 mw PVP according to MacKenzie (21,47). The horizontal axis is % PVP w/w. The T_m curve is the equilibrium melting curve, the T_g curve is the glass transition curve, the T_h curve is the homogeneous nucleation curve, the T_r curve is the ice recrystallization curve (upon warming), the T_d curve is the devitrification curve, the (T_c) curve is the hypothesized collapse temperature curve (where the glassy melt begins to flow noticeably in the lab time frame of reference). (T_m) is an extrapolated section of the melting curve. The dotted arrows I have added to show to what composition the homogeneous nucleation of the solution will asymptote at several temperatures. Note that the arrows correspond to compositions that are completely stable on warming, thus the lack of devitrification events after homogeneous nucleation. In the composition region between 45 and 55%, where devitrification is observed, it is presumed that some homogeneous nuclei form in the temperature zone between the T_d and T_g curves on both cooling and warming, but that the volume of ice formed is microscopic and undetectable with presently available instrumentation. The crossing of the T_g and T_m curves is the equilibrium glass transition. Note that there is a fairly large composition region (55-65%) between the most dilute stable glass former and the actual equilibrium glass forming composition. This composition region can be cooled or warmed at any rate and no ice will form as long as heterogeneous nucleators are not present. This corresponds well with the observation that the glass forming moieties in the Populus are stable at compositions somewhat more dilute than the $-28^{\circ}C$ equilibrium glass transition solution.

equilibrium until somewhat above the T_g-T_m crossover.

It is harder to explain the dual homogeneous nucleation (as opposed to the single event in PVP-H_2O) in the Populus by a difference in cooling rates between the experiments. However, considering the number of compartments in the wood it is not surprising that more than one major T_h curve would be recorded. For the same reason it is not surprising that multiple glass transitions are recorded in the Populus upon warming after cooling from a lethally high subzero annealing temperature ($\geq$-15°C). The death of virtually all the cells in the tissue under such circumstances, coupled with the fact that after quench cooling from $\leq$-20°C even xylem often shows callose development, and is virtually never injured in twigs with healthy cambium and phloem, all implies that the multiple glass transition - devitrifications are not representative of behavior anatomically localized to different cell groups. This assumes that the devitrifications are lethal.

The glass forming moiety with an equilibrium glass transition $\leq$-70°C is similar in that behavior to the contents of the tender Populus (see Thermogram 4). Note, however, that when the tender material is annealed at -22°C and quickly cooled, it appears to devitrify upon rewarming. This is in sharp contrast to -20°C quenched superhardy material (Thermograph (13)). This indicates the greater resistance to nucleation/devitrification of the very low temperature glass forming moiety in the hardy material. Note also in Thermograph (5) that tender Populus has a higher heat capacity below -40°C than hardy Populus, presumably due to a larger amount of very low temperature glass forming material, then a lower heat capacity from -40°C to -20°C, due to the large amount of glassy melt forming in that temperature range in the hardy cells, and finally a higher apparent heat capacity above -20°C due to the greater amount of ice melting (due to the initially much more dilute intra-

cellular contents in the tender material).

One might assume that the normal component of intracellular salts or small organic molecules, concentrated by plasmolysis, is the very low temperature glass forming moiety in both the tender and hardy wood albeit with an altered profile of individual molecular species. Figure (2) shows that a mixture of NaCl, KCl, with small amounts of divalent salts (Hanks balanced salt solution, Sigma Chemicals) with or without an initial concentration of 5% fetal calf serum shows glass transition-devitrification behavior in the -60°C to -80°C range. The third curve in that figure shows what happens when a third glass forming component, dimethyl sulfoxide, is added. Note that two large glass transitions are observed. This shows that the multiple glass transition-devitrifications observed in the Populus can occur in the same solution; they need not be in separate subcellular compartments.

It is quite possible that the instability of this very low temperature glass former is the primary reason why the superhardy cells are not resistant to quench cooling from temperatures above -20°C. If we refer back to the PVP-H_2O diagram, Figure (1), we see that a PVP solution in equilibrium at -15°C is quite stable to both homogeneous nucleation and vitrification, with a glass transition at about -60°C. This is not surprising since extensive measurements by MacKenzie and Rasmussen (61) have shown that suppression of homogeneous nucleation is $\geq$1.8 x suppression of equilibrium freezing. For polymers the coefficient of suppression relative to ΔTm can be as high as 5x. Thus the homogeneous nucleation temperature of the main glass forming components of the Populus would be $\leq$-70°C and $\leq$-100°C if it is a typical polymer. The transitions in the DSC of partially superhardy Populus annealed only 3 min at -10°C imply that this is below the two high temperature glass transitions when the wood is in equilibrium at -15°C. Thus, since homogeneous nucleation will not occur in the solid glassy solution, it could only occur in

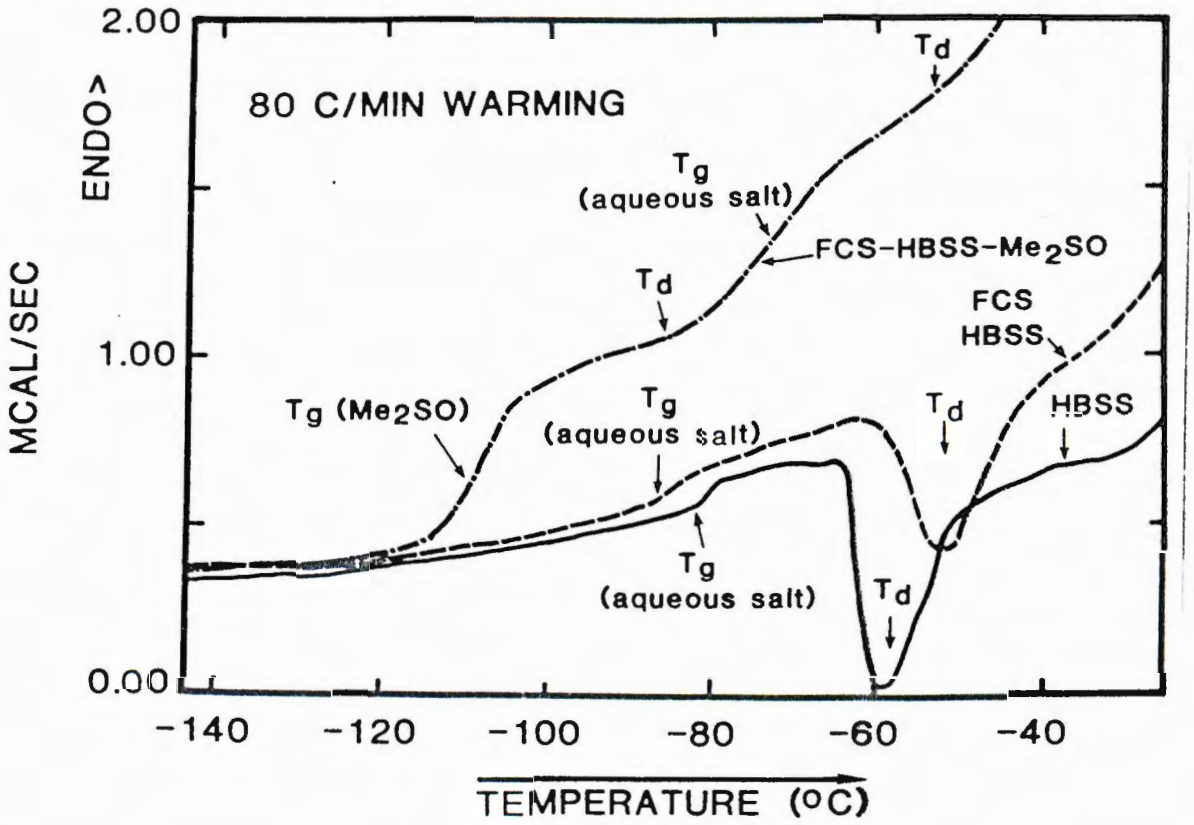

Figure 2

This is the fast warming (80°C/min) record after 100°C/min cooling of various solutions containing 300 mM NaCl, KCl and some divalent salts (Hanks balanced salt solution, Sigma Chemical Co.). The solid curve is just salts and water. The dashed curve has in addition an initial concentration of 5% fetal calf serum. Note that the glass transition is actually at a slightly lower temperature in the protein containing solution, perhaps due to sequestering of salt by the protein, but the devitrification is inhibited (less area above the curve). When an initial concentration of 1 molar DMSO is added (dot-dashed curve) an additional DMSO-H_2O glass transition is observed (-120°C) and most devitrification is suppressed. Note though, that the position of the aqueous salts' T_g is largely unaffected while its magnitude appears dramatically increased. This latter observation is not easily explained. The record demonstrates that a single solution can exhibit multiple glass transition-devitrifications in various microdomains.

the remaining microdomain with a Tg below -80°C. It is very important to grasp that without homogeneous (or heterogeneous) nucleation on cooling no devitrification will occur on warming unless the warming rate is significantly slower so that homogeneous (or heterogeneous) nucleation has more time to occur during the warming cycle. Even extremely slow warming after very fast cooling from -20°C produced neither biological, microscopic, nor DSC evidence of devitrification, so by -20°C even the Tg of the low temperature transition microdomain must be at or above its T_h.

Given that the cells are partitioned into subcellular domains, it is reasonable to inquire whether some domains are more or less stable than others to devitrification after quench cooling. The figures series (3) micrographs answer this question for at least the cytoplasmic vs. vacuolar compartment. The partially superhardy material was quench cooled from -20°C, followed by reinsertion at -27°C, to allow devitrification to proceed (according to the DSC data (Thermograms (7-12)) indicating that -27°C is in the middle of a devitrification region in material in equilibrium at ~-15°C). Only the vacuoles froze, but the twig from which the sample was taken (and all others in that group) died. Fully superhardy material was devoid of thermal evidence of devitrification after quick cooling from -20°C and was also unetched in the micrographs. The -15°C quenched fully superhardy material shows no etching if held below -70°C, but the same material shows significant cytoplasmic etching if warmed to -27°C and then recooled. This again is in complete agreement with the DSC results (Thermographs (18-26)). Thus mortality does not appear to be strictly a function of cytoplasmic freezing in these circumstances but is a consequence of freezing in either cytoplasmic or vacuolar compartments.

In the DSC and microscope results much attention is paid to calculations of the amount of water leaving the cells and cell configuration as a function

of temperature below freezing, respectively. This study is crucial to understanding what strains the hardy cells might be avoiding (when compared with the tender cells) and as a further test of the consistency of the glass forming model as a predictor of the physical behavior of the system. The study was far from wholly successful in attaining these goals. This is in part due to the fact that much of the relevant DSC and electron microscope data on hardy wood was taken on partially superhardy wood and partially due to the fact that attempts to measure cell volume and configuration in actual frozen samples by light microscopy were a complete failure due to the complex refraction and reflection problems encountered in ice filled wood.

Several interesting conclusions can nevertheless be drawn from the quantitative freezing, solution plasmolysis, and drying data. First, the partially superhardy wood that was used for the DSC study (Thermogram (2)) had an intracellular osmolality in the unstressed state of ~1200 mOsm, almost the same as fully superhardy wood. Thus it is not a bad model for the fully superhardy system. The DSC data (Thermograms (1) and (2) show that both the tender wood and superhardy wood seem to freeze nearly ideally to quite low temperatures (-9°C for the tender material, -20°C for the hardy material). One can ask whether this is consistent with (1) a small organic molecule such as sucrose or glycerol as a cryoprotectant, or (2) a large polymer, perhaps a polysaccharide like hydroxyethyl starch, as a cryoprotectant. Actually, glycerol and disaccharides such as sucrose can be ruled out because they form unstable glasses which have glass transition temperatures when in equilibrium at -20°C of $\leq$-70°C (45) and that is not taking into account the fact that the depression of the freezing point in the superhardy cells' cytoplasm is partly due to concentration of the normal background of KCl, protein, etc.

However, the question of a large polymer remains. If one uses polyethylene glycol (PEG, mw 8000) as a model the volumetric data are very encouraging, but the amount of water frozen out by -20°C in polyethylene glycol solution is inconsistent with the DSC observations of hardy wood. The calculations are as follows (physical data from (32,45)): for a starting concentration of 800 mOsm of PEG in pure H_2O a starting volume of one liter contains about 200 gm PEG and about 800 gm H_2O. The final density is about 1.12 and the final wt. % PEG at equilibrium at -20°C is 52%. Then the equations we want are $200/x = 52/48$, $(200+x)/1.12$ = final volume. Thus the final volume would be 34% of initial volume. A similar calculation yields 41% of initial volume if the initial osmolality is 1300 mOsm. By comparison the figures are 20% and 29% of initial volume for sucrose and 11% and 15% for

NaCl. Thus a mixture of salt and small organic molecules and PEG would tend to have a smaller volume than 1300 mOsm of pure PEG concentrated by freezing to -20°C but a larger volume than 800 mOsm so concentrated. The range of 34% to 41% is in remarkable agreement with the biological (light microscope) volume vs. external osmolality data, for Populus. The DSC data for H_2O frozen out are in sharp disagreement however. The respective figures in that calculation are 77% of H_2O frozen out for a starting concentration of 800 mOsm of PEG in pure H_2O and 72% frozen out for a starting concentration of 1300 mOsm. The calculation for sucrose yields 88% H_2O frozen out for a starting concentration of 800 mOsm and 82% for 1300 mOsm. For NaCl the figures are 92% and 86%. Thus the mixture of PEG, salt, and all organic molecules would be expected to lose about 75% of its water. The best explanation for this error is the tendency of the DSC to overestimate heats of fusion in samples with very poor heat conductivity. This point is discussed in some detail in DSC materials and methods. An examination of the other model polymer in this study, 30,000 MW PVP, gives essentially the same figure for water freezing out. The apparent molecular weight of the polymer (in ~1 molal solutions) based on colligativity is 330 (47). Thus an 800 mOsm solution is about 21 wt.% and a 1300 mOsm solution is about 30 wt.%. The final concentration at equilibrium at -20°C (see Figure 1) is about 62 wt.%. Thus at 800 mOsm 84% of the water freezes out, whereas at 1300 mOsm starting concentration 74% of the initial water would freeze. Thus the percent water freezing out would be only about 8-10% low instead of 15% low as in the PEG-salt-protein system. Nevertheless, unless the biological material were an unusually low density polymer, the smaller discrepancy in enthalpy data engendered by PVP like behavior would be negatively compensated by an estimated volume that was too small. Still, if the polymer actually was in equilibrium with ice at -20°C in a 62% solution

while the starting concentration at 800 mOsm was 21%, and if the final density was about 1.12, as PEG, then the estimated final volume range would be between 30% and 43% of initial. This is still reasonable.

This PVP-like model is not consistent with electron micrograph data on dried Populus in which wood that was predried to 60% of normal water content was shown to be alive before freezing and resistant to homogeneous nucleation when quench cooled from 0°C (see Micrograph 1(e)). For PVP at a starting concentration of 800 mOsm, removal of 40% of the water would raise the concentration to 1.3 osm. Thus the cellular freezing point depression would be less than 6°C if it behaved in essentially the same manner. One possible explanation is that the uneven drying of the wood and the random nature of the fracturing process combined to give replicas of cells that were considerably drier than the mean of the whole wood.

The information presented in the electron microscopic results on cell configuration is relevant to a number of current theories on why plant cells die at subzero temperatures. The work of Burke and others (15,26,43) has confirmed that xylem ray parenchyma in many northern woody plants supercool and then freeze at temperatures ranging from -10°C to -45°C. Microscopic evidence indicates that in many of the deep ($\leq$-40°C) supercoolers little or no cell collapse occurs (12). Clearly the evidence presented in this thesis points to viscoelastic collapse of the Populus cells' walls concurrent with cellular shrinkage to maintain equilibrium with the external ice.

Since the minimum cell volume is 30-40% only about 30% of the linear dimensions need be lost during this collapse. Since it must be difficult to collapse secondary cell wall beyond a certain point, this large minimum volume may be an important element in the complete cold resistance conferred by the glass forming intracellular contents. In addition, the fact that the cell membrane appears to stick to the cell wall during osmotic collapse implies

that sudden deep freezing of many plants at temperatures considerably above the homogeneous nucleation temperature of water may be the result of negative osmotic tensions that build up in the membranes as a result of resistance of the cell walls to collapse beyond a certain point (12,41,43,95,96). This could lead to the membranes tearing away from the cell wall and resultant ice penetration at some temperature defined by each membrane's resistance to such stress. The very low minimum volume of the tender cells supports this notion, since loss of 60% of the linear dimensions of the cells would engender a very large deformation of something as stiff as a mature cell wall.

In those plant cells that die from some osmotic strain other than sudden intracellular freezing (non-supercoolers) it has been traditional to postulate that direct injury to membranes is the primary cause of damage (22-25,28,47,52,55,96). Work on wheat cells in this laboratory by R. J. Williams (95) and the extensive work on rye protoplasts by Steponkus (96) has shown that, in water solution, osmotically stressed hardy cells appear to reversibly lose plasma membrane lipid to internal depots while tender cells appear to lose membrane lipid to external depots. In both cases this appears to occur by membrane blebbing (local invagination). If the freezing rate is not too high (<10x ambient cooling rates) intracellular freezing does not play a part. The results reported in this thesis shed grave doubt on the applicability of these studies to the in vivo situations in very hardy woody plants. There is no electron microscopic evidence of local invagination inward of the super-hardy cells plasma membrane during deep freezing. There is evidence of wrinkling (and thus possible mechanical disruption) of tender cell plasma membranes during deep freezing, but the lack of an external solution makes it difficult to imagine losing lipid to the external medium. There is no evidence, in either superhardy nor tender cells slowly frozen that organellar

membranes are grossly disrupted (see Micrographs (2a,c) and (2g,h,i)). Thus the electron microscope evidence does not support the notion that the internal cellular membrane system has to be reconstituted after severe freeze dehydration. Such a model has been proposed in the case of desiccation injury at temperatures >0°C (6). Just as important is the evidence that even superhardy Populus cells, if immersed in dilute aqueous solution, freeze intracellularly upon cooling at ambient rates (<5°C/hr). Thus, it is safest to assume that woody plants are quite different than the herbaceous monocots now being used as models, and even the monocots may be behaving quite differently in vivo than in vitro.

Speculation

This study has concentrated on the physical aspects of extreme freezing resistance: the state of water in superhardy cells and the morphology of those cells as a function of freezing stress. The discovery that the cells become largely an amorphous solid between -25°C and -30°C prompts several predictions that have yet to be tested. The 3 glass model predicts that the hydrostatic pressure resistance of the wood should increase markedly below -30°C due to the fact that non-fluid cytoplasmic components cannot leak through membranes or as easily denature. This increased resistance could help mediate the effects of massive pressures (≥2000 atmospheres) that build up inside frozen trees at temperatures well below 0°C. Early in this study preliminary work indicated that hardy Populus could withstand 1000 atmospheres for 10 minutes at 0°C. Higher pressures were not tolerated. Repeated attempts to measure resistance at higher pressures and lower temperatures have failed due to technical difficulties.

Another prediction that emerges from the model is that extreme centrifugation of the cells at ≤-30°C should produce very little sedimentation of cell

contents as examined by freeze fracture-freeze etch electron microscopy. Attempts to carry out experiments of this type have floundered on inability to maintain a low enough temperature during centrifugation.

The model clearly implies that Tq (the maximum quenching temperature for survival equal to that of controls) ought to rise significantly if the low temperature bath is at dry ice temperature as opposed to LN_2. Preliminary work with partially superhardy material (survived quenching to LN_2 from -50°C) showed no change in Tq when twigs were plunged into liquid freon in dry ice. This work will be repeated with fully superhardy material. Certainly, the inability to see second freezes above -50°C when the tissue is cooled at 50°C/min from temperatures as high as -4°C in the DSC is evidence that the Populus cryoprotective system is quite useful in preventing winter injury of the sunscald type (41). The latter is presumed to occur when the winter sun warms tissue several tens of degrees above ambient air temperature and, when the sun disappears behind a cloud or a physical obstruction in the environment, rapid cooling (several degrees C/min) occurs. This is assumed to lead to a large degree of intracellular supercooling and consequent intracellular freezing.

The next phase of this work is to characterize the chemical nature of the major glass forming moieties and thence to ascertain the genes involved in the production and regulation of those products. It is hoped that the superhardiness gene system of the Populus will prove amenable to transfer to less hardy woody plants at some future date. It is also hoped, in this laboratory, that the glass forming moiety of the Populus may prove to either (1) bolster the effects of penetrating cryoprotectants when used as an extracellular cryoprotectant and/or (2) be introducible into mammalian cells, perhaps through liposome packaging, as an enzymatically degradable intracellular glass former. There is ample evidence from work done by Dr. Takahashi and me that synthetic

extracellular glass formers, such as hydroxyethyl starch, perform as in (1) above, halving the lower limit of initial DMSO concentration conferring complete cryoprotection in human monocytes. Little information is available on hypothesis (2) above, but the plant rapidly (<2 weeks) degrades its cryoprotectant (on the basis of loss of hardiness) in warm, long day conditions, so the enzymatic machinery for rapid, controlled degradation is potentially available. Since there is evidence that when penetrating cryoprotectants are needed in high concentration, different organs may require different cryoprotectants (35) to withstand frozen storage, the hopes for preservation of whole organisms with high concentrations of penetrating cryoprotectants alone seems remote.

Conclusions

The main points of this study are summarized as follows:

1. Populus balsamifera var virginiana Sarg. appears to make, as part of its hardening off process for the winter, at least 2 major high temperature aqueous glass forming substances and one low temperature aqueous glass forming material.

2. The above substances appear to have T_g-T_m crossover points on the supplemented phase diagram of circa -75°C for the low temperature system, -47°C for the intermediate temperature moiety, and -28°C for the high temperature material.

3. Despite the fact that both high temperature glass forming substances go through glass transitions well above any observable homogeneous nucleation when the cell sap solution is in equilibrium at -15°C, slow rewarming from a LN_2 quench from -15°C is invariably fatal. This appears to be due to the third low temperature glass forming moiety which devitrifies under such conditions upon warming. Thus, after quenching from -15°C, the intracellular solution appears to contain ice nuclei. The fact that the -28°C glass former goes through its glass transition below -50°C when the cell is in equilibrium at -15°C provides ample opportunity for this intracellular ice seed to grow upon slow warming between -50°C and the -28°C equilibrium glass transition point. This hypothesis is borne out by both DSC and electron microscope data.

4. Quench cooling is not lethal to completely superhardy twigs of equilibrated samples from -20°C or below no matter what the cooling/warming regimen below this temperature. In part, this may be due to the fact that by -20°C even the lowest temperature glass former goes through its glass transition at a temperature above or at its homogeneous nucleation point. Thus, upon slow warming, no intracellular nucleation and devitrification occurs to seed the additional glassy melts that form at higher temperatures.

5. In tender tissue significantly more ice melts at high subzero temperatures, upon warming after a very slow freeze, than melts in hardy tissue so treated. Nevertheless, the heat capacity of hardy tissue between -40°C and -20°C is much higher. This is taken as further proof that more water is locked in high temperature aqueous glasses at very low temperature in the hardy tissue.

6. The presence of significant extracellular water is lethal to slow cooled superhardy cells due to penetration of the cells by extracellular ice above -35°C.

7. Neither superhardy nor fully tender cells freeze intracellularly upon slow cooling to very low temperatures under normal in vivo conditions, despite the fact that fully tender cells are killed at $\geq$-2°C.

8. Superhardy cells show no evidence of significant membrane strain upon slow freezing, and they stick to the cell wall. Slow frozen tender cells show extensive membrane wrinkling and stick to the cell wall as well.

9. The intracellular membrane systems of superhardy cells slow frozen to -70°C or quench cooled from $\leq$-20°C are apparently completely intact as far as can be ascertained by freeze fracture-freeze etch electron microscopy. Both blebbing and abnormal clustering of membrane associated particles are absent.

Most of the conclusions reached in this study are new. Natural intracellular glass formation has not been heretofore reported. The reason for extensive loss of extracellular water during 'hardening off' of woody plants has not been reported. The state of membranes and the packing of cellular constituents in hardy wood as a function of deep freezing in vivo, unbiased by synthetic cryoprotection or fixation artifacts, has not been reported. Finally, the demonstration that resistance to freeze damage is resistance to devitrification during very slow warming in quench cooled superhardy wood is a substantial extension of the pioneering work of Sakai (64-74).

Appendix I

Experimental Number	Collection Time	Treatment		Mortality	Callosing	Pmot*	Pcall**
1	Nov. 25, 1981	-20°C store until June 1982, then controls just thawed at 3°/hour; experimental plunged into LN_2 from -20°C, reinserted -50°C, then 3°C/hr to -20°C, hold 1 day, then 3°C/hr to thaw	**Exp.**	0/10	10/10	.44	.07
			Cont.	1/8	5/8		
	super						
2	Nov. 25, 1981	-20°C store until June 14, 1982, then quench into LN_2 from -20°C, then reinsert into -50°C, then run 3°C/hr to -35°C, then 1°C/min to -50°C, then 3°C/hr to thaw; controls to -50°C 3°C/hr, 1°C/min to -35°C 3°C/hr to -50°C, then 3°C/hr to thaw	**Exp.**	1/6	3/6	.3	.58
			Cont.	4/8	2/8		
	super						
3	Dec., 1981	Stored -20°C, then plunge to LN_2 or -75°C on August 11 (results had to be pooled versus control), hold 1 day, then 3°C/hr to thaw; control just 3°C/hr from -20°C	**Exp.**	9/10	1/10	.076	.077
			Cont.	2/5	3/5		
	partially						
4	Dec. - Jan. 1981-82	-20°C store, LN_2 quench in August 1982, reinsert -75°C 3 days, then 12°C/hr to -35, then 4°C/hr to thaw vs. plunge of -20°C material into -75°C, then same	**Exp.**	4/6	1/6	1.0	1.0
			Cont.	5/7	2/7		
	partially						
5	Jan., 1981	-20°C, then quench to LN_2, reinsert -50°C April 15, 1981, 3°C/hr to thaw (on May 6 mortality assessed); controls to -50°C 3°C/hr from -20°C, 3°C/hr to thaw	**Exp.**	0/4	1/4	1.0	1.0
			Cont.	2/9	2/8		
	super						

* = probability that the mortality of the experimental and control samples was from the same pooled set plus the probability of seeing all less likely mortality data based on random drawing from the same pool.

** = same as * but comparing callosing/bud break instead of mortality.

Experimental Number	Collection Time	Treatment		Mortality	Callosing	Pmot*	Pcall**
6	Mar. 3, 1982 partially	Stored 0°C (frozen extracellularly), then controls 3°C/hr to -50°C, then 1°C/min to thaw, then 1 month +4°C; experimental to -50°C, 3°C/hr, then quench LN_2, reinsert -50°C, then 1°C/min to thaw; done on wood stored 0°C early March to late April	**Exp.** **Cont.**	13/13 3/7	0/13 4/7	.007	.007
7	Mar. 3, 1982 super	Stored -20°C until July 15, 1982 then plunged directly to LN2, reinsert -75°C, then 2°C/hr thaw; control just 3°C/hr thaw	**Exp.** **Cont.**	0/4 1/8	3/4 5/8	1.0	1.0
8	Mar. 3, 1982 super	Stored -20°C until July 15, then plunge into -75°C bath from -20°C, then 2°C/hr to thaw; control just thaw 3°C/hr	**Exp.** **Cont.**	0/4 1/8	2/4 5/8	1.0	1.0
9	Mar. 3, 1982	-20°C store, then quenched to LN_2, reinsert dry ice 5 days, then slow thaw in insulated box, or quench directly to dry ice (2 quenches, -196°C and -75°C had to be pooled for statistics) vs. just thaw control	**Exp.** **Cont.**	7/9 3/7	2/9 3/7	.3	.6
10	Mid Nov. 1982 no natural frost partially super	to -18°C at 3°C/hr, quench to LN_2, reinsert -18°C, 3°C/hr to thaw; control to -18°C and from -18°C, 3°C/hr	**Exp.** **Cont.**	16/16 3/13	0/16 8/13	.001	.001
11	Mid Nov. 1982 partially super	to -60°C at 5°C/hr, then quench to LN_2, reinsert -60°C, then 5°C/hr to thaw; control no freeze at all	**Exp.** **Cont.**	2/10 4/31	3/10 11/31	.6	1
12	Dec. 1982 collected partially	to -20°C at 3°C/hr, then quench to LN_2, reinsert -20°C, controls to -20°C and back at	**Exp.** **Cont.**	5/8 4/18	2/8 8/18	.08	.42

Experimental Number	Collection Time	Treatment		Mortality	Callosing	Pmot*	Pcall**
13	Jan. 1983 collected very mild conditions partially	to -20°C at 3°C/hr, then quench to LN_2, reinsert -20°C; control to -20°C at 3°C/hr	**Exp.**	13/13	0/13	10^{-7}	10^{-7}
			Cont.	0/12	0/12		
14	Jan. 1983 mild conditions partially	to -20°C at 3°C/hr, then LN_2 quench, then reinsert -20°C, controls to -20 at 3°C/hr.	**Exp.**	17/17	0/17	10^{-9}	.01
			Cont.	4/33	10/33		
15	Jan. 1983 mild conditions continue partially	to -20°C at 3°C/hr, then LN_2 quench, reinsert -20°C, control to -20°C at 3°C/hr	**Exp.**	26/30	0/30	10^{-5}	10^{-5}
			Cont.	1/12	8/12		
16	Jan. 1983 mild conditions partially	to -25°C at 3°C/hr, quench to LN_2 reinsert -50°C, then 3°C/hr to -62°C, 1°C/min to -50°C then 3°C/hr to thaw, control same except slow to -62°C and no quench	**Exp.**	22/29	4/29	.045	.1
			Cont.	11/24	8/24		
17	Feb. 1983 super	3x hardened Feb. 1983 by 0-20°C at 3°C/hr, then to -14.5°C, LN_2 quench, reinsert -50°C 1 day then 2 months dry ice, warm 3°C/hr to thaw out to warm May 2; control to -50°C slow, slow thaw	**Exp.**	30/30	0/30	10^{-16}	
			Cont.	2/37	7/37		
18	Jan. 1983 Artificially hardened by 3 daily excursions to -20°C and back to 0°C at 3°C/hr	to -20°C at 3°C/hr, quench to LN_2, reinsert -20°C control just to -20°C at 3°C/hr	**Exp.**	7/37	11/37	1	.4
			Cont.	7/39	8/39		

Experimental Number	Collection Time	Treatment		Mortality	Callosing	Pmot*	Pcall**
19	Jan. 1983 not artificially hardened partially	to -20°C at 3°C/hr, LN_2 quench reinsert -50°C, 3°C/hr warm; control to -50°C slow	**Exp.**	32/32	0/32	.0035	.03
			Cont.	31/40	6/40		
20	Jan. 1983 artificially hardened 3x to -20°C super	to -20°C at 3°C/hr, quench LN_2, reinsert -20°C, warm 3°C/hr; control to -20°C at 3°C/hr	**Exp.**	13/37	13/37	.81	.31
			Cont.	12/39	9/39		
21	Jan. 1983 Populus 3x artificially hardened: 0°C to -20°C super	to -35°C at 3°C/hr, quench LN_2, reinsert -50°C hold 1 day, then plunge into dry ice 6 days, reinsert at -60°C, then 3°C/hr until thaw; control 3°C/hr to -50°C, hold 1 day, then plunge into dry ice, reinsert after 6 days at -60°C, then thaw at 3°C/hr	**Exp.**	0/15	12/15	1.0	1.0
			Cont.	0/13	10/13		
22	Mar. 1, 1983 after very mild Jan., Feb. 7x hardened: 0°C to -15°C including one accidental excursion to -50°C at 1°C/min super	After 7 cycles to -15°C and one fast cycle to -50°C, 3°C/hr to -15°C, quench LN_2, reinsert -30°C then 3°C/hr to -50°C, then 3°C/hr to warm; control same 7x hardening and fast to -50°C, but slow to -50°C, but slow to -50°C and back, no quench	**Exp.**	22/22	0/22	$2x10^{-9}$	.01
			Cont.	4/24	8/24		
23	Late Feb. 1983 3x hardened super	0°C to -20°C, 3x then plunge to LN_2 from -25°C reinsert -50°C 1 day, then 2 months dry ice then thaw 3°C/hr from -70°C on May 5, to warmth May 9, mortality measured May 17; control to -50°C slow otherwise the same	**Exp.**	0/17	10/17	1.0	.45
			Cont.	0/19	10/19		

Experimental Number	Collection Time	Treatment		Mortality	Callosing	Pmot*	Pcall**
24	Feb. 1983	cooled 3°C/hr to -20°C then plunged into dry ice, starting on May 6 reinserted -20°C then 3x hardened -20°C to -6°C and back once per day then quench to LN_2 from -21.6°C reinsert dry ice 1 week then 3°C/hr from -70°C; Controls to dry ice after hardening instead of LN_2	**Exp.**	4/17	9/17	.35	.72
			Cont.	1/13	8/13		
	super						
25	Jan. 1984	cooled at 3°C/hr to -20°C then plunged into dry ice, stored until early March 1984 then inserted into -20°C, held 3 hours at -20°C ,plunged into LN_2, reinserted at -27°C for 12 hrs, plunged back into a -70°C cooling bath and warmed at 3°C/hr to thaw; Control is an average of all previous controls not cooled below -20°C with the control group assumed as large as the experimental	**Exp.**	7/24	--	.49	--
			Cont.	4/24	--		
	super						

Appendix II

```
C       THIS PROGRAM SOLVES THE PROBLEM OF COMPUTING THE PROBABILITY OF
C       PICKING N LIVE TWIGS AND M DEAD TWIGS OUT OF A HAT CONTAINING
C       A LIVE TWIGS AND B DEAD TWIGS,WHERE A .GE. N AND B .GE. M,PLUS
C       THE PROBABILITY OF ALL LESS LIKELY EVENTS.THIS IS:
C       (N+M)!A!B!((A+B)-(N+M))!/N!M!(B-M)!(A-N)!(A+B)!;FOR EACH
C       POSSIBLE M AND N.THUS THE COMPUTATION IS THE SUM OF ALL SUCH EX-
C       PRESSIONS .LE. THE EXPRESSION FOR  THE GIVEN N AND M.
C
C
1       IMPLICIT REAL*8(A-Z)
2       DATA SALIVE,SDEAD,TALIVE,TDEAD/3.0,3.0,5.0,7.0/
2222    DIMENSION TMS(0.0:100.0)
3       DIMENSION APROB(0.0:100.0,0.0:100.0)
4       DIMENSION TPROB(0.0:100.0,0.0:100.0)
5       DIMENSION AS(0.0:100.0),DS(0.0:100.0),AT(0.0:100.0)
6       DIMENSION DT(0.0:100.0),ASPDS(0.0:100.0)
7       DIMENSION DTMDS(0.0:100.0),ATMAS(0.0:100.0)
8       DIMENSION ATPDT(0.0:100.0),ST1(0.0:100.0)
9       DIMENSION PROB(0.0:100.0)
10      OPEN (UNIT=2, FILE='STAT.DAT',STATUS='NEW')
101     TMS(0)=1.0
61      AS(0)=1.0
72      DS(0)=1.0
83      AT(0)=1.0
94      DT(0)=1.0
105     ASPDS(0)=1.0
1161    DTMDS(0)=1.0
127     ATMAS(0)=1.0
138     ATPDT(0)=1.0
149     ST1(0)=1.0
11      S=SALIVE+SDEAD
12      T=TALIVE+TDEAD
13      DDT=TDEAD
14      AAT=TALIVE
15      AAS=-1.0
18      IF ((AAS .LT. S) .AND. (AAS .LT. AAT))   THEN
19         AAS=AAS+1.0
16         DDS=S-AAS
21         GOTO 221
20      ELSE
           GOTO 28
22      END IF
221     IF (DDS .GT. DDT) THEN
222        DDS=DDT
223        AAS=(S-DDS)-1.0
224        GOTO 18
225     END IF
C
C
C
1511    DO 69 J=1.0,T
```

```
1611        CJ=J
1711        IF (CJ .GT. AAS) THEN
1811           AS(J)=1.0
1911        ELSE
2011           AS(J)=J
2111        END IF
2211        IF (CJ .GT. DDS) THEN
2311           DS(J)=1.0
2411        ELSE
2511           DS(J)=J
2611        END IF
2711        IF (CJ .GT. AAT) THEN
2811           AT(J)=1.0
2911        ELSE
3011           AT(J)=J
3111        END IF
3211        IF (CJ .GT. DDT) THEN
3311           DT(J)=1.0
3411        ELSE
3511           DT(J)=J
3611        END IF
3711        IF (CJ .GT. S) THEN
3811           ASPDS(J)=1.0
3911        ELSE
4011           ASPDS(J)=J
4111        END IF
4211        IF (CJ .GT. (AAT-AAS)) THEN
4311           ATMAS(J)=1.0
4411        ELSE
4511           ATMAS(J)=J
4611        END IF
4711        IF (CJ .GT. (DDT-DDS)) THEN
4811           DTMDS(J)=1.0
4911        ELSE
5011           DTMDS(J)=J
5111        END IF
6000        IF (CJ .GT. T-S) THEN
6001           TMS(J)=1.0
6002        ELSE
6003           TMS(J)=J
6004        END IF
5211        ATPDT(J)=T-J+1.0
5311        RATIO=(ASPDS(J)/AS(J))*(DT(J)/DS(J))*(AT(J)/DTMDS(J))*
            1(TMS(J)/ATMAS(J))*(1.0/ATPDT(J))
5511        ST1(J)=ST1(J-1)*RATIO
5611        PROB(AAS)=ST1(T)
69          CONTINUE
C
C
26          APROB(AAS,DDS)=PROB(AAS)
27          GOTO 18
28          TPROB(SALIVE,SDEAD)=APROB(SALIVE,SDEAD)
29          DO 33 J=0.0,AAS
30          IF (APROB(J,S-J) .GT. APROB(SALIVE,SDEAD)) GOTO 33
```

```
31          IF (J .EQ. SALIVE) GOTO 33
32          TPROB(SALIVE,SDEAD)=TPROB(SALIVE,SDEAD)+APROB(J,S-J)
33          CONTINUE
34          WRITE (2,*) 'TOTAL ALIVE,TOTAL DEAD;SAMPLE ALIVE,DEAD;
            1PROBABILITY FOLLOW:'
            WRITE (6,*) 'TOTAL ALIVE,TOTAL DEAD;SAMPLE ALIVE,DEAD;
            1PROBABILITY FOLLOW:'
            WRITE (2,116) TALIVE,TDEAD,SALIVE,SDEAD,
            1TPROB(SALIVE,SDEAD)
            WRITE (6,116) TALIVE,TDEAD,SALIVE,SDEAD,
            1TPROB(SALIVE,SDEAD)
116         FORMAT (1H ,4G15.5,G18.9)
            STOP
            END
```

References

1. Angell, C.A. and Sare, E.J. (1969). Glass-forming composition regions a glass transition temperatures for aqueous electrolyte solutions. J. Chemical Physics **523**, 1058-1068.

2. Angell, C.A. (1970). The data gap in solution chemistry. J. Chemical Education **47**, 583-587.

3. Angell, C.A. (1978). Glass transition temperatures for simple molecular liquids and their binary solutions. J. Phys. Chem. **82**, 2622-2629.

4. Angell, C.A. and Tucker, J.C. (1979). Heat capacity changes in glass-forming aqueous solutions and the glass transition in vitreous water. J. Phys. Chem. **84**, 268-272.

5. Angell, C.A. and Sare, E.J. (1980) Glass formation in aqueous sodium sal solutions. Cryo-Letters **1**, 257-260.

6. Bewley,J.D (1979).Physiological aspects of desiccation tolerance. Ann. Rev. Plant Physiol. 30,195-238

7. Bittenbender, H.C. and Howell Jr., G.S. (1975). Interactions of temperature and moisture content on spring de-acclimation of flower buds of highbush blueberry. Can. J. Sci **55**, 447-452.

8. Bixby, J.A., and Brown, G.N. (1975). Ribosomal changes during induction of cold hardiness in black locust seedlings. Plant Physiol. **56**, 617-621.

9. Brown, G.N., and Bixby, J.A. (1973b). Quantitative and qualitative changes in total protein and soluble protein during induction of cold hardiness in black locust stem tissues. Cryobiology **10**, 529-530.

10. Brown, G.N., and Bixby, J.A. (1975). Soluble and insoluble protein patterns during induction of freezing tolerance in black locust seedlings. Physiol. Plant. **34**, 187-191.

11. Bruggler, P. and Mayer, E. (1980). Complete vitrification in pure liquid water and dilute aqueous solutions. Nature **288**, 569-571.

12. Burke, M.J. Personal communication.

13. Chen, P.M. and Li, P.H. (1977). Induction of frost hardiness in stem cortical tissues of Cornus stolonifera Michx. by water stress. II. Biochemical changes. Plant Physiol. **59**, 240-243.

14. Chen, P.M., Burke, M.J., and Li, P.H. (1976). The frost hardiness of several Solanum species in relation to the freezing of water, melting point depression, and tissue water content. Bot. Gaz. 137 313-317.

15. Chen, P.M., Li., P.H., and Burke, M.J. (1977). Induction of frost hardiness in stem cortical tissues of Cornus stolonifera michx. by water stress. I. Unfrozen water in coritcal tissues and water status in plants and soil. Plant. Physiol. 59, 236-239.

16. Clegg,J.S. (1978).Hydration dependent metabolic transitions and the sta of water in Artemia. In Dry Biological Systems (Crowe, J.H. and Clegg, J.S., eds.), Academic Press, New York.

17. Crowe J.H., Jackson,S., and Crowe,L.M. (1983). Nonfreezable water in anhydrobiotic nematodes. Mol. Physiol. 3, 99-105.

18. Dubochet, J., Lepault, J., Freeman, R., Berriman, J.A., and Homo, J.-C. (1982). Electron microscopy of frozen water and aqueous solutions. Journal of Microscopy 128, 219-237.

19. Engle, A.G., Fukunaga, H., and Osame, M. (1982). Stereometric estimatior of the area of the freeze-fractured membrane. Muscle & Nerve Nov/Dec, 682-685.

20. Espevik, T. and Elgsaeter, A. (1981). In situ liquid propane jet-freezing and freeze-etching of monolayer cell cultures. Journal of Microscopy 123 105-110.

21. Franks, F., Asquith, M.H., Hammond, C.C., Skaer, H.L.B, and Echlin, P. (1977). Polymeric cryoprotectants in the preservation of biological ultrastructure. Low temperature, states of aqueous solutions of hydrophilic polymers. J. Microsc. 110, 223-238.

22. Garber, M.P., and Steponkus, P.L. (1973b). Alterations in chloroplast membranes during cold acclimation and freezing. Cryobiology, 10, 532.

23. Garber, M.P., and Steponkus, P.L. (1973a). Alterations in chloroplast membranes during cold acclimation and freezing. II. Alterations during cold acclimation. Cryobiology, 10, 531.

24. Garber, M.P., and Steponkus, P.L. (1976a). Alterations in chloroplast thylakoids during an in vitro freeze-thaw cycle. Plant Physiol 57, 673-680.

25. Garber, M.P., and Steponkus, P.L. (1976b). Alterations in chloroplast thylakoids during cold acclimation. Plant Physiol 57, 681-686.

26. George, M.F., and Burke, M.J. (1977a). Cold hardiness and deep supercooling in xylem of shagbark hickory. Plant Physiol. **59**, 319-325.

27. Gusta, L.V., Burke, M.J., and Kapoor, A.C. (1975). Determination of unfrozen water in winter cereals at sub-freezing temperatures. Plant Physiol. **56**, 707-709.

28. Heber, U. (1970). Proteins capable of protecting chloroplast membranes against freezing. In The Frozen Cell (G.E. Wolstenholme and M. O'Connor, eds.) J. and A. Churchill, London, pp. 175-188.

29. Hodgman, C.D., Weast, R.C., and Wallace, C.W. (1953). Handbook of Chemistry and Physics (C.D. Hodgman, R.C. Weast, and C.W. Wallace, eds.), Chemical Rubber Publ. Co., Cleveland, Ohio., 35th Edition.

30. Itoh, T. (1974). Fine structure of the membranes and organelles in parenchyma cells of poplar shoot observed by freeze etching technique. Wood Research **57**, 31-47.

31. Johansson, N.-O. (1970). Ice formation and frost hardiness in some agricultural plants. Nat. Swed. Inst. Plant Protection Contrib. **14**, (132), 364-382.

32. Johansson, N.-O., and Krull, E. (1970). Ice formation, cell contraction, and frost killing of wheat plants. Nat. Swed. Inst. Plant Protection Contrib. **14**(131), 343-362.

33. Johnson, J.E., Jr. Current Trends in Morphological Techniques, Vol. II, **5**, CRC Press, 131- .

34. Kanno, H. and Angell, C.A. (1977). Homogeneous nucleation and glass formation in aqueous alkali halide solutions at high pressures. J. Physical Chemistry **81**, 2639-2643.

35. Karow, Jr., A.M. and Pegg, D.E. (1981). Organ Preservation for Transplantation, Marcel Dekker Inc., New York, 2nd Ed.

36. Kauzmann, W. (1948). The nature of the glassy state and the behavior of liquids at low temperatures. Chem. Revs. **43**, 219-256.

37. Krasavtsev, O.A. (1969). Effect of prolonged frost on trees. Fiziol. Rast. **16**, 228-236.

38. Kull, U. (1973). Temperature independent accumulation of raffinose in barks of Populus. Ber. dtsch. bot. Ges. **86**, 499-503.

39. Lehmann, H. and Schultz, D. (1976). Alternations in frozen aqueous media during storage in liquid nitrogen. J. Submicr. Cytol. **8**(4), 285-291.

40. Levitt, J. (1956). The Hardiness of Plants. 278 pp. Academic Press, New York.

41. Levitt, J. (1980). Responses of Plants to Environmental Stresses Vol. I. (J. Levitt, Ed.), Academic Press, New York, 2nd Edition.

42. Li, P.H., and Weiser, C.J. (1967). Evaluation of extraction and assay methods for nucleic acids from red osier dogwood and RNA, DNA, and protein changes during cold acclimation. Proc. Amer. Soc. Hort. Sci. **91**, 716-727.

43. Li, P.H. and Sakai, A. (1978). Plant Cold Hardiness and Freezing Stress, (Li, P.H. and Sakai, A., Eds.) Academic Press, New York.

44. Luyet, B. and Rasmussen, D. (1967). Study by differential thermal analysis of the temperatures of instability in rapidly cooled solutions of polyvinyl-pyrrolidone. Biodynamica **10** (209), 137-147.

45. Luyet, B. and Rasmussen, D. (1967). Study by differential thermal analysis of the temperatures of instability of rapidly cooled solutions of glycerol,ethylene glycol,sucrose and glucose. Biodynamica **10** (209), 167-192.

46. MacKenzie, A.P. and Luyet, B.J. (1967). Electron microscope study of recrystallization in rapidly frozen gelatin gels. Biodynamica **10** (206), 95-121.

47. MacKenzie, A.P. (1977). Non-equilibrium freezing behaviour of aqueous systems. Phil. Trans. R. Soc. Lond. **278**, 167-189.

48. McKenzie, J.S., Wieser, C.J., and Li, P.H. (1974c). Changes in water relations of Cornus stolonifera during cold acclimation. J. Am. Soc. Hortic. Sci. **99**, 223-228.

49. McKenzie, J.S., Weiser, C.J., and Li, P.H. (1974a). Effects of red and far red light on the initation of cold acclimation in Cornus stolonifera Michx. Plant Physiol. **53**, 783-789.

50. McKenzie, J.S., Weiser, C.J., Stadelmann, E.J, and Burke, M.J. (1974). Water permeability and cold hardiness of cortex cells in cornus stolonifera michx. - a preliminary report. Plant Physiol. **54**, 173-176.

51. Mayer, E. and Bruggeller, P. (1982). Vitrification of pure liquid water by high pressure jet freezing. Nature **298**, 715-718.

52. Meryman, H.T. (1971). Osmotic stress as a mechanism of freezing injury. Cryobiology **8**, 489-500.

53. Miller, K.R., Prescott, C.S., Jacobs, T.L., and Lassignal, N.L. (1983). Artifacts associated with quick-freezing and freeze-drying. J. Ultrastructure Research **82**, 123-133.

54. Nagano, M., Kodama, K., Bara, N., Kanaya, K., and Osumi, M. (1982). Filamentous structure in yeast mitochondria by freeze-etching of replica combined with rapid freezing. J. Electron Microsc. **31** (3), 268-272.

55. Olien, C.R. and Smith, M.N. (1981). Analysis and Improvement of Plant Cold Hardiness (C.R. Olien & M.N. Smith, Eds.), CRC Press, Boca Raton, Florida.

56. Parish, G.R. (1974). Seasonal variation in the membrane structure of differentiating shoot cambial-zone cells demonstrated by freeze-etching. Cryobiologie **9**, 131-143.

57. Parker, J. (1972). Spatial arrangements of some cryoprotective compounds in ice lattics. Cryobiology **9**, 247-250.

58. Rasmussen, D. (1969). A note about "phase diagrams" of frozen tissues. Biodynamica **10** (221), 333-339.

59. Rasmussen, D. and Luyet, B. (1970). Contribution of the establishment of the temperature-concentratin curves of homogeneus nucleation in solutions of some cryoprotective agents. Biodynamica **11** (225), 33-43.

60. Rasmussen, D.H. and MacKenzie, A.P. (1970). The glass transition in amorphous water. application of the measurements to problems arising in cryobiology. J. Physical Chemistry **75** (7), 967-973.

61. Rasmussen, D.H. and MacKenzie, A.P. Effect of solute on ice-solution interfacial free energy; calculation from measured homogeneous nucleaton temperature. In Water Structure at the Water-Polymer Interface (H.H.G. Jellinek, Ed.), Plenum Publ. Corp, New York, N.Y.

62. Sagisaka, S. (1972). Decrease in the metabolic activity in poplar twigs to a fetal level during storage in frozen state. Low. Temp. Sci. Ser. B. Biol. Sci. **30**, 15-21.

63. Sagisaka, S. (1974). Effect of low temperature on amino acid metabolism in wintering poplar: Arginine-glutamine relationships. Plant Physiol. **53**, 319-322.

64. Sakai, A. (1956). The effect of temperature on the hardening of plants. Low Temp. Sci. Ser. **B14**, 7-15.

65. Sakai, A. (1958). Survival of plant tissue at super-low temperature. II. Low Temp. Sci. Ser. **B16**, 41-53.

66. Sakai, A. (1960). Survival of the twigs of woody plants at -196°C. Nature, **185**, 393-394.

67. Sakai, A. (1962). Studies on the frost-hardiness of woody plants. I. The causal relation between sugar content and frost-hardiness. Contr. Inst. Low. Temp. Sci. Ser. **B11**, 1-40.

68. Sakai, A. (1965). Studies of frost hardiness in woody plants. II. effect of temperature on hardening. Plant Physiol. **11**, 353-359.

69. Sakai, A. and Otsuka, D. (1967). Survival of plant tissue at super low temperature V. An electron microscope study of ice in cortical cells cooled rapidly, Plant Physiol. **42**, 1680- .

70. Sakai, A. and Yashida, S. (1968a). The role of sugar and related compounds in variations of freezing resistance. Cryobiology **5**, 160-174.

71. Sakai, A. (1970a). Freezing resistance in willows from different climates. Ecology **51**, 485-491.

72. Sakai, A. (1973). Characteristics of winter hardiness in extremely hardy twigs of woody plants. Plant Cell Physiol. **14**, 1-9.

73. Sakai, A., and Sugawara, Y. (1973). Survival of poplar callus at super-low temperatures after cold acclimation. Plant Cell Physiol. **14**, 1201-1204.

74. Sakai, A. (1974). Characterictics of winter hardiness in extremely hardy twigs. Fiziol. Rast. **21**, 141-147.

75. Schonbeck, M.W. and Bewley, J.D. (1981). Responses of the moss Tortula ruralis to desiccation treatments. II. variations in desiccation tolerance. Can. J. Bot. **59**, 2707-2712.

76. Severs, N.J. and Green, C.R. (1983). Rapid freezing of unpretreated tissues for freeze-fracture electron microscopy. Biology of the Cell, **47**, 193-204.

77. Simatos, D., Faure, M., Bonjour, E., and Couach, M. (1975). The physical state of water at low temperatures in plasma with different water contents as studied by differential thermal analysis and differential scanning calorimetry. Cryobiology **12**, 202-208.

78. Siminovitch, D., and Briggs, D.R. (1949). The chemistry of the living bark of the black locust tree in relation to frost hardiness. I. Seasonal variations in protein content. Arch. Biochem. Biophys. **23**, 8-17.

79. Siminovitch, D., and Briggs, D.R. (1953a). Studies on the chemistry o the living bark of the black locust tree in relation to frost hardiness. III. The validity of plasmolysis and desiccation tests for determining the frost hardiness of bark tissue. Arch. Biochem. Biophys. **28**, 15-34.

80. Siminovitch, D., and Briggs, D.R. (1953b). Studies on the chemistry of the living bark of the black locust tree in relation to frost hardiness. IV. Effects of ringing on translocation, protein synthesis and the development of hardiness. Plant Physiol. **28**, 177-200.

81. Siminovitch, D., and Briggs, D.R. (1954). Studies on the chemistry of the living bark of the black locust in relation to its frost hardiness. VII. A possible direct effect of starch on the susceptibility of plants to freezing injury. Plant Physiol. **29**, 331-337.

82. Siminovitch, D., Rheaume, B., and Sachar, R. (1967a). Seasonal increase in protoplasm and metabolic capacity in the cells during adaptation to freezing. In Molecular Mechanisms of Temperature Adaptation (C.L. Prosser, ed.), Pub. No. 84. Amer. Assoc. Adv. Sci. Washington, D.C, pp. 3-40.

83. Siminovitch, D., Rheaume, B., Pomeroy, K., and Lepage, M. (1968). Phospholipid, protein, and nucleic acid increases in protoplasm and membrane structures associated with development of extreme freezing resistance in black locust tree cells. Cryobiology **5**, 202-225.

84. Sjolund, R.D. and Shih, C.Y. (1983). Freeze-fracture analysis of phloem structure in plant tissue cultures I. The sieve element reticulm. J. of Ultrastructure Research **82**, 111-121.

85. Sjolund, R.D. and Shih, C.Y. (1983). Freeze-fracture analysis of phloem structure in plant tissue cultures II. The sieve element plasma membrane. J. of Ultrastructure Research **82**, 189-197.

86. Sjolund, R.D. and Shih, C.Y. (1983). Freeze-fracture analysis of phloem structure in plant tissue cultures III. P-protein, sieve area pores, and wounding. J. of Ultrastructure Research **82**, 198-211.

87. Steere, R.L. and Erbe, E.F. (1983). Supporting freeze-etch specimens with "lexan" while dissolving biological remains in acid. Proceedings of the 41st Annual Meeting of the Electron Microscopy Society of America, San Francisco Press, Inc.

88. Suzuki, E. and Nagashima, N. (1982). Freezing-thawing hysteresis phenomena of biological systems by the new method of proton magnetic resonance. Bull. Chem. Soc. Jpn. **55**, 2730-2733.

89. Takahashi, T., and Asahina, E. (1974). Injury by extracellular freezi the egg cells of sea urchins, a preliminary report. Low Temp. S Ser. B. 32, 9-18.

90. Talstad, I., Dalen, H., Scheie, P., and Roli, J. (1981) Patterns in quench-frozen, freeze-dried, blood proteins Scanning Electron Microscopy II, 319-326.

91. Tumanov, I. and Krasavtsev, O. (1959). Hardening of northern woody plants by temperatures below zero. Soviet Plant Physical 6 (6), 663- .

92. Wall, F.T. (1974). Chemical Thermodynamics A Course Study, W.H. Freeman and Company, San Francisco, Calif., Third Edition.

93. Weiser, C.J. (1970). Cold resistance and acclimation in woody plants. Hort Science 5(5), 3-10.

94. Williams, R.J. (1973). Osmotic properties of glycopeptides from hardy Cornus spp. Cryobiology 10, 530.

95. Williams, R.J., Personal communication.

96. Wolfe, J. and Steponkus, P.L. (1983). Mechanical properties of the plasma membrane of isolated plant protoplasts. mechanism of hyperosmotic and extracellular freezing injury. Plant Physiol 71 (2), 276- .

97. Yoshida, S., and Sakai, A. (1973). Phospholipid changes associated with the cold hardiness of cortical cells from poplar stem. Plant Cell Physiol. 53, 509-511.

98. Young, R., and Yelenosky, G. (1973). Effect of freezing on cell ultrastructure in Citrus tissues. Cryobiology 10, 531-532.